SHIPPING TO AMERICA

XIWEN BAI
Tsinghua University

JESÚS FERNÁNDEZ-VILLAVERDE
University of Pennsylvania

YILIANG LI
Peking University HSBC Business School

RICARDO MARTO
Federal Reserve Bank of St. Louis

FRANCESCO ZANETTI
University of Oxford

June 2026

We study the macroeconomic impact of route-specific shipping disruptions on the U.S. economy and their implications for trade policy. Using high-frequency satellite data on the *universe* of U.S.-bound container vessels between 2016 and 2025, we construct novel measures of potential and effective shipping capacity that account for disruptions arising from port congestion, Suez and Panama Canal bottlenecks, slow steaming, and vessel rerouting. These measures allow us to document new facts about the evolution of U.S.-bound shipping capacity, the sources of capacity losses, and changes in shipping efficiency. We develop a multi-route general equilibrium model to quantify the impact of shipping disruptions. The 2021 West Coast port congestion during the COVID-19 pandemic reduced welfare by 0.9% of GDP, while the security threats from the 2023–2024 Houthi attacks led to a welfare loss of 0.4% of GDP. The U.S. Navy's intervention in the Red Sea helped contain the effect of these attacks, yielding a benefit of 0.2% of GDP at a fiscal cost of 0.02%. Tariffs, by alleviating route congestion, can mitigate or even reverse the standard inflationary effect, although the effect on welfare depends on the degree of retailers' market power.

KEYWORDS: AIS, shipping capacity, shipping disruptions, port congestion, maritime transportation, general equilibrium, trade policy, tariffs, maritime security, supply chains.

JEL CLASSIFICATION: E23, L91, O18, O41, R40.

Xiwen Bai: xiwenbai@tsinghua.edu.cn
Jesús Fernández-Villaverde: jesusfv@econ.upenn.edu
Yiliang Li: yiliang_li@phbs.pku.edu.cn
Ricardo Marto: ricardo.marto@stls.frb.org
Francesco Zanetti: francesco.zanetti@economics.ox.ac.uk

We thank Simon Fuchs, Myrto Kalouptsidi, Fernando Leibovici, Nicolas Morales, Theodore Papageorgiou, and Stephen Redding for their insightful comments and suggestions. We are also grateful to seminar and conference participants at the Bank of Portugal Winter Research Conference, the NBER Summer Institute, the NBER meeting on Transportation Networks and the Spatial Distribution of Economic Activity, the Federal Reserve Bank of San Francisco, the SED Meetings in Copenhagen, the Federal Reserve Bank of St. Louis, the Symposium of the Society for Nonlinear Dynamics & Econometrics, the 3rd HKU Macroeconomics Workshop, and SUFE. We thank Hoang Le and Shengyao Xu for excellent research assistance. The views expressed here are those of the authors and do not necessarily reflect the views of the Federal Reserve Bank of St. Louis or the Federal Reserve System.

1. Introduction

A sequence of high-profile shocks—the COVID-19 pandemic, the 2021 Suez Canal blockage, the Red Sea crisis of 2023–2024, and the 2025–2026 tensions in the Strait of Hormuz—has highlighted how disruptions in seaborne shipping propagate through global supply chains. Yet standard macroeconomic models treat shipping costs as exogenous, abstracting from the endogenous allocation of shipping capacity across routes and its response to congestion, security threats, and other disruptions. We challenge the traditional paradigm by combining novel measurement and theory, showing that the shipping sector is a strategic intermediary whose endogenous responses—through capacity reallocation and speed adjustments—reshape prices, quantities, and the macroeconomic effects of supply chain shocks and trade policy.

We make five contributions. *First*, we construct a novel dataset covering the universe of container vessels shipping to the U.S. from January 2016 through March 2025, combining high-frequency Automatic Identification System (AIS) satellite signals with vessel-level characteristics from the Lloyd's List registry. We use it to build granular, route-specific measures of *potential* and *effective* shipping capacity and of *shipping efficiency*, the ratio of the two. We decompose the wedge between potential and effective capacity into four operational frictions: port congestion, Suez and Panama canal bottlenecks, vessel rerouting, and slow steaming. *Second*, we develop a multi-region, multi-route general equilibrium model in which monopolistically competitive shipping firms allocate capacity across routes, choose sailing speeds and loading factors, and set prices subject to route-specific congestion externalities. *Third*, we map the model to the data and quantify the welfare costs of the two most consequential recent disruption episodes—the 2021 West Coast port crisis during the COVID-19 pandemic and the 2024 Red Sea attacks. *Fourth*, we use the framework to assess the U.S. Navy's protection of commercial vessels in the Red Sea, providing, to our knowledge, the first structural estimate of the macroeconomic benefits of a maritime security operation. *Fifth*, we study tariffs with explicit shipping frictions and identify a "decongestion effect" whereby tariffs relieve congestion by reallocating shipping capacity away from saturated routes, although the effect on welfare depends on the degree of retailers' market power.

Our empirical analysis uncovers several new facts about U.S.-bound container shipping. First, the 2021–2022 expansion of potential shipping capacity was highly asymmetric. Total deadweight tonnage of U.S.-bound vessels surged more than 60% above pre-pandemic levels by early 2022—reaching 48 million metric tons despite a much smaller increase in world fleet capacity—and was disproportionately concentrated on the Asia–West Coast route (Section 2). Africa, Latin America, and the Caribbean bore the cost of this reallocation, losing over 12% of their direct liner connections during 2021–2022.

Second, shipping efficiency collapsed during the recent disruption episodes (Section 3). Pre-pandemic, the U.S.-bound fleet translated roughly 89% of its potential capacity into effective service. At the peak of the supply chain crisis in 2021–2022, aggregate shipping efficiency fell below 70%. Nearly one-third of deployed potential capacity was absorbed by ships waiting at anchor, slow steaming across the Pacific, or diverting around logistical bottlenecks. The Red Sea crisis produced an analogous, route-specific shock. After Houthi attacks began in late 2023, shipping firms rerouted via the Cape of Good Hope, adding 700–1,200 nautical miles to voyages from Asia and the Middle East to the U.S. East Coast.

To interpret these patterns and quantify their aggregate implications, we develop a general equilibrium model of the shipping sector (Section 4). Monopolistically competitive shipping firms hold fleets that can be idle or allocated across six major U.S.-bound routes. On each route, firms choose sailing speed, loading intensity, and price. A key ingredient is an endogenous route-specific congestion externality: greater capacity flowing into a route lowers its shipping efficiency, capturing port and canal congestion in reduced form. Importers source from four global regions, choosing both how much to import along each route (intensive margin) and whether to specialize on it at all (extensive margin). Consumers have nested CES preferences over domestic goods and imports.

The model clarifies why the aggregate effects of shipping disruptions cannot be inferred from the size of the directly affected route alone. A route-specific disruption propagates through the entire shipping network because shipping firms reallocate vessels and capacity across routes, while importers adjust both import volumes and sourcing patterns. These responses reshape congestion and prices across routes and interact with markups and entry in the shipping and retail sectors. The macroeconomic consequences of a disruption therefore depend on these endogenous adjustment margins, rather than only on a route's Domar weight, the domestic expenditure share, or the trade elasticity. We calibrate the model to AIS data for February 2016 and simulate it forward through March 2025, matching route-level shipping efficiency, potential capacity, sailing speeds, and import shares (Section 5).

We use the calibrated model to quantify the welfare costs of two major disruption episodes (Section 6). For the 2021 West Coast port congestion, we construct a counterfactual that holds Asia–West Coast shipping efficiency at its January 2020 value, roughly 1.5 times its end-2021 trough. In this counterfactual, the import share of GDP at end-2021 rises from 12.7% to 14.0%, the retail price of Asian goods falls by about 14%, and the aggregate price index is 1.4% lower than in the baseline. Measured as an equivalent variation, the welfare cost of the 2021 disruptions amounts to 0.9% of GDP.

For the 2024 Houthi attacks, an analogous counterfactual holds Asia–Suez and Middle East–East Coast shipping efficiency at August 2023 values, more than 26 percentage points above

their May 2024 troughs. The import share rises by 0.5 percentage points in May 2024 (from 11.2% to 11.7% of GDP), the retail prices of Asian and Middle Eastern goods fall by 5.8% and 21.3%, respectively, and the aggregate price index is 0.5% lower. Between late 2023 and March 2025, the annualized welfare cost of the Red Sea crisis amounts to 0.4% of GDP.

The 2024 welfare cost was contained by U.S. naval forces, whose destroyers intercepted projectiles targeting commercial vessels (Section 7). Without the intervention, continued efficiency losses through early 2025 would have made the Red Sea crisis substantially costlier. We value the Navy's intervention at 0.2–0.3% of GDP, against a fiscal cost of roughly 0.02% of GDP; the implied return, about ten to one, is best read as an upper bound. To our knowledge, this is the first structural estimate of the macroeconomic value of a maritime security operation.

A final set of results evaluates trade policy and port infrastructure in this environment (Sections 8 and 9). Tariffs are *not* universally welfare-reducing. By suppressing import demand for Asian goods, a tariff induces shipping firms to reallocate capacity away from congested Asian routes. This "decongestion effect" acts as a productivity boost that lowers shipping prices and expands retail supply, and can more than offset the tariff's direct consumer-price effect—a textbook example of a second-best correction in the presence of a pre-existing distortion. In our baseline, an 18% tariff on Asian goods raises consumer welfare by 1.3% of income—including the 0.9% of GDP in tariff revenue rebated lump-sum to consumers—and lowers retail prices of imported goods by about 3%. The result is sensitive to two structural objects. Raising the congestion externality by 50%—mimicking a severely bottlenecked environment—flips the sign: the same tariff costs the economy 0.6% of output. Raising the retail markup from 25% to 50% likewise lets tariff pass-through dominate the decongestion gain, leaving consumers worse off. Port fees, which tax shipping firms rather than importers, raise less revenue than tariffs yet generate large welfare losses once congestion or markups bind.

Related literature. This paper connects to four main strands of literature. *First*, we build on the industrial organization of global shipping. Stopford (2008) provides the classic synthesis of the industry, while Greenwood and Hanson (2015) and Kalouptsidi (2014) document the long lags in shipbuilding that make the extensive margin of fleet capacity slow to adjust. Dunn and Leibovici (2023) study how these capacity dynamics interact with trade flows. A growing literature characterizes how search frictions, ballast trips, congestion, and market structure shape trade costs (Bai et al., 2024, Brancaccio et al., 2020, 2024, 2025, Ganapati et al., 2024), and Hummels et al. (2009) document the trade-reducing effects of market power among liner carriers. This literature focuses on the slow-moving extensive margin of fleet capacity. We focus instead on the intensive margin—how existing fleets are deployed across routes—which accounts for the bulk of U.S.-bound capacity losses during the 2021 and 2024 episodes.

Second, we contribute to research on the endogenous determinants of international shipping costs and their role in shaping trade patterns (Asturias, 2020, Hummels and Skiba, 2004, Hummels, 2007, Limão and Venables, 2001, Wong, 2022). A complementary strand quantifies how transportation networks and infrastructure shape welfare in spatial equilibrium (Allen and Arkolakis, 2022, Fajgelbaum and Schaal, 2020), and Coşar et al. (2024) estimate the long-run macroeconomic effects of transportation productivity in the United States. Closest to our measurement strategy, Heiland et al. (2025) use AIS-based shipping data to study how local shocks propagate through global shipping networks. We introduce route-specific congestion externalities into the general equilibrium analysis and use vessel-level satellite data to discipline how shipping firms reallocate capacity, choose speeds, and price in response to them.

Third, we contribute to the literature on the macroeconomic effects of supply chain disruptions. A long-standing strand of work studies how shocks propagate through input–output networks and firm-to-firm linkages (Acemoglu et al., 2012, Boehm et al., 2019, Carvalho et al., 2021, Qiu et al., 2026). Closer to our episode of interest, Alessandria et al. (2023), Bai et al. (2024), and Bai et al. (2026) document the aggregate effects of the 2020–2022 global supply chain disruptions, while Carrière-Swallow et al. (2023), Comin et al. (2023), di Giovanni et al. (2023), Isaacson and Rubinton (2023), and LaBelle and Santacreu (2022) quantify their inflationary consequences. Notteboom et al. (2024) and Yap and Yang (2024) study the Red Sea crisis from a transportation-geography perspective, Lugovskyy et al. (2025) examine speed adjustments and their environmental margins, and Fernández-Villaverde et al. (2025) show that illicit oil shipping affects prices and output through global supply chains. Blaum et al. (2026) and Xu et al. (2025) study how firms reorganize input sourcing in response to disruption risk and adjustment costs. We advance this literature by mapping granular vessel-level micro-data into a structural general equilibrium model, measuring their macroeconomic impact. Methodologically, our central proposition extends Hulten (1978) and Baqaee and Farhi (2019, 2020) to a congestible shipping sector, and shows that the welfare impact of a route disruption departs from both the Domar-weight benchmark and the domestic-share sufficient statistic of Arkolakis et al. (2012) once trade costs are the endogenous price of reallocating capacity across a shared network.

Fourth, our results speak to the economics of trade policy and port pricing amid shipping frictions. The recent empirical literature on the 2018–2019 U.S. tariffs documents near-complete pass-through to U.S. import prices and quantifies welfare losses for importers and consumers (Amiti et al., 2019, Cavallo et al., 2021, Fajgelbaum et al., 2020). Quantitative trade models with multiple sectors and dynamic adjustment have likewise been used to evaluate the welfare effects of tariff regimes (Caliendo and Parro, 2015, Caliendo et al., 2019). We contribute by showing that, when the shipping market is imperfectly competitive and routes are congested,

tariffs can serve as a second-best corrective to a route-specific congestion externality—an application of the classic theory of policy intervention under pre-existing domestic distortions (Bhagwati and Ramaswami, 1963). This mechanism connects directly to the transportation literature on optimal port pricing (De Borger et al., 2011, Strandenes and Marlow, 2000) and to the broader analysis of congestion pricing with market power (Brueckner, 2002). Finally, our valuation of the U.S. Navy's intervention in the Red Sea relates to a smaller literature on the economic cost of trade insecurity and conflict (Anderson and Marcouiller, 2002, Glick and Taylor, 2010).

The remainder of the paper proceeds as follows. Sections 2 and 3 present the data and empirical facts; Sections 4–6 develop, calibrate, and quantify the model; Sections 7–9 evaluate the Navy intervention, tariffs, port fees, and infrastructure; and Section 10 concludes. The online appendix provides additional empirical evidence, robustness exercises, and model derivations.

2. U.S.-BOUND POTENTIAL SHIPPING CAPACITY

We quantify the evolution of U.S.-bound potential shipping capacity at the route level using high-frequency satellite data on ship movements. Potential capacity is the upper bound on the shipping services a route could deliver absent disruptions and with vessels operating at full efficiency. We measure it in metric tons or ton-miles, the latter being one metric ton of goods carried one nautical mile (Stopford, 2008).

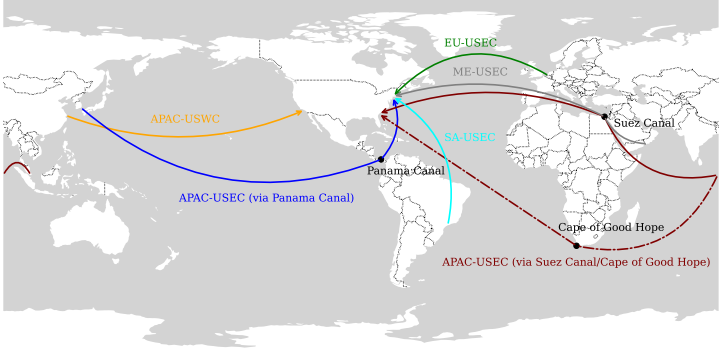
Data. Our analysis relies on two primary data sources. The first is the Automatic Identification System (AIS), which the International Maritime Organization (IMO) requires on all ships above 300 gross tonnage engaged in international voyages. AIS reports the IMO ship identification number, position, and speed at high frequency. Vessels transmit as often as every two seconds. We focus on container ships, as they are the main mode of transport for manufactured goods.[1] The second data source is the Lloyd's List vessel registry, which provides ship-level characteristics, including deadweight tonnage (DWT) and ownership.

Combining these sources lets us reconstruct the full population of container-ship voyages arriving at U.S. ports, linked to ship-level characteristics, from January 2016, when AIS data became publicly available with comprehensive global coverage, through March 2025. In our benchmark analysis, we use weekly data unless otherwise stated.

[1]Dry bulk shipping carries bulk commodities such as iron ore, coal, and grain, and oil tankers carry oil. In 2024 these segments held 43% and 28% of world fleet capacity, respectively; container ships and other general cargo ships made up the rest (UNCTAD, 2024). In the U.S., container shipping carries more tonnage (nearly one billion short tons) and value (more than 0.7 trillion dollars) than any other transport mode, over 50% of U.S. trade by weight and roughly 30% by value (Bureau of Transportation Statistics, 2021). Some high-value items, such as computer chips, go by air, but these products depend on other components, such as motherboards, that travel by container ship.

Routes and trips. We classify vessel trips into six major U.S.-bound trade routes: (1) Asia-Pacific to the U.S. West Coast (APAC–USWC); (2) Asia-Pacific to the U.S. East Coast (APAC–USEC) via the Panama Canal; (3) Asia-Pacific to the U.S. East Coast via the Suez Canal or the Cape of Good Hope; (4) Europe to the U.S. East Coast (EU–USEC); (5) the Middle East to the U.S. East Coast (ME–USEC); and (6) South America to the U.S. East Coast (SA–USEC).[2] Figure 2.1 plots these six trade routes. Together, they capture the bulk of U.S.-bound shipping dynamics, about 80–90% of all U.S. containerized maritime imports.

FIGURE 2.1.—Major U.S.-bound trade routes



Unlike dry bulk vessels or tankers, container ships operate on fixed service loops connecting predetermined sets of origin and destination ports. To distinguish U.S. inbound from outbound trips, we define a trip as the journey that begins when a vessel departs its last port in the foreign region of origin (Asia-Pacific, Europe, the Middle East, or South America) and ends on its arrival at the first port on either the U.S. East Coast or West Coast, possibly after some intermediate port calls (a port call is the arrival of a ship at a port where it docks to load and unload cargo). When a vessel's itinerary includes stops in multiple foreign regions, we record a separate trip for each region. This granularity lets us focus on shipping dynamics along the intercontinental legs of vessels' service loops, while limiting the effect of domestic and within-region movements on the measurement of shipping services provided to the U.S.[3]

Figure 2.2 shows a representative round trip between Asia-Pacific and the U.S. East Coast via the Suez Canal. Along the voyage, the vessel calls, among others, at Port Klang, Malaysia

[2]For route (3), we combine the Suez Canal and Cape of Good Hope paths because the latter emerged in response to the Houthi attacks in the Red Sea in late 2023 and is not a regular route throughout the period.

[3]Extending the analysis to cover within-region legs or the additional U.S.-bound routes (e.g., SA–USWC) is feasible but computationally intensive.

FIGURE 2.2.—Representative service loop: Asia-Pacific to U.S. East Coast via Suez



Note: A representative port rotation (U.S.-inbound leg in blue, U.S.-outbound leg in gray) for a container service connecting the Asia-Pacific and Middle East regions to the U.S. East Coast via the Suez Canal. The route follows a fixed sequence of port calls, beginning in East Asia (Qingdao, Shanghai, Ningbo, and Nansha), continuing through Southeast Asia (Port Klang) and the Middle East (Jeddah), and stopping at Damietta in Egypt before reaching U.S. East Coast ports (Newark, Norfolk, Charleston, and Jacksonville). The vessel then returns to Asia to complete the round trip. The schedule on the left reports the pro forma departure day at each port along the service loop. *Source:* SeaLead.

(Asia-Pacific) and Jeddah, Saudi Arabia (Middle East) before arriving at Newark (U.S. East Coast). This voyage serves both the APAC–USEC via Suez route and the ME–USEC route.[4]

TABLE 2.1

KEY PORTS AND U.S.-BOUND TRADE ROUTES

Rank	Destination Port	Trips (%)	Rank	Origin Port	Trips (%)	Major Routes
1	Newark, NJ	19.6	1	Busan, South Korea	19.3	APAC-USWC, APAC-USEC (Panama)
2	Los Angeles, CA	11.4	2	Cartagena, Colombia	9.8	SA-USEC
3	Long Beach, CA	9.0	3	Shanghai, China	6.8	APAC-USWC, APAC-USEC (Panama)
4	Savannah, GA	5.3	4	Yantian, China	5.5	APAC-USWC, APAC-USEC (Panama)
5	Fort Lauderdale, FL	4.3	5	Ningbo-Zhoushan, China	4.8	APAC-USWC, APAC-USEC (Panama)
6	Seattle, WA	4.0	6	Valencia, Spain	4.6	EU-USEC
7	Tacoma, WA	3.9	7	Bremerhaven, Germany	3.5	EU-USEC
8	Houston, TX	3.8	8	Le Havre, France	3.0	EU-USEC
9	Miami, FL	3.6	9	Colombo, Sri Lanka	2.6	APAC-USEC (Suez/Cape)
10	Philadelphia, PA	2.7	10	Tokyo, Japan	2.4	APAC-USWC, APAC-USEC (Panama)
11	Charleston, SC	2.7	11	Yokohama, Japan	2.2	APAC-USWC
12	New York, NY	1.6	12	Kaohsiung, Taiwan	1.9	APAC-USWC, APAC-USEC (Panama)
13	Norfolk, VA	1.4	13	Santa Marta, Colombia	1.8	SA-USEC
14	Oakland, CA	1.3	14	Singapore, Singapore	1.7	APAC-USEC (Suez/Cape)
15	Portsmouth, VA	1.2	15	Point Lisas, Trinidad & Tobago	1.5	SA-USEC
16	Boston, MA	0.9	16	Antwerp, Belgium	1.5	EU-USEC
17	Chester, PA	0.9	17	Mundra, India	1.5	APAC-USEC (Suez/Cape)
18	Palm Beach, FL	0.6	18	St Georges, Grenada	1.4	SA-USEC
19	Mobile, AL	0.6	19	Melbourne, Australia	1.3	APAC-USEC (Panama), APAC-USWC
20	New Orleans, LA	0.4	20	Xiamen, China	1.3	APAC-USWC

Note: The third column shows the percentage of total container ship trips to each destination port listed in the second column during the sample period 2016–2025. Similarly, the sixth column presents the percentage of total trips originating from each origin port listed in the fifth column during the same period.

[4] A key limitation of AIS-based shipping data is the inability to track cargo origins and destinations, which prevents precise measurement of cargo flows on individual routes. Integrating AIS records with U.S. bills of lading offers a promising way to overcome the limitation, and we leave it for future research.

Table 2.1 summarizes the main destination and origin ports in our sample, along with the routes they follow and the share of trips they represent over 2016–2025. The sample records 58,582 trips and includes 218 unique ports appearing as either destinations or foreign-origin ports, comprising 58 destination ports and 160 origin ports. The principal U.S. destination ports are Newark on the East Coast, Los Angeles and Long Beach on the West Coast, and Savannah in the Southeast. The leading Asia-Pacific origin ports are Busan in South Korea and Shanghai, Yantian, and Ningbo-Zhoushan in China, primarily associated with the APAC–USWC and APAC–USEC routes. Cartagena, Colombia is the dominant South American origin port on the SA–USEC route. The main European origin ports are Valencia in Spain, Bremerhaven in Germany, and Le Havre in France, which are associated with the EU–USEC route.

Potential shipping capacity. The potential shipping capacity in *metric tons* along route r in week t is the total DWT of the container ships operating on it, where a vessel's DWT is the maximum weight of cargo it can carry:

$$\texttt{Potential Capacity}^{\text{tons}}_{r,t} = \sum_{i \in \boldsymbol{\mathcal{I}}_t} \mathbf{1}_{i,r,t} \times \texttt{DWT}_i, \tag{2.1}$$

where $\boldsymbol{\mathcal{I}}_t$ denotes the set of active container ships in week t (vessels recording at least one AIS signal), and $\mathbf{1}_{i,r,t}$ is equal to one if ship i operates on route r in week t and zero otherwise.[5]

The potential shipping capacity in *ton-miles* is the product of total DWT and the potential distance vessels could travel in one week, assuming they operate at the maximum speed observed over the sample period. Let $\overline{\texttt{Speed}}_{r,t}$ denote the DWT-weighted average vessel speed along route r in week t:

$$\overline{\texttt{Speed}}_{r,t} = \sum_{i \in \boldsymbol{\mathcal{I}}_t} \left(\frac{\mathbf{1}_{i,r,t} \times \texttt{DWT}_i}{\sum_{i \in \boldsymbol{\mathcal{I}}_t} \mathbf{1}_{i,r,t} \times \texttt{DWT}_i} \right) \times \texttt{Speed}_{i,t}. \tag{2.2}$$

Since the distance traveled is the product of speed and time, the weekly potential shipping capacity in *ton-miles* is:

$$\texttt{Potential Capacity}^{\text{ton-miles}}_{r,t} = \texttt{Potential Capacity}^{\text{tons}}_{r,t} \times \underbrace{\left(\max_{t \in \boldsymbol{\mathcal{T}}} \left\{ \overline{\texttt{Speed}}_{r,t} \right\} \times 24\,\text{hours} \times 7\,\text{days} \right)}_{\text{potential distance}}. \tag{2.3}$$

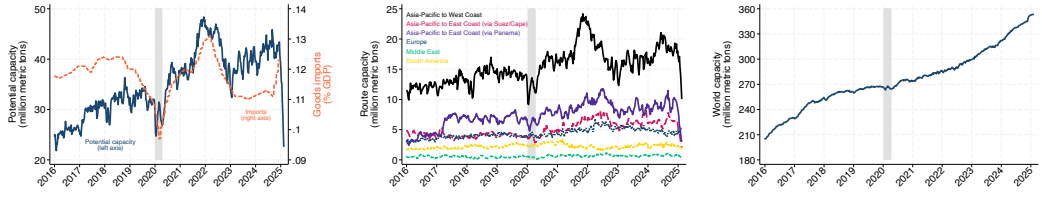
We use the maximum observed speed over the sample period ($\boldsymbol{\mathcal{T}}$) because it represents a technological upper bound independent of transient operational slowdowns. The metric captures not only the weight of the goods transported but also the distance over which they move. Mov-

[5] DWT enters directly into the ton-mile calculation. By contrast, Dunn and Leibovici (2023) measure capacity by the number of container ships and their TEU capacity, a volume rather than weight measure.

ing 10,000 tons of cargo 5,000 nautical miles demands far more shipping capacity than moving the same cargo 500 nautical miles.

The supply of U.S.-bound capacity. Panel 2.3a plots the aggregate potential shipping capacity in tons, summed across all routes.[6] From early 2016 onward, the total DWT of U.S.-bound ships rose steadily, averaging about 30 million metric tons just before the COVID-19 pandemic. After the onset of the pandemic, potential capacity surged by more than 60%, reaching 48 million metric tons in January 2022. This expansion reflected both the entry of new firms and the redeployment of vessels from other regions to capture historically high freight rates on American routes. Total DWT then contracted from its peak as import demand normalized, before rebounding toward the end of 2024. In early 2025, potential shipping capacity fell sharply, foreshadowing the U.S.-China trade war.[7]

FIGURE 2.3.—U.S.-bound potential shipping capacity (tons), January 2016–March 2025



(a) U.S.-bound potential capacity (b) Route-level potential capacity (c) World potential capacity

Note: The shaded area indicates recessions.

Panel 2.3b shows that the expansion of shipping capacity toward the U.S. was also uneven across routes. The largest increase occurred on the APAC–USWC route, which absorbed most of the new capacity after 2020.[8] This route was the primary target for new entrants and the main beneficiary of incumbents redeploying vessels from other regions.

Finally, Panel 2.3c shows that the world's total capacity evolved much more steadily, suggesting that reallocation occurred mostly across regions. Africa, Latin America, and the Caribbean were most affected by this redeployment, losing 12.4% and 13.5% of their respective direct liner shipping connections between late 2020 and mid-2022 (UNCTAD, 2022). The preference for the APAC–USWC route reflects its shorter sailing distance. Before the pandemic, shipments

[6] Aggregating across routes may overstate potential capacity because a single vessel can serve multiple routes. Figure A.1 of Appendix A addresses this with the set of unique container ships on U.S.-bound routes; the magnitudes differ slightly but the dynamics are essentially the same as in Figure 2.3.

[7] The series in ton-miles (Panel 3.5a) traces the same path, from slightly more than 80 billion before the pandemic to a peak of 135 billion in early 2022, about 110 billion in 2023–2024, and below 70 billion by the end of the sample. The number of container ships serving U.S. ports moved through the same cycle (Figure A.2 of Appendix A), rising from about 360 a week before the pandemic to 550 in early 2022 before correcting in 2023.

[8] By the end of 2021, the APAC–USWC route accounted for roughly half of total U.S.-bound potential capacity in tons, up about 6 percentage points from early 2020.

from Asia-Pacific to the West Coast averaged 2.2 weeks, against about 4 weeks for shipments from Asia to the East Coast.[9] The shorter duration let carriers maximize fleet turnover, drawing potential capacity to the West Coast during the peak in import demand.

Although less visible, potential shipping capacity from Asia-Pacific to the East Coast (via either Panama or Suez/Cape) also expanded gradually, peaking toward the end of 2022. The delayed adjustment reflects operational and economic frictions: rerouting to the East Coast required longer sailing distances, higher fuel costs, and more time to reposition fleets, so carriers concentrated new and redeployed capacity first on the more profitable APAC–USWC route (Notteboom et al., 2021). Similar patterns emerged on the EU–USEC and ME–USEC routes. By contrast, the SA–USEC route saw a prolonged and substantial decline in capacity from early 2021 to mid-2022, as Latin America and the Caribbean lost connectivity when shipping lines reassigned vessels to the Asia–U.S. routes.

3. Effective capacity and shipping efficiency

While potential shipping capacity surged after 2020, not all of it translated into effective shipping services. Port congestion, bottlenecks at Panama and Suez Canals, and rerouting around conflict zones constrained the shipping supply to U.S. importers, both by stalling vessels at ports or canals and by forcing ships to sail farther or slower.

To measure the actual provision of shipping services, we compute effective capacity in ton-miles, the capacity that remains after accounting for operational frictions, or

$$\begin{aligned}\texttt{Effective Capacity}_{r,t}^{\text{ton-miles}} = \texttt{Potential Capacity}_{r,t}^{\text{ton-miles}} - \texttt{Port Congestion}_{r,t}^{\text{ton-miles}} \\ - \texttt{Canal Congestion}_{r,t}^{\text{ton-miles}} - \texttt{Rerouting}_{r,t}^{\text{ton-miles}} \\ - \texttt{Vessel Slowdown}_{r,t}^{\text{ton-miles}}.\end{aligned} \tag{3.1}$$

Our measure of shipping efficiency corresponds to the ratio of effective to potential shipping capacity, i.e.,

$$\texttt{Shipping Efficiency}_{r,t} = \texttt{Effective Capacity}_{r,t}^{\text{ton-miles}} / \texttt{Potential Capacity}_{r,t}^{\text{ton-miles}}. \tag{3.2}$$

Shipping efficiency summarizes these disruptions in a single unit-free statistic, analogous to TFP in growth accounting. It is the share of potential capacity that survives the four frictions, comparable across routes and over time, unlike days of delay or queue lengths. We next quantify each wedge in turn.

[9] For shipments originating in Europe, the Middle East, and South America, the pre-pandemic averages were roughly 1.7, 2.9, and 1.3 weeks, respectively.

Port congestion. We measure port congestion using AIS records of vessel speed and anchorage duration. Congestion occurs when ships must wait in a port's anchorage area until a berth becomes available (Bai et al., 2024). Ideally, a ship proceeds straight to a berth on arrival. In practice, disruptions ranging from labor shortages and inland transport delays to surges in import demand force vessels to queue at anchor, reducing the actual supply of shipping services.

We quantify this loss in ton-miles per route at a weekly frequency. First, we map the geographic boundaries of berth and anchorage areas for all container ports worldwide.[10] Next, for each port call we compute the time the vessel spends in that anchorage area, attributing the full wait to the week in which the call began. Let $\texttt{Port Waiting Time}_{i,p,r,t}$ denote the hours vessel i spends in anchorage at port p during a port call initiated in week t on a trip along route r.

To convert this waiting time into foregone nautical miles, we assume that absent congestion the vessel would have sailed at the route's average speed. We therefore multiply the anchorage duration by the DWT-weighted average speed of all vessels on route r in week t ($\overline{\texttt{Speed}}_{r,t}$ in Equation (2.2)) and then by the vessel's DWT, yielding:

$$\texttt{Port Congestion}^{\text{ton-miles}}_{r,t} = \sum_{i \in \boldsymbol{\mathcal{I}}_t} \mathbf{1}_{i,r,t} \times \underbrace{\texttt{DWT}_i}_{\text{tonnage}} \times \underbrace{\left(\overline{\texttt{Speed}}_{r,t} \times \sum_{p \in \boldsymbol{\mathcal{P}}_{i,r,t}} \texttt{Port Waiting Time}_{i,p,r,t} \right)}_{\text{foregone distance}}, \tag{3.3}$$

where $\boldsymbol{\mathcal{P}}_{i,r,t}$ is the set of port calls initiated by vessel i along route r in week t, and $\boldsymbol{\mathcal{I}}_t$ is the set of active container ships in week t.

Panel 3.1a shows the average waiting time at port anchorages. Across all routes, ships spent roughly 6 hours at anchor before the pandemic. Driven by a surge in consumer demand and pandemic-related labor shortages at the Ports of Los Angeles and Long Beach, average waiting times on the APAC–USWC route exceeded 60 hours throughout the summer and fall of 2021. As bottlenecks intensified on the West Coast while nationwide demand stayed elevated, shipping companies redirected capacity toward East Coast ports. This reallocation eased congestion on the APAC–USWC route while intensifying it on the East Coast. The ME–USEC route saw severe delays, with average anchorage times peaking above 80 hours in some weeks.[11]

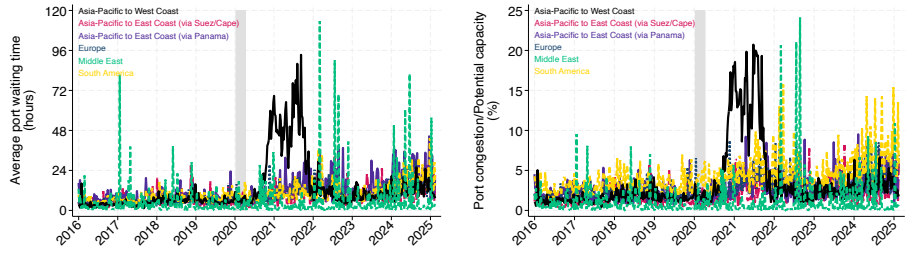
Panel 3.1b plots port congestion as a fraction of potential capacity in ton-miles. Port congestion cut potential shipping capacity on the APAC–USWC route by as much as one-fifth in 2021, a substantial efficiency loss. The effect was similarly severe on the ME–USEC route,

[10] We use AIS data with the IMA-DBSCAN (Iterative Multi-Attribute Density-Based Spatial Clustering of Applications with Noise) algorithm for this task; see Bai et al. (2023) for details.

[11] This instability reflects the "lumpiness" of a trade lane served by a very small fleet, fewer than 10 vessels for most of the sample period. With so few ships, the operational decisions of individual vessels, or delays at regional chokepoints, can skew the aggregate measure.

where port congestion absorbed nearly a quarter of potential capacity at the peak of the bottlenecks in late 2022.

FIGURE 3.1.—Port congestion across routes, January 2016–March 2025



(a) Average port waiting time (b) Port congestion/potential capacity

Note: The shaded area indicates recessions.

Canal congestion. Like port congestion, bottlenecks at the Suez and Panama Canals can restrict shipping supply. We quantify them by tracking vessel movements within the canal zones, identifying periods when ships are stalled or delayed, and computing the ton-miles lost to queuing at these chokepoints.

First, we delineate the geographic boundaries of the Suez and Panama Canals with polygons. Within these boundaries, we identify all vessel transits and extract the sequence of AIS signals each vessel broadcasts. For every pair of consecutive signals, we compute the time elapsed, the distance traveled, and the implied speed over that interval.

To measure congestion, we isolate intervals where a vessel is stationary or moving well below normal transit speed because of canal bottlenecks, filtering for intervals where speed is one knot or less. For these delayed intervals, we compute the foregone distance, the distance the vessel would have covered at the route's benchmark speed minus the distance it actually covered. The benchmark speed is $\overline{\texttt{Speed}}_{r,t}$ from Equation (2.2).[12]

The measure of canal congestion multiplies the foregone distance by the vessel's DWT and sums across all valid intervals for all ships on the route:

$$\texttt{Canal Congestion}_{r,t}^{\text{ton-miles}} = \sum_{i \in \mathcal{I}_t} \mathbf{1}_{i,r,t} \times \underbrace{\texttt{DWT}_i}_{\text{tonnage}} \times \underbrace{\left[\sum_{k \in \mathcal{K}_{i,r,t}} \mathbf{1}_{\texttt{Speed}_{i,k} \leq 1} \times \left(\overline{\texttt{Speed}}_{r,t} - \texttt{Speed}_{i,k} \right) \times \tau_{i,k} \right]}_{\text{foregone distance}}, \tag{3.4}$$

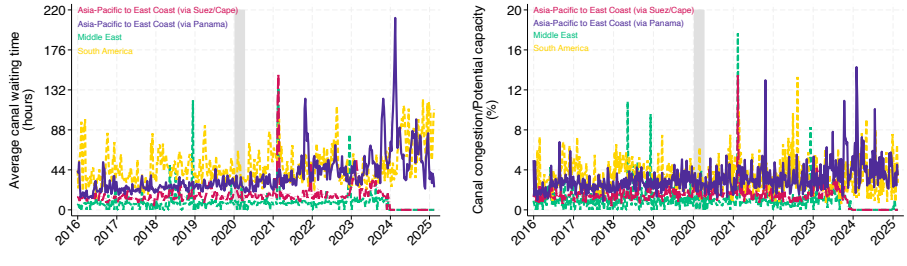
[12] In Equation (3.3), we do not subtract the distance traveled, since vessels in anchorage are mostly stationary at zero speed. In the canal congestion calculation we account for the fact that waiting vessels may still move slowly through the canal in queues.

where $\tau_{i,k}$ is the duration in hours of each interval k between consecutive AIS signals within the boundaries of the Suez or Panama Canal for vessel i, and $\mathcal{K}_{i,r,t}$ is the set of intervals during a trip along route r in week t. $\texttt{Speed}_{i,k}$ is the vessel's observed speed in interval k, and the indicator $\mathbf{1}_{\texttt{Speed}_{i,k} \leq 1}$ ensures we aggregate foregone miles only during periods when the vessel was effectively stalled.

Panel 3.2a shows the average waiting time at the Suez and Panama Canals for routes from Asia-Pacific, the Middle East, and South America to the U.S. East Coast.[13] Before the pandemic, ships queued only modestly at the two canals, averaging 11 and 34 hours. Since then the two have diverged. The Suez Canal saw two short-lived spikes: one in March 2021, from the *Ever Given* blockage, and another in January 2023, when the bulk carrier *M/V Glory* ran aground but was quickly refloated, causing only minor delays. Since early 2024, unrest in the Red Sea has pushed many carriers onto the longer route around the Cape of Good Hope (see Figure 3.3 below), cutting Suez traffic and waiting times to near zero. Waiting times at the Panama Canal, by contrast, have risen since 2023, reflecting reduced transit capacity from severe drought and the onset of El Niño.

Panel 3.2b plots canal congestion as a fraction of potential capacity across routes. Suez congestion accounted for less than 2% of potential capacity on the APAC–USEC and ME–USEC routes for most of the sample, then fell to zero as the Red Sea crisis escalated. The loss from the 2023–2024 drought and El Niño at the Panama Canal was more sustained, absorbing more than 4% of potential capacity on the APAC–USEC and SA–USEC routes.

FIGURE 3.2.—Canal congestion across routes, January 2016–March 2025



(a) Average canal waiting time (b) Canal congestion/potential capacity

Note: The shaded area indicates recessions.

Rerouting. We now turn to rerouting episodes that forced vessels off their planned course onto a longer or costlier alternative to reach U.S. ports. Often a response to changing market

[13] These chokepoints are not relevant for the APAC–USWC and EU–USEC routes, which rely on direct trans-Pacific or trans-Atlantic connections.

conditions or major external events such as the 2024 Red Sea crisis, these diversions can add substantial costs to the provision of shipping services.

Using AIS tracking data, we first group container-ship trips along each U.S.-bound route by their origin–destination (o–d) port pairs. We focus on routes that historically offer multiple routing options (e.g., Suez and the Cape of Good Hope).[14] Under normal conditions, vessels traverse the shortest available path to minimize fuel consumption and transit time. For each o–d pair, we therefore identify the trip with the shortest travel distance and use the corresponding vessel's trajectory as the benchmark. Let $\texttt{Min Distance}_{o,d,r}$ denote the shortest trip distance between origin o and destination d along route r, and let $\texttt{Trip Distance}_{i,j,o,d,r}$ denote the distance for vessel i's trip j from o to d along route r, in nautical miles.

We classify a trip j as rerouted if it deviates from the benchmark trajectory. Since trips span varying durations, we measure the intensity of the deviation as a rate. The additional nautical miles of travel in a week are

$$\texttt{Weekly Extra NM}_{i,j,o,d,r} \equiv \underbrace{\frac{\max\left(0, \texttt{Trip Distance}_{i,j,o,d,r} - \texttt{Min Distance}_{o,d,r}\right)}{\texttt{Trip Duration}_{i,j,o,d,r}}}_{\text{extra nautical miles per hour}} \times 24\,\text{hours} \times 7\,\text{days},$$

where $\texttt{Trip Duration}_{i,j,o,d,r}$ is the trip duration in hours.

Consequently, the weekly measure of rerouting in ton-miles is

$$\texttt{Rerouting}^{\text{ton-miles}}_{r,t} = \sum_{o \in \mathcal{O}_r} \sum_{d \in \mathcal{D}_r} \sum_{j \in \mathcal{J}_{o,d,r,t}} \sum_{i \in \mathcal{I}_t} \mathbf{1}_{i,j} \times \underbrace{\texttt{DWT}_i}_{\text{tonnage}} \times \underbrace{\texttt{Weekly Extra NM}_{i,j,o,d,r}}_{\text{foregone distance}}, \tag{3.5}$$

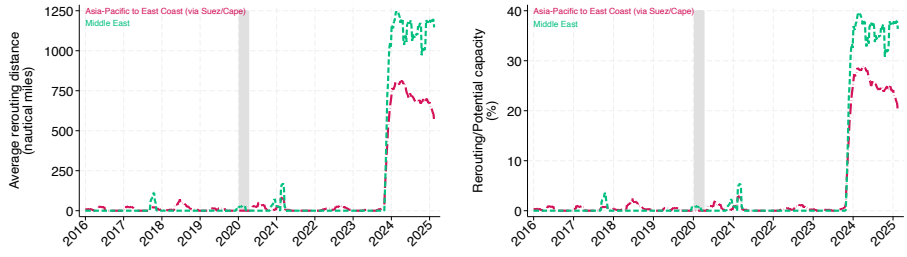
where $\mathcal{O}_r$ and $\mathcal{D}_r$ are the sets of origin and destination ports along route r, $\mathcal{J}_{o,d,r,t}$ is the set of rerouted trips between o and d along route r in week t, and $\mathcal{I}_t$ is the set of active vessels in week t. The indicator $\mathbf{1}_{i,j}$ equals one if vessel i performed trip j.

Panel 3.3a shows the average additional distance in nautical miles incurred by vessels rerouting along shipping lanes that normally transit the Suez Canal. The March 2021 Suez blockage caused negligible deviations, but the Red Sea crisis beginning in late 2023 brought a sustained shift in routing. Diverting vessels around the Cape of Good Hope added between 700 and 1,200 nautical miles to voyages from the Asia-Pacific and Middle East to the U.S. East Coast, sharply raising both fuel consumption and transit time.

To quantify the supply-side implications of these longer voyages, Panel 3.3b reports the share of potential capacity absorbed by rerouting. The diversions consumed a large part of the capacity deployed on the APAC–USEC and ME–USEC routes, roughly 25% and 36% of potential capacity in early 2024.

[14] This ensures the measured deviations reflect strategic rerouting rather than minor navigational adjustments on a single fixed route.

FIGURE 3.3.—Vessel rerouting, January 2016–March 2025



(a) Average rerouting distance

(b) Rerouting/potential capacity

Note: The shaded area indicates recessions.

Vessel slowdown. Finally, we account for reductions in shipping capacity from adjustments in vessel speed. Even when not stationary at anchor or diverting to longer routes, vessels may operate below their maximum observed speed, a practice known as "slow steaming," to save fuel or manage arrival times at congested ports.

Vessel slowdown is the gap between the average fleet speed ($\overline{\texttt{Speed}}_{r,t}$ from Equation (2.2)) and the route's technological potential, the maximum average speed observed on route r over the sample period $\mathcal{T}$. The capacity lost to vessel slowdown is the product of aggregate deployed tonnage and the distance foregone per week by sailing below this maximum:

$$\texttt{Vessel Slowdown}_{r,t}^{\text{ton-miles}} = \left[\sum_{i \in \mathcal{I}_t} \mathbf{1}_{i,r,t} \times \underbrace{\texttt{DWT}_i}_{\text{tonnage}}\right] \times \underbrace{\left[\left(\max_{t \in \mathcal{T}} \left\{\overline{\texttt{Speed}}_{r,t}\right\} - \overline{\texttt{Speed}}_{r,t}\right) \times 24\,\text{hours} \times 7\,\text{days}\right]}_{\text{foregone distance}}. \tag{3.6}$$

Panel 3.4a plots the evolution of average vessel speed across the six U.S.-bound routes. Operating speeds fell structurally, most sharply on the major East-West lanes. Before the pandemic (2016–2019), vessels on the APAC–USWC route averaged about 16 knots. The figure dropped sharply during the pandemic, bottoming out near 10 knots in 2022. The deceleration owed largely to a new virtual queuing system at the Ports of Los Angeles and Long Beach in late 2021.[15] Meant to reduce safety risks and pollution from ships waiting near port, the system assigned queue positions by departure time, removing the "hurry up and wait" incentive and encouraging vessels to slow steam across the Pacific.

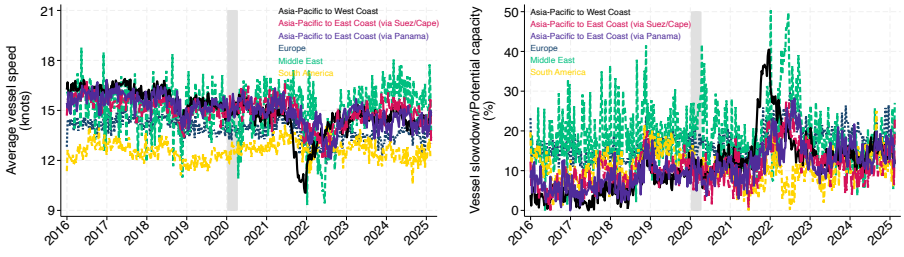
The trend extends beyond the West Coast: average speeds on the EU–USEC and APAC–USEC (via Panama) routes also drifted down, from pre-pandemic averages of 14.2 and 15.5 knots to about 13.5 and 14.5 knots in the recent period. Rising fuel prices in 2022 and new environmental regulations, such as the IMO's Carbon Intensity Indicator, sustained this broad

[15] See MXSOCAL (2021) (accessed Dec 17, 2025) for details.

deceleration.[16] Speeds have recovered slightly since mid-2023 but remain below pre-pandemic levels.

Panel 3.4b reports the share of potential capacity absorbed by vessel slowdown. On the APAC–USWC route, slow steaming accounted for about 6% of potential capacity before the pandemic, but nearly 40% at the height of the supply chain crisis. The loss is not unique to the Pacific: on the EU–USEC route the share rose from 15% pre-pandemic to 20% more recently. Across the major U.S.-bound corridors, vessel slowdown continues to absorb a substantial share of potential capacity.

FIGURE 3.4.—Vessel slowdown across routes, January 2016–March 2025



(a) Average vessel speed

(b) Vessel slowdown/potential capacity

Note: The shaded area indicates recessions.

The shipping efficiency collapse. Panel 3.5a presents potential versus effective shipping capacity (in ton-miles) aggregated across all U.S.-bound routes. The gap between the two series is the total capacity lost to shipping disruptions. The panel also reports aggregate shipping efficiency.

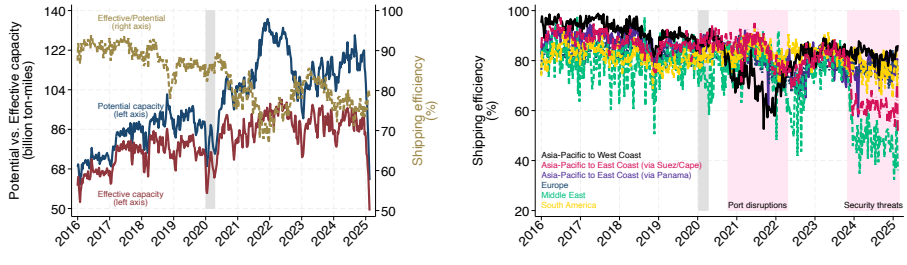
Figure 3.5 reveals a striking divergence. Before the pandemic (2016–2019), the U.S.-bound shipping network ran efficiently: about 89% of the fleet's potential capacity became effective service, with the remaining 11% lost to normal operational friction. This relationship broke down during the supply chain disruption of 2021–2022. As carriers aggressively deployed new capacity, driving potential capacity to record highs, effective capacity stagnated. At the peak of the disruption, the aggregate efficiency of the U.S.-bound fleet fell below 70%. Nearly one-third of deployed capacity was "deleted" from the market, absorbed by ships waiting at anchor, steaming slowly, or diverting around maritime bottlenecks. The network has not regained its pre-pandemic efficiency. More recently, rerouting after the 2024 Houthi attacks in the Red Sea held aggregate efficiency around 79%.

[16] IMO 2023 (EEXI/CII) regulations have forced many older vessels to permanently reduce sailing speeds to meet carbon intensity targets.

The aggregate decline masks wide heterogeneity across routes. Panel 3.5b plots shipping efficiency for each of the six U.S.-bound routes. The APAC–USWC route was the epicenter of the pandemic-era collapse. Historically the most efficient corridor, converting over 92% of potential capacity into effective supply before the pandemic, it saw efficiency fall to 53% in late 2021. At the height of the crisis, nearly half the capacity on the trans-Pacific trade was absorbed by port congestion and speed adjustments. The route has since recovered but remains well below its historical norm.

The recent deterioration, by contrast, owes largely to geopolitical instability following the Houthi attacks in the Red Sea. Efficiency on the Middle East and Asia-Pacific routes to the U.S. East Coast via the Suez Canal has fallen sharply since late 2023, to 48% and 61%. Diverting vessels around the Cape of Good Hope drives much of this loss, since ships travel longer distances without delivering additional cargo.

FIGURE 3.5.—U.S.-bound effective capacity and shipping efficiency, January 2016–March 2025



(a) Aggregate trends (b) Shipping efficiency

Note: The shaded area indicates recessions.

4. A MODEL OF THE SHIPPING MARKET WITH MULTIPLE ROUTES

The evidence in Sections 2 and 3 points to two complementary forces in U.S.-bound shipping. Shipping firms allocate and reallocate capacity across routes, while exogenous disruptions from port congestion, canal bottlenecks, and security threats absorb large shares of potential capacity, cutting the effective supply reaching U.S. ports.

To quantify these patterns, we develop a multi-route general equilibrium model with both forces: (i) the endogenous allocation of capacity across routes by profit-maximizing firms, and (ii) exogenous disruptions that govern how much potential capacity becomes effective shipping services. The model lets us trace how shocks propagate through the shipping sector to trade flows and prices, and evaluate counterfactuals central to trade policy.

4.1. *Environment*

Consider an economy with consumers, producers, retailers, and shipping firms. Besides domestically produced goods, consumers enjoy foreign goods that must be shipped from one of the four ports of origin $o \in \mathcal{O} = \{A, E, M, S\}$ (Asia, Europe, the Middle East, and South America) to one of the two arrival ports $a \in \mathcal{A} = \{E, W\}$ (the East and West Coasts of the United States). Imported goods from different regions are imperfect substitutes.

Shipping firms operate a fleet of container vessels, competing across multiple U.S.-bound routes. They carry the manufactured goods produced in one of the four regions to a destination port along a route $r \in \mathcal{R}$. The six routes are *Asia to West Coast*, *Asia to East Coast via Panama Canal*, *Asia to East Coast via Suez Canal*, *Europe to East Coast*, *Middle East to East Coast*, and *South America to East Coast*.[17] A shipping firm first decides how to allocate vessel capacity across routes, subject to a capacity constraint and costs of reshuffling fleets, repurposing vessels, and repositioning crews. Given its optimal capacity allocation, the firm then makes the operational decisions of which sailing speeds to adopt on each route and how intensively to load ships. Once ships arrive, importers resell the goods to consumers.

Domestic goods producers. A representative firm produces domestic goods d with a linear technology in labor with productivity z_d. The firm hires domestic labor, l_d, at the wage rate w and sells the goods directly to consumers at price p_d. Profit maximization requires:

$$p_d z_d = w. \tag{4.1}$$

Foreign goods producers. Foreign firms produce goods for export in each origin region. They supply any quantity demanded at the price $\overline{p}_o$ (in dollars) for goods originating in region $o \in \mathcal{O}$. Foreign producers sell to retailers, but for simplicity, we have the shipping firms act as intermediaries. The producers are indifferent to the routes shipping firms take and so do not price discriminate across them (though relaxing this assumption is an easy extension).

The shipping market. There is a continuum of monopolistically competitive shipping firms of measure N. Each shipping firm is endowed with total capacity κ that can be optimally allocated among different routes or remain idle. The capacity allocated to each route r is denoted by κ_r and idle capacity (or capacity allocated to unmodeled routes) is $\overline{\kappa}$.[18] The capacity constraint

[17] In line with the evidence, there is only one route and one arrival port for goods produced in Europe, the Middle East, or South America. Goods from Asia come in three variants: they go to either East Coast or West Coast ports, and those bound for the East Coast can be routed through the Panama Canal or the Suez Canal.

[18] Idle capacity only plays a role in counterfactual experiments as it puts an upper bound on how much capacity shipping firms can reallocate to U.S.-bound routes. As new ships take on average three years to build (Kalouptsidi, 2014), this can represent a binding constraint in any given period.

of a shipping firm can be expressed as

$$\kappa = \sum_{r \in \mathcal{R}} \kappa_r + \overline{\kappa}. \tag{4.2}$$

Shipping technology. Along each route r, shipping firms choose the average speed of their ships, s, and the quantity of goods loaded on them, ℓ, to produce the shipping service q_r.

The technology to produce the shipping service is a function of the number of trips made along the route, $n_r(s)$, and the quantity of goods transported per trip, $\ell\kappa_r$:

$$\underbrace{q_r}_{\text{effective supply}} = z_r \underbrace{n_r(s)\,\ell\kappa_r}_{\text{potential supply}}. \tag{4.3}$$

Here z_r is a firm- and route-specific productivity term, shaped by disruptions from congestion, weather, wave or storm intensity, or piracy. It corresponds to the effect of shipping disruptions on shipping supply in Sections 2 and 3, so a fall in z_r is an increase in shipping disruptions.

Shipping productivity is given by

$$z_r = \frac{x_r}{g(K_r)}, \tag{4.4}$$

where x_r is an exogenous component and $g(K_r)$ is a congestion externality that rises with the market capacity allocated to route r, K_r.

The number of trips made within a period is

$$n_r(s) = A_r s^{\alpha}, \tag{4.5}$$

where A_r is a route-specific efficiency term translating nautical miles per hour into number of trips and $\alpha > 0$ is a parameter. The average speed of ships is the ratio of the distance traveled along route r, d_r, to the time traveled within the period, τ, that is, $s \equiv d_r/\tau$.[19]

Finally, the loading of ships, $\ell \in [0, 1]$, is the fraction of the capacity allocated to the route, κ_r, used to transport goods. If $\ell = 0$, ships travel empty; if $\ell = 1$, they are at full capacity.

Congestion. The congestion factor disrupting route r depends on the aggregate capacity deployed along the route by all N competing shipping firms:

$$g(K_r) = \varepsilon_k \left(\int_0^N \kappa_r(j) dj \right)^{\phi}, \tag{4.6}$$

[19] The distance along route r is exogenous and common to all shipping firms, so increases in speed reduce the time traveled between origin and arrival ports.

where ε_k is a shifter and ϕ is the elasticity of the congestion externality to total capacity traveling along route r. The more capacity traveling along a route, the more congested and disrupted it is.

Shipping costs. The transportation cost per trip is $\overline{p}_n$, assumed common across routes. The longer the distance, the fewer trips a shipping firm makes and the costlier it is to transport goods (more fuel, for example). The total cost of shipping along route r is

$$tc_r = \overline{p}_n (n_r(s))^{\zeta} + \overline{p}_o (\ell \kappa_r)^{\nu}. \tag{4.7}$$

The cost exponents are such that $\zeta, \nu \geq 1$ and $1/\zeta + 1/\nu = 1$. This restriction ensures the total cost function is homogeneous of degree 1 in the shipping service output.[20] The total cost is convex in trips and in goods transported, reflecting diminishing returns to, or rising adjustment costs from, faster sailing (more engine maintenance, more specialized sailors) or heavier loading (the cranes and workers needed to stack containers grow costlier).

Operational decisions. The shipping firm's problem has a two-stage structure. The firm first commits to a cross-route capacity allocation, then chooses speed and loading on each route to maximize per-route profits. The optimal sailing speed and loading, s_r and ℓ_r, solve the firm's cost-minimization problem, Equation (4.7), taking the capacity allocated to the route κ_r as given and subject to the technological constraint, Equation (4.3), and the loading constraint $\ell \in [0, 1]$. When the optimal load is interior, that is $\ell_r < 1$, the solution yields the marginal cost of shipping through route r:

$$mc_r = \frac{g(K_r)}{x_r} \left[\frac{\overline{p}_n}{1/\zeta}\right]^{1/\zeta} \left[\frac{\overline{p}_o}{1/\nu}\right]^{1/\nu}. \tag{4.8}$$

The marginal cost of shipping goods rises with shipping disruptions, congestion, the transportation price, and the price of goods at the origin port. When the ship is fully loaded, it also rises with capacity.[21]

Shipping profits per route. A shipping firm maximizes its profits along route r by choosing the price of its shipping services, p, taking the retailers' demand $\mathtt{y}_r(p)$ as given. The profit maximization problem for route r is

$$\pi_r = \max_p \left(p - mc_r\right) q_r, \tag{4.9}$$

[20] The exponents $1/\zeta$ and $1/\nu$ in the cost function are isomorphic to having the exponents ζ and ν in the production technology.

[21] When the optimal load is at the boundary $\ell_r = 1$, the marginal cost of shipping through route r is $mc_r = \frac{g(K_r)}{x_r}\left[\frac{\overline{p}_n}{1/\zeta}\right]^{1/\zeta}\left[\frac{\overline{p}_o}{1/\nu} + \frac{\mu_r}{\kappa_r^{\nu}}\right]^{1/\nu}$, where $\mu_r > 0$ is the Lagrange multiplier on the load's upper-bound constraint. The multiplier can be written as a function of capacity, number of trips, and input prices: $\mu_r = \zeta \overline{p}_n n_r(s_r)^{\zeta} - \nu \overline{p}_o \kappa_r^{\nu}$.

subject to supply meeting demand, $q_r = \mathtt{y}_r(p)$.

The solution yields a route-specific price, p_r, equal to a markup over marginal cost:

$$p_r = m\, mc_r. \tag{4.10}$$

The markup depends on retailers' price elasticity of demand, $\xi \equiv -(\partial \mathtt{y}_r(p_r)/\partial p_r)(p_r/\mathtt{y}_r(p_r))$, through $m = \xi/(\xi - 1)$. The demand in Equation (4.18) has constant elasticity $\xi = 1/(1-\sigma)$, so the markup is the same on every route,

$$m = \frac{1}{\sigma}. \tag{4.11}$$

Optimal capacity per route. The capacity allocated to each route r is chosen to maximize the shipping firm's aggregate profit, π, the sum of per-route profits net of the cost of deploying ships across routes. That cost is a quadratic capacity-adjustment term priced at $\overline{p}_\kappa$, capturing the expense of repositioning ships, repurposing vessel types, and reshuffling crews across routes. Aggregate profit is

$$\pi = \max_{\{\kappa_r\}_{r\in\mathcal{R}}} \left\{ \sum_r \pi_r - \overline{p}_\kappa \sum_r \frac{\kappa_r^2}{2} \right\}, \tag{4.12}$$

subject to the capacity constraint (4.2). The optimal capacity per route follows from substituting the Lagrange multiplier on the capacity constraint into the firm's first-order condition for problem (4.12). The firm does not internalize the effect of its capacity choice on congestion, and hence on output.

The optimal capacity per route equates the marginal benefit of additional capacity to its marginal cost. Adding capacity on one route raises that route's profit per ton traveled relative to the firm's average, but it also raises the cost of deploying capacity there relative to the average. The more congested a route, the lower its profit per ton traveled, and the more likely the firm is to reallocate capacity to other routes. The first-order condition, when the optimal loading is interior ($\ell_r < 1$), is

$$\underbrace{\frac{(p_r - mc_r)\, x_r n_r(s_r^\star)\ell_r^\star}{g(K_r)}}_{\text{profit per ton traveled along route } r} - \underbrace{\frac{1}{|\mathcal{R}|}\sum_h \frac{(p_h - mc_h)\, x_h n_h(s_h^\star)\ell_h^\star}{g(K_h)}}_{\text{average profit per ton traveled}} = \overline{p}_\kappa \left[\kappa_r - \underbrace{\frac{1}{|\mathcal{R}|}(\kappa - \overline{\kappa})}_{\text{average capacity per route}} \right], \tag{4.13}$$

where $|\mathcal{R}|$ is the number of routes (6), and speed and loading are at their optimum. The left-hand side is the marginal benefit of reallocating capacity to route r, its profit per ton traveled relative to the firm's average. The right-hand side is the marginal cost, the cost of deployment to route r relative to the average.

When $\ell_r = 1$, the firm faces additional marginal cost pressure from the loading constraint. With a fully loaded ship, adding capacity lowers the firm's marginal cost of shipping along route r relative to its average cost, since the firm can now fully load a larger ship, raising profit on route r relative to the others.[22]

Entrants in the shipping market. A firm that enters earns the expected profit from operating in the market, $\left(\int_0^N \pi(j)dj\right)/N$, while staying out delivers zero. The free-entry condition determines the number of shipping firms, N.

Importers. A measure $\mathcal{I}$ of identical importers sources goods from different regions and routes. They buy manufactured goods from a shipping firm j operating route r at the price $p_r(j)$ and resell them to consumers at the final price p_o for $o \in \mathcal{O}$. The final price depends only on the origin of the goods, since consumers are indifferent to the arrival port or route by which they arrive.

The output of importers sourcing goods from route r uses a decreasing-returns-to-scale technology that aggregates all services produced by shipping firms operating along the route, with elasticity of substitution $1/(1-\sigma)$:

$$y_r = \left[\chi_r \left(\int_0^N y_r(j)^\sigma dj\right)^{1/\sigma}\right]^\theta, \tag{4.14}$$

where χ_r is the productivity of importers specializing in manufactured goods delivered along route r, and $\theta \in (0,1)$ governs returns to scale from dealing with shipping firms, common across routes.

Importers' profit per route. Importers' profit from each route r is

$$\Pi_r = \max_{\{y_r(j)\}} \left\{ p_o \chi_r^\theta \left(\int_0^N y_r(j)^\sigma dj\right)^{\theta/\sigma} - \int_0^N p_r(j) y_r(j) dj - f \right\}, \tag{4.15}$$

where $f > 0$ is the fixed cost of operating in the retail sector. Since $\theta < 1$, importers can make profits on some routes.

Optimal sourcing decision. We make importers' sourcing decision endogenous, giving shipping disruptions both an intensive and an extensive margin. Disruptions then alter both the quantity importers demand and their distribution across routes. We introduce idiosyncratic taste shocks for goods sourced from different routes, so importers choose the route r they

[22] The first-order condition when the optimal load along route r is at the upper bound ($\ell_r = 1$) is $\frac{(p_r - mc_r)x_r n_r(s_r)\ell_r}{g(K_r)} - \frac{1}{|\mathcal{R}|}\sum_h \frac{(p_h - mc_h)x_h n_h(s_h)\ell_h}{g(K_h)} = \overline{p}_\kappa \left[\kappa_r - \frac{1}{|\mathcal{R}|}(\kappa - \overline{\kappa})\right] + \frac{\partial mc_r}{\partial \kappa_r} q_r - \frac{1}{|\mathcal{R}|}\sum_h \frac{\partial mc_h}{\partial \kappa_h} q_h$, where $\partial mc_h/\partial \kappa_h = -(mc_h/\kappa_h)\,\mu_h/\left[\nu \overline{p}_o \kappa_h^\nu + \mu_h\right] < 0$ when $\ell_h = 1$.

source from according to the discrete choice problem

$$\Pi = \max_{r \in \mathcal{R}} \{\Pi_r + \epsilon_r\}, \tag{4.16}$$

where ϵ_r are taste shocks for goods from route r, assumed mean-zero Type I extreme value with scale parameter $\lambda > 0$.

The optimal sourcing decision for goods from route r is governed by the following expression

$$o_r = \frac{e^{\lambda \Pi_r}}{\sum_{x \in \mathcal{R}} e^{\lambda \Pi_x}}. \tag{4.17}$$

More profitable routes are more likely to have more importers.

Importers' demand for shipping services. Total demand for goods sourced from route r and carried by firm j, $\mathtt{y}_r(j)$, is the per-importer quantity $y_r(j)$ times the mass of importers sourcing route r, $o_r\mathcal{I}$:

$$\mathtt{y}_r(j) \equiv y_r(j) o_r \mathcal{I} = \left[\frac{\theta \chi_r^{\sigma} p_o y_r^{(1-\sigma/\theta)}}{p_r(j)} \right]^{1/(1-\sigma)} o_r \mathcal{I}, \tag{4.18}$$

where the final expression replaces $y_r(j)$ with the solution to the importer's problem (4.15).

Entrants in the retail market. A potential importer that enters earns the expected profit from sourcing the best route after taste shocks realize, $\frac{1}{\lambda} \ln \sum_{r \in \mathcal{R}} e^{\lambda \Pi_r}$; one that stays out earns zero. Free entry drives this to zero and determines the measure of importers, $\mathcal{I}$.

Consumers. A unit measure of consumers each holds one unit of time, supplied inelastically at wage w. They also receive profits Λ from the retail and shipping firms they own. Consumers buy domestic goods d at price p_d and imports c_o from Asia, Europe, the Middle East, and South America ($o \in \mathcal{O}$) at price p_o. Thus, the budget constraint of a consumer is:

$$\sum_{o \in \mathcal{O}} p_o c_o + p_d d = w + \Lambda. \tag{4.19}$$

Goods from different regions are imperfect substitutes, with elasticity of substitution $1/(1-\rho)$. The imported bundle is

$$c = \left(\sum_{o \in \mathcal{O}} \gamma_o c_o^{\rho} \right)^{1/\rho}, \tag{4.20}$$

where γ_o is an origin-specific utility weight with $\sum_{o \in \mathcal{O}} \gamma_o = 1$. Goods from the same region sourced via different routes are perfect substitutes.

A consumer derives utility from domestic goods and the imported bundle, with elasticity of substitution $1/(1-\varrho)$. The consumer solves

$$u = \max_{c_A, c_E, c_M, c_S, d} \left[\gamma_d d^{\varrho} + (1-\gamma_d) c^{\varrho}\right]^{1/\varrho}, \tag{4.21}$$

subject to the budget constraint (4.19) and the imported bundle (4.20).

4.2. *Equilibrium*

Definition (**EQUILIBRIUM**). An equilibrium is a solution for: (1) the domestic goods price and domestic labor demand, $\{p_d, l_d\}$; (2) each shipping firm's profit, output, trips, sailing speed, price, load, and capacity along each route $r \in \mathcal{R}$, $\{\pi_r(j), q_r(j), n_r(j), s_r(j), p_r(j), \ell_r(j), \kappa_r(j)\}$, and total profits $\pi(j)$, for all firms $j \in [0, N]$; (3) importers' demand for the services of each shipping firm j, $\mathrm{y}_r(j)$, output y_r, profits Π_r, and sourcing decision o_r for each route $r \in \mathcal{R}$; (4) consumers' demand for domestic goods d and imports c_o from each region $o \in \mathcal{O}$; (5) the wage w; (6) retail prices p_o for each region $o \in \mathcal{O}$; (7) the number of shipping firms N; (8) the number of importers $\mathcal{I}$; (9) aggregate profits Λ. These satisfy:

1. The domestic firms' problem satisfies (4.1), and labor demand is
$$l_d = 1 - \frac{1}{w} \int_0^N \sum_{r \in \mathcal{R}} \left\{ \zeta \overline{p}_n n_r(j)^{\zeta} - \frac{\mu_r(j)}{\nu} + \overline{p}_\kappa \frac{\kappa_r(j)^2}{2} \right\} dj.$$
2. Given the transport price $\overline{p}_n$ and origin-port goods prices $\overline{p}_o$, each shipping firm j maximizes profits $\pi_r(j)$ per (4.9), yielding $\{q_r(j), n_r(j), s_r(j), p_r(j), \ell_r(j)\}$ along each route r that satisfy $\ell_r(j) = \min\left\{1, \left(\frac{\zeta}{\nu}\frac{\overline{p}_n}{\overline{p}_o}\right)^{1/\nu} n_r(j)^{\zeta/\nu}/\kappa_r(j)\right\}$, (4.3), (4.5), (4.8), (4.10), and (4.11). Total profits $\pi(j)$ and capacity per route $\kappa_r(j)$ satisfy (4.12) and (4.13).
3. Given shipping prices $p_r(j)$ and retail prices p_o, importers' allocations $\{y_r, \Pi_r, o_r\}$ and $\{\mathrm{y}_r(j)\}_0^N$ satisfy (4.14), (4.15), (4.17), and (4.18) for each route $r \in \mathcal{R}$.
4. Given prices p_d and p_o, the wage w, and profits Λ, consumers' demands for d and c_o, $o \in \mathcal{O}$, maximize utility (4.21) subject to the budget constraint (4.19) and the imported bundle (4.20).
5. The shipping-importer market clears on each route r:
$$\int_0^N q_r(j) dj = o_r \mathcal{I} \left[\theta \chi_r^{\sigma} p_o y_r^{(1-\sigma/\theta)}\right]^{1/(1-\sigma)} \int_0^N p_r(j)^{1/(\sigma-1)} dj.$$

6. The importer-consumer market clears: $c_A = (o_{AEP}y_{AEP} + o_{AES}y_{AES} + o_{AW}y_{AW})\mathcal{I}$ for Asian goods and $c_j = o_{jE}y_{jE}\mathcal{I}$ for regions $j \in \{E, M, S\}$, determining retail prices p_o for each $o \in \mathcal{O}$.
7. Free entry in shipping holds, $\int_0^N \pi(j)dj = 0$, determining N.
8. Free entry in retail holds, $\frac{1}{\lambda}\ln\sum_{r\in\mathcal{R}} e^{\lambda\Pi_r} = 0$, determining $\mathcal{I}$.
9. Retail entry costs are rebated to consumers, $f\mathcal{I} = \Lambda$.

4.3. *Unpacking the impact of shipping disruptions*

Akin to Hulten (1978)'s theorem (see Baqaee and Farhi, 2019, 2020), Proposition 4.1 gives closed-form expressions for how shipping disruptions along a route transmit to aggregate output and consumer welfare. The impact depends on the route's importance in aggregate output (its Domar weight), with amplifying or dampening effects through the retail sector via importers' output and sourcing decisions. Because shipping firms reallocate capacity across routes, spillovers across routes can soften the blow. The rest operates through general equilibrium effects on the incentives to enter the retail and shipping markets.

Let $X_r \equiv \left[\int_0^N x_r(j)^{\sigma/(1-\sigma)}dj\right]^{(1-\sigma)/\sigma}$ denote aggregate route-r shipping productivity net of congestion, which bundles the exogenous primitives $x_r(j)$ across the endogenous measure of shipping firms N. Although the $x_r(j)$ are exogenous, X_r is endogenous because N adjusts in equilibrium. A fall in X_r, driven by a deterioration in $x_r(j)$, is an adverse shipping disruption along route r. Our measured route-r disruptions, which include the endogenous effect of congestion, are $Z_r \equiv X_r/g(K_r)$, with $Z_r \equiv \left[\int_0^N z_r(j)^{\sigma/(1-\sigma)}dj\right]^{(1-\sigma)/\sigma}$. The proposition below can be stated equivalently in terms of X_r or Z_r.

PROPOSITION 4.1: (IMPACT OF SHIPPING DISRUPTIONS ON REAL AGGREGATE OUTPUT) The impact of route-r shipping disruptions on real aggregate output Y is

$$\frac{\partial Y}{\partial X_r}\frac{X_r}{Y} = \sum_{h\in\mathcal{R}} \underbrace{\left(\begin{smallmatrix}\text{Route } h\text{'s share in}\\ \text{aggregate output}\end{smallmatrix}\right)}_{\text{Domar weight}} \times \left(\underbrace{\frac{\partial y_h}{\partial X_r}\frac{X_r}{y_h}}_{\text{intensive margin}} + \underbrace{\frac{\partial o_h}{\partial X_r}\frac{X_r}{o_h}}_{\text{sourcing reallocation}}\right)$$
$$+ \left(\begin{smallmatrix}\text{Import share in}\\ \text{aggregate output}\end{smallmatrix}\right) \times \underbrace{\left(\frac{\partial \mathcal{I}}{\partial X_r}\frac{X_r}{\mathcal{I}}\right)}_{\text{retail entry}} + \left(\begin{smallmatrix}\text{Domestic share in}\\ \text{aggregate output}\end{smallmatrix}\right) \times \underbrace{\left(\frac{\partial d}{\partial X_r}\frac{X_r}{d}\right)}_{\text{domestic spillovers}},$$

where route h's share in aggregate output is $p_{o(h)}y_h o_h \mathcal{I}/(w+\Lambda)$, with $o(h)$ the origin region of route h and $p_{o(h)}$ the retail price of goods from that origin. The first-order impact of the congestion externality $g(K_r)$, or of total disruptions Z_r, on real output follows.

PROOF: See Appendix B.1. *Q.E.D.*

The proposition has a few important implications. Hulten (1978)'s theorem summarizes the first-order impact of a route-r productivity shock on real output by route r's Domar weight alone, since the envelope theorem eliminates every reallocation term once marginal value products are equalized. That benchmark fails here.

First, a shock to route r enters the term of *every* route h in the sum, not only its own. Disruptions on one route propagate to all others because shipping firms reallocate a common pool of capacity across the six routes. Were capacity non-transferable, the cross-route terms ($h \neq r$) would vanish and the impact would collapse to route r's own Domar-weighted effect. These capacity linkages give the decomposition its network structure.

Second, the equilibrium is inefficient. Imports carry a markup over marginal cost—compounding the shipping firms' markup ($1/\sigma$) and the importers' markup ($1/\theta$)—so reallocation across these heterogeneous wedges changes welfare at the margin. The route-specific congestion externality, $g(K_r)$, is not internalized by individual shipping firms, thereby making cross-route reallocation welfare-relevant. Without it, the cross-route reallocation terms would cancel to first order as the retail markup is identical across routes.

Third, importers convert shipped goods into retail output with diminishing returns. Thus, the gains from absorbing rerouted capacity are bounded, and additional demand is met partly through the entry of new importers (the retail entry term) rather than the expansion of existing ones. Together, these forces imply that route r's Domar weight is *not* a sufficient statistic for the welfare impact of a disruption.

These channels also distinguish our benchmark from canonical quantitative trade models. Arkolakis et al. (2012) show that, across a class of models, the welfare effect of a change in trade frictions is captured by two sufficient statistics, the domestic expenditure share and the trade elasticity. The result relies on iceberg trade costs and an efficient economy. Melitz and Redding (2015) show that its sufficiency breaks once production linkages are present, even in efficient models. Our framework departs on both counts. Trade costs are not exogenous. They are the equilibrium price of a shipping service whose capacity is reallocated across a shared, congestible network, so a route shock has spillovers that a single-trade elasticity cannot capture. Second, the equilibrium is inefficient, the joint result of congestion externalities, markups, and the sourcing externality. The domestic share is not a sufficient statistic, since the same change in the import share can map to different welfare changes depending on which margin adjusts.

Propositions B.1 and B.2 in Appendix B show how shipping disruptions affect importers' output and sourcing decisions in partial equilibrium. Section 6 uses the model to compute the route-specific Domar weights and the elasticity of importers' output and sourcing to a shipping productivity shock along each route, taking their general equilibrium effects into account.

4.4. *The constrained social planner's problem*

The decentralized equilibrium has three sources of inefficiency. First, the route-specific congestion externality $g(K_r)$ is not internalized by individual shipping firms when they allocate capacity. Second, shipping firms have monopoly power and charge a markup $m = 1/\sigma$ over marginal cost. Third, and relatedly, decreasing returns in importers' technology ($\theta < 1$) together with idiosyncratic sourcing tastes generate retail profits that shape entry and sourcing incentives across routes, which shipping firms ignore when setting prices. These forces distort the efficient allocation.

We now study the efficient allocation chosen by a constrained social planner and compare it to the decentralized equilibrium. The planner chooses imported goods from each region o, $\{c_o\}_o$, labor in domestic production, l_d, and, for each route r, the aggregate shipping capacity, loading, average speed, social price of shipping, and importers' demand, $\{K_r, \ell_r, s_r, v_r^{\text{social}}, Y_r^{\text{input}}\}_r$, to maximize consumer welfare

$$\max_{\substack{\{c_o\}_{o\in\mathcal{O}}, l_d, \\ \{K_r,\ell_r,s_r,v_r^{\text{social}},Y_r^{\text{input}}\}_{r\in\mathcal{R}}}} \mathbb{E}_{\boldsymbol{\epsilon}}[u] \quad \text{with } d = z_d l_d. \tag{4.22}$$

The planner respects the aggregate capacity constraint, $\sum_{r\in\mathcal{R}} K_r + \overline{K} = K$, the free-entry conditions in retail and shipping that determine the masses of importers and shipping firms, $\mathcal{I}$ and N, and the importers' taste shocks across routes. As in the decentralized equilibrium, the planner takes as given the disruption shocks, domestic productivity, taste shocks, the remaining efficiency terms, and the transportation, capacity-adjustment, and foreign-goods prices. The planner internalizes the congestion externality and how importers reallocate across routes. Appendix B.3 describes the problem.

There are two notable differences in how the planner allocates capacity across routes. First, the first-order condition yields an expression like Equation (4.13), summed over all N shipping firms. Because the planner internalizes the congestion externality, the marginal cost of shipping along route r rises by a factor of ϕ, which lowers the benefit of reallocating ships across routes. Second, to cover the cost of redeploying ships across routes, the planner sets a social price of shipping on each route that includes a markup. This markup does not depend on the elasticity of substitution between shipping services, σ. The relevant elasticity is now θ, the elasticity of retail output with respect to total import demand. Because the planner also internalizes how shipping prices affect importers' sourcing decisions, the shipping-service markup includes a further term for the sourcing response.

5. TAKING THE MODEL TO DATA

We match the model to U.S. data to capture the shipping trends in Sections 2 and 3.[23] The strategy has two steps. We calibrate to a pre-disruption economy using February 2016 data, then simulate from March 2016 through March 2025.

Parameters. The framework has 42 parameters: 7 consumer preference parameters, $\{\rho, \varrho, \gamma_d, \gamma_o\}$ for $o \in \mathcal{O}$; 10 governing the importers' problem, $\{\chi_r, \theta, \sigma, f, \lambda\}$ for $r \in \mathcal{R}$; 18 for the shipping market, $\{x_r, A_r, \varepsilon_k, \phi, \alpha, \zeta, \nu, \overline{\kappa}\}$ for $r \in \mathcal{R}$; the productivity of domestic producers, z_d; and 6 exogenous prices (capacity redeployment, transportation, and foreign goods), $\{\overline{p}_\kappa, \overline{p}_n, \overline{p}_o\}$ for $o \in \mathcal{O}$.

Our calibration strategy splits these parameters into three groups. The first consists of parameters that either have direct empirical counterparts or can be normalized. The second is backed out from the equilibrium conditions to match specific data targets exactly. The rest are calibrated jointly to minimize the distance between model-implied moments and their empirical targets. Table 5.1 summarizes the full set of estimated parameters. Table 5.2 contrasts the targeted model moments with the data as of February 2016.

5.1. *Exogenous and externally estimated parameters*

Consumer elasticity of substitution. A large literature estimates trade elasticities of substitution. A robust finding is that the elasticity across goods from different countries exceeds the one between domestic and foreign goods: consumers substitute more readily among import sources than away from domestic varieties. Feenstra et al. (2018), using U.S. data from 1992 to 2007, find a "micro-Armington" elasticity (across foreign goods) of 3.22 to 4.05 and a "macro-Armington" elasticity (domestic versus foreign) near 2 for most sectors. We set the substitution parameter between imported goods to $\rho = 0.75$ (elasticity of 4) and between foreign and domestic goods to $\varrho = 0.5$ (elasticity of 2).

Shipping technology and costs. We estimate α, the elasticity of the number of trips to sailing speed, directly from the data. Using satellite-based AIS data from January 2016 through March 2025, we find that intercontinental voyages often span much of a calendar month, so observed monthly trip counts cluster at an integer boundary. To recover α without censoring bias, we reconstruct the average number of trips per ship from the DWT-weighted average trip duration (in hours) along route r in month t,

$$\overline{\texttt{Number of Trips}}_{r,t} = \frac{730}{\overline{\texttt{Trip Duration}}_{r,t}},$$

[23] Weekly data are aggregated to monthly frequency.

where 730 is the approximate number of hours in a month and the weighted average trip duration is

$$\overline{\texttt{Trip Duration}}_{r,t} = \sum_{i \in \boldsymbol{\mathcal{V}}_t} \left(\frac{\mathbf{1}_{i,r,t} \times \texttt{DWT}_i}{\sum_{i \in \boldsymbol{\mathcal{V}}_t} \mathbf{1}_{i,r,t} \times \texttt{DWT}_i} \right) \times \texttt{Trip Duration}_{i,r,t},$$

and $\texttt{Trip Duration}_{i,r,t}$ is the average number of hours vessel i spends on a trip on route r in month t. The DWT-weighted average sailing speed follows Equation (2.2) at monthly frequency.

To recover α, we regress the average number of trips on average sailing speed in logs. Table C.1 in Appendix C.1 reports the full results, comparing OLS with weighted least squares (WLS) specifications that use total route DWT as analytical weights to dampen idiosyncratic monthly noise. For the baseline we set $\alpha = 0.663$, from the preferred WLS specification with route, year, and month fixed effects.

Shipping costs are increasing and strictly convex in both the number of trips and the quantity transported per trip. Lacking granular firm-level data to estimate these elasticities, we impose a quadratic cost structure and set the elasticity to the number of trips at $\zeta = 2$. The constant-returns restriction $1/\zeta + 1/\nu = 1$ then pins down the elasticity to the transported quantity at $\nu = 2$.

Congestion. We estimate the congestion exponent ϕ as the elasticity of total congestion time to the total number of port calls. Using vessel-level AIS data and the IMA-DBSCAN algorithm from Section 2, we build a monthly panel of total port calls and total congestion times for major global container ports from January 2016 through March 2025. We compute the total hours container ships wait in a port's anchorage before berthing, then regress this on the total number of port calls in logs. Table C.2 in Appendix C.1 reports the results. The preferred WLS specification, weighting by total port calls and controlling for port, year, and month fixed effects, yields a precisely estimated elasticity of 1.296. We set $\phi = 1.296$ and normalize the congestion shifter ε_k to 1.

Importer technology and sourcing. We normalize importer productivities to one on most routes, except those from Asia. Because goods from the same origin are perfect substitutes, the productivities of two of the three Asian routes must be calibrated internally to match observed shipping supply shares. We jointly estimate χ_{AES} and χ_{AW} (more below) and normalize $\chi_{AEP} = \chi_{EE} = \chi_{ME} = \chi_{SE} = 1$.

The price elasticity of importers' demand for shipping services is $\xi_r = 1/(1-\sigma)$, implying a shipping-firm markup of $1/\sigma$. We target a shipping markup of 25%, which pins down $\sigma = 0.8$. The marginal cost of importers conditional on sourcing a route is θp_o, yielding a markup of $1/\theta$.

We set $\theta = 0.8$ to match a retail markup of 25%. Finally, we normalize the scale parameter of the mean-zero Gumbel sourcing shock to $\lambda = 1$. Lower values of λ raise the variance of importers' idiosyncratic taste shocks and give a more dispersed sourcing distribution.

Domestic producers. We normalize the productivity of domestic producers to $z_d = 1$, so the price of domestic goods equals the aggregate wage. With the wage as numeraire, $p_d = 1$.

TABLE 5.1

PARAMETER VALUES

Parameter	Description	Value	Identification
Consumer preferences			
ϱ	Elast. of sub. between imported and domestic goods	0.500	Feenstra et al. (2018)
ρ	Elast. of sub. among imported goods	0.750	Feenstra et al. (2018)
γ_d	Cons. weight, domestic goods	0.955	Total import share
γ_o	Cons. weight, Asia, Europe, Middle East, South America	0.368, 0.359 0.093, 0.180	Regional import shares
Retail market			
χ_r	Importer prod., Asia to East Coast via Panama/Suez/to West Coast	1.000, 1.082, 1.229	Potential shipping supply,
	Europe, Middle East, South America to East Coast	1.000, 1.000, 1.000	normalization
θ	Returns to scale	0.800	Retail markup
σ	Elast. of sub. between shipped goods	0.800	Shipping markup
f	Entry cost in retail market	0.024	Number of retail firms
λ	Scale parameter in optimal shipping route	1.000	Normalization
Shipping market			
x_r	Route prod., Asia to East Coast via Panama/Suez/to West Coast	2.755, 3.487, 5.632	Shipping disruptions
	Europe, Middle East, South America to East Coast	3.252, 1.557, 2.101	
A_r	Speed eff., Asia to East Coast via Panama/Suez/to West Coast	0.300, 0.382, 0.563	Average speed
	Europe, Middle East, South America to East Coast	0.406, 0.107, 0.262	
ε_k	Congestion shifter	1.000	Normalization
ϕ	Congestion exponent	1.296	Congestion time
α	Exponent on speed	0.663	Elast. trip number wrt speed
ζ	Exponent on number of trips	2.000	Exogenous
ν	Exponent on quantity transported	2.000	
$\overline{\kappa}$	Idle capacity	0.569	Non-US shipping supply
$\overline{p}_\kappa$	Redeployment price	0.028	Number of shipping firms
$\overline{p}_n$	Transportation price ($\times 100$)	0.004	Average number of trips
Producers			
z_d	Productivity of domestic firms	1.000	Normalization
$\overline{p}_o$	Origin prices, Asia, Europe, Middle East, South America	0.058, 0.126 0.038, 0.048	Potential shipping supply

5.2. *Internally calibrated parameters*

Import shares. The consumption weights on domestic and imported goods, $\{\gamma_d, \gamma_A, \gamma_E, \gamma_M, \gamma_S\}$, help match the total goods import share of output from the BEA and each region's share of U.S. merchandise trade from the Census Bureau, as of February 2016. Regional import shares are the ratio of containerized vessel values from a region to the total across all four origins.[24] In February 2016, the aggregate import share of GDP was 11.8%, with 8.7% from Asia, 2.2% from Europe, 0.2% from the Middle East, and 0.8% from South America.

[24]The BEA data are available here and the Census Bureau trade data here. Countries are assigned to regions following the World Bank's classification (here).

Given equilibrium prices and the consumer elasticities, we back out γ_d and $\{\gamma_o\}_{o\in\mathcal{O}}$ to match these four targets exactly, subject to $\sum_{o\in\mathcal{O}}\gamma_o = 1$. Solving the consumer's problem in (4.21) gives the expenditure share on domestic goods, $\omega_d \equiv p_d d/(w+\Lambda)$,

$$\omega_d = \gamma_d^{1/(1-\varrho)}\left(\frac{p_d}{P^{\text{total}}}\right)^{\varrho/(\varrho-1)},$$

and the share on imports from region $o \in \mathcal{O}$, $\omega_o \equiv p_o c_o/(w+\Lambda)$,

$$\omega_o = \gamma_o^{1/(1-\rho)}\left(\frac{p_o}{P^{\text{imp}}}\right)^{\rho/(\rho-1)}(1-\omega_d).$$

Here $P^{\text{total}} \equiv \left[\gamma_d^{1/(1-\varrho)}p_d^{\varrho/(\varrho-1)} + (1-\gamma_d)^{1/(1-\varrho)}\left(P^{\text{imp}}\right)^{\varrho/(\varrho-1)}\right]^{(\varrho-1)/\varrho}$ is the economy-wide ideal price index, and $P^{\text{imp}} \equiv \left(\sum_{o\in\mathcal{O}}\gamma_o^{1/(1-\rho)}p_o^{\rho/(\rho-1)}\right)^{(\rho-1)/\rho}$ the ideal price index for imports.

Shipping disruptions. Route-specific shipping efficiency, z_r, maps to the ratio of effective to potential shipping supply from Section 3 and Figure 3.5b. Given the endogenous congestion externality $g(K_r)$, we back out the exogenous component of shipping efficiency, $\{x_r\}_{r\in\mathcal{R}}$, to match the empirical ratio exactly.

Potential shipping capacity. The origin prices $\{\overline{p}_A, \overline{p}_E, \overline{p}_M, \overline{p}_S\}$ and the retail productivities for Asia to the East Coast via Suez and to the West Coast, χ_{AES} and χ_{AW}, help match potential shipping capacity (in DWT) by route as of February 2016 (see Figure 2.3b). The theoretical counterpart is $\int_0^N n_r(j)\ell_r(j)\kappa_r(j)dj$. Given the speed and cost exponents (α, ν, ζ), speed efficiencies (A_r), sailing speeds (s_r), and the mass of shipping firms (N), the origin prices and retail productivities exactly match the observed route-specific tonnages.

Average sailing speeds. We identify the speed efficiency shifters $\{A_r\}_{r\in\mathcal{R}}$ from the average sailing speed of vessels on each route, derived from Equation (2.2) using February 2016 satellite data (Figure 3.4a). Given the targeted speed s_r and the optimal number of trips n_r per route, A_r is uniquely identified.

Average number of trips. The price per trip, $\overline{p}_n$, makes the model's average number of trips per firm per route per month match the AIS data. The theoretical average is

$$\overline{n} = \frac{\sum_{r\in\mathcal{R}}\int_0^N n_r(j)dj}{N|\mathcal{R}|}.$$

In February 2016, a vessel completed 2.021 U.S.-bound trips per route per month on average, with trips ranging from 7 to 26 days.

Idle capacity. Idle capacity, $\overline{\kappa}$, matches the fraction of global capacity allocated to U.S.-bound routes. In the model this share is

$$\varpi_{US} = \frac{\int_0^N \sum_{r \in \mathcal{R}} \ell_r(j)\kappa_r(j)dj}{\int_0^N \sum_{r \in \mathcal{R}} \ell_r(j)\kappa_r(j)dj + N\psi\overline{\kappa}},$$

where $\psi = 0.8$ is an assumed load-factor adjustment for non-U.S.-bound ships. We use AIS data to track the global fleet and define the target as the ratio of U.S.-bound potential capacity (inbound and outbound) to total global potential capacity. In February 2016, 59.8% of the world's DWT was allocated to non-U.S.-bound routes and the rest to U.S.-bound routes.

Number of importers and shipping firms. The retail entry cost, f, normalizes the measure of importers, $\mathcal{I}$, to one. The capacity redeployment price, $\overline{p}_\kappa$, helps match the average number of shipping firms, N, across U.S.-bound routes. In February 2016, the average was 33 firms.

5.3. *Tracing the evolution of U.S.-bound shipping between 2016 and 2025*

We simulate the model to trace our measure of shipping disruptions, import shares across regions, route-specific potential shipping capacity in DWT, world capacity, average sailing speeds, and the number of firms from March 2016 to March 2025. We solve for the exogenous shipping disruptions, speed efficiencies, idle capacity, redeployment price, retail productivities, retail entry cost, and origin prices, $\left\{\{x_{r,t}\}_{r\in\mathcal{R}}, \{A_{r,t}\}_{r\in\mathcal{R}}, \overline{\kappa}_t, \overline{p}_{\kappa,t}, \{\chi_{r,t}\}_{r\in\mathcal{R}}, f_t, \{\overline{p}_{o,t}\}_{o\in\mathcal{O}}\right\}$. The algorithm finds the values that minimize the distance between model-implied aggregates and the targeted data at each date from March 2016 to March 2025. All other parameters are held constant over time. These simulations are the baseline for the counterfactual experiments in Sections 6 and 7.

Figure C.1 in Appendix C.1 presents the targeted time series, Figure C.2 the exogenous variables needed to match the data, and Figure C.3 other aggregates of interest.

The model matches the targeted series exactly. The congestion externality, $g(K_r)$, rises markedly on most routes from summer 2020 to the end of 2022, in line with the fall in measured shipping productivity, z_r (Panels C.1a, C.2a, and C.3a). The rise in congestion was driven by a fall in idle capacity, $\overline{\kappa}$, and so an increase in U.S.-bound potential capacity, K_r (Panels C.1b, C.2b, and C.3b). With the fall in the capacity redeployment price, $\overline{p}_\kappa$, these forces help explain the rise in the number of shipping firms in 2021–2022, N, and in world capacity, K (Panels C.1c, C.1d, and C.2c).

The 2022 shipping disruptions added about 3 days of delays along Asian routes, slowed average sailing speeds, s_r, and raised loading factors, ℓ_r, for container ships departing Asia

TABLE 5.2

TARGETED MOMENTS: DATA VS. MODEL (FEBRUARY 2016)

Moment	Model	Data	Source
Import shares of output, ω_o			
Total	0.118	0.118	BEA
Asia	0.087	0.087	Census
Europe	0.022	0.022	Census
Middle East	0.002	0.002	Census
South America	0.008	0.008	Census
Shipping efficiency (effective/potential capacity), z_r			
Asia to East Coast via Panama Canal	0.849	0.849	AIS
Asia to East Coast via Suez Canal	0.882	0.882	AIS
Asia to West Coast	0.953	0.953	AIS
Europe to East Coast	0.823	0.823	AIS
Middle East to East Coast	0.821	0.821	AIS
South America to East Coast	0.797	0.797	AIS
Potential shipping capacity (in DWT), $N\,q_r\,/\,z_r$			
Total	24.143	24.143	AIS
Asia to East Coast via Panama Canal	2.921	2.921	AIS
Asia to East Coast via Suez Canal	4.714	4.714	AIS
Asia to West Coast	11.056	11.056	AIS
Europe to East Coast	3.202	3.202	AIS
Middle East to East Coast	0.478	0.478	AIS
South America to East Coast	1.773	1.773	AIS
Sailing speeds, s_r			
Asia to East Coast via Panama Canal	15.433	15.433	AIS
Asia to East Coast via Suez Canal	15.325	15.325	AIS
Asia to West Coast	16.264	16.264	AIS
Europe to East Coast	14.018	14.018	AIS
Middle East to East Coast	15.824	15.824	AIS
South America to East Coast	12.149	12.149	AIS
Other targets			
Average number of trips	2.021	2.021	AIS
Non-U.S.-bound capacity (% of world capacity)	0.598	0.598	AIS
Number of shipping firms	33.0	33.0	AIS
Number of importers	1.0	1.0	Normalization

relative to other routes. They did not, however, much reduce the number of trips per ship, n_r. Speed efficiency and origin prices, A_r and $\overline{p}_o$, helped sustain these trends (Panels C.1e, C.2d, C.2e, C.3c, C.3d, C.3e, and C.3f).

Retail productivity and entry costs, χ_r and f, fell during the COVID-19 pandemic and recovered quickly afterward, which helps explain the changes in the import share of goods from Asia (Panels C.1f, C.2f, C.2g). The fall in the Asian import share is sustained by higher retail prices, lower Asian route shares of output, and a reallocation of retailers' sourcing (Panels C.3g, C.3h, and C.3i).

6. THE MACROECONOMIC IMPACT OF SHIPPING DISRUPTIONS

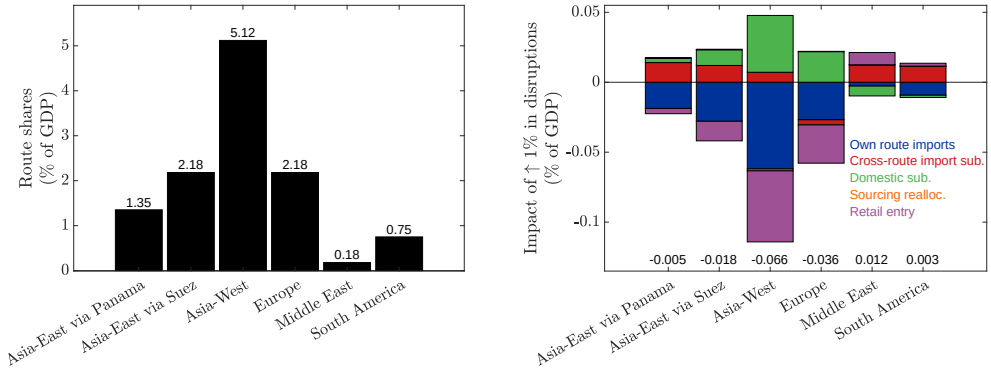
Using the calibrated model, we revisit Proposition 4.1 and quantify the macroeconomic effects of route-specific shipping disruptions. We then focus on two specific disruption events and study their macroeconomic effects. The first event is the unprecedented global port congestion

at the outset of the COVID-19 pandemic in late 2021 (Bai et al., 2024), which disproportionately affected the Asia-West Coast route. The second event is the rerouting away from the Suez Canal following Houthi attacks in the Red Sea in early 2024, which significantly affected the Asia-East Coast route via the Suez Canal and the Middle East-East Coast route. In both scenarios, counterfactual economies without the measured disruptions are simulated and compared to our baseline economy. Comparing the counterfactual and baseline economies isolates the macroeconomic effects of each disruption.

6.1. *Revisiting Proposition 4.1 on the impact of shipping disruptions on aggregate output*

We use the model calibrated to February 2016 data to compute the elasticity of aggregate output with respect to a route-specific shipping-efficiency shock at the pre-disruption equilibrium, accounting for general equilibrium effects. Figure 6.1a shows each route's share in U.S. aggregate output (akin to the route's Domar weight) as of February 2016. For instance, the Asia-West Coast route accounted for nearly 5% of aggregate output, while the Asia-East Coast route via the Suez Canal and the Europe-East Coast route represent about 2% of aggregate output each. The sum of the route weights corresponds to the total import share.

FIGURE 6.1.—The impact of shipping disruptions on aggregate output



(a) Route shares in aggregate output

(b) Elasticity of real output to shipping disruptions

Note: Panel (a) shows each route's share in aggregate output (equivalent to its Domar weight). Panel (b) shows the elasticity of aggregate real output to shipping disruptions, $-\frac{\partial Y}{\partial X_r}\frac{X_r}{Y}$, taking into account the general equilibrium effects, computed with automatic differentiation.

Figure 6.1b shows the elasticity of aggregate output to shipping efficiency shocks along each of the six routes, computed using automatic differentiation.[25] A 1% fall in route r's aggregate

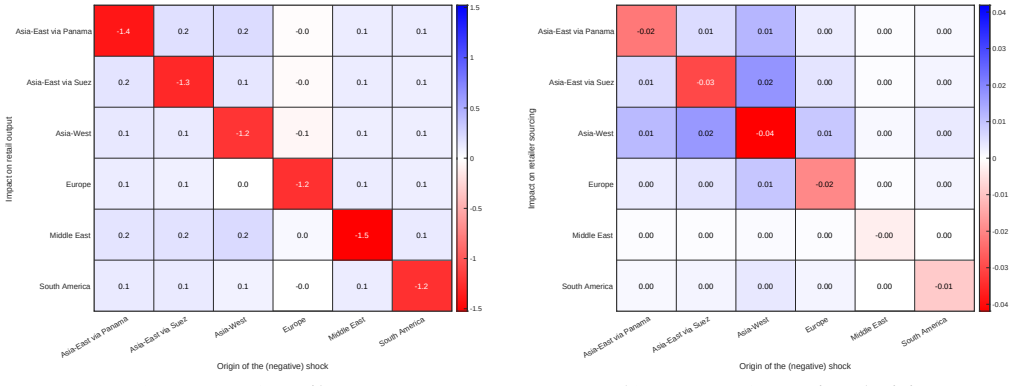
[25]The elasticities take general-equilibrium effects fully into account. We compute the partial derivatives of the equilibrium conditions via automatic differentiation and recover the full general-equilibrium Jacobian by applying the implicit function theorem. This approach yields accurate numerical derivatives.

shipping efficiency, X_r, reduces aggregate real output by about 0.07% along the Asia-West Coast route and by 0.02% along the Asia-East Coast route via the Suez Canal. The output effects are smaller for the remaining routes. They are marginally negative for the Middle East and South America to the East Coast routes as disruptions along those routes slightly raise aggregate output because shipping firms reallocate capacity toward higher-value routes.

To understand the forces driving the magnitude of these shocks, Figure 6.1b also shows the contribution of changes in imports from the disrupted route, in the demand for domestic goods and imported goods from other routes, in importers' sourcing decisions, and in retail entry. Shipping disruptions lead to a reduction in imported goods from the disrupted route as importers shift away toward goods sourced from other routes and an increase in demand for domestic goods. Shipping disruptions also impact aggregate output through retail exit of importers.

We now zoom in on imports. Figure 6.2a shows the impact of a route-specific disruption shock on each good type's output, $-(\partial \log y_h / \partial \log X_r)$, and Figure 6.2b displays the impact of disruptions on importers' sourcing decisions, $-(\partial \log o_h / \partial \log X_r)$. Disruptions along a particular route tend to reduce retail output from that same route (diagonal cells in the matrix) and to increase output on goods sourced from competing routes (off-diagonal cells). For instance, a 1% disruption shock tends to reduce retail output from the same route by about 1.2 to 1.5% and to increase retail output from competing routes by up to 0.2%. The spillover effects are heterogeneous between routes. A shock along the Asian routes tends to raise retail output across all other routes by more than a shock in the other regions. The intensity of the color denotes the strength of the effect.

FIGURE 6.2.—The effect of shipping disruptions on importers' output and sourcing decisions



(a) Importers' retail output

(b) Importers' sourcing decisions

Note: Panel (a) displays the elasticity of importers' output from goods transported along route h to disruptions along route r, $-(\partial y_h / \partial X_r)(X_r / y_h)$. Panel (b) displays the elasticity of importers' sourcing of goods from route h to disruptions along route r, $-(\partial o_h / \partial X_r)(X_r / o_h)$. Color intensity denotes the strength of the effect.

The elasticity of retail output to shipping disruptions depends on the response of retail prices and congestion, as shown in Proposition B.1 in Appendix B. Figures C.4a and C.4b in Appendix C.2 display the effect of disruptions on retail prices and congestion. Shipping disruptions increase the retail price consumers pay and have a stronger impact on the price of goods from the same region as the shock. For instance, a 1% disruption shock tends to raise retail prices of goods from the same region by about 0.05% to 0.5%. Disruptions along the routes departing from Asia have stronger spillovers on retail prices as goods from all regions become more expensive. Similarly, disruptions tend to reduce congestion along the affected route, diverting ships to competing U.S.-bound routes or leaving them idle. In particular, disruptions along the Asia-East Coast route via the Suez Canal, the Asia-West Coast route, and routes from Europe tend to increase congestion in competing routes the most.

6.2. *Port congestion in the summer and fall of 2021*

The summer and fall of 2021 saw a record number of ships waiting at the ports of Los Angeles and Long Beach. This unprecedented strain put massive pressure on the shipping sector, in particular along the Asia-West Coast route. Although port congestion only became news in the summer of 2021, our satellite-based measure of disruptions started signaling a fall in shipping efficiency as early as November 2020, reaching its lowest value by the end of 2021. Along the Asia-West Coast route, shipping efficiency fell 20 p.p. in November 2021 relative to the prior year.

To study the aggregate impact of the 2021 shipping disruptions along the Asia-West Coast route, we build a counterfactual economy in which shipping disruptions along that route are absent. In particular, we solve for the values of x_{AW} in each month that keep the shipping efficiency, z_{AW}, at its value as of January 2020, while preserving all the other parameter values at their baseline levels. Next, we contrast that counterfactual economy with the baseline economy.

Figure C.5 in Appendix C.3 shows the evolution of the key aggregates. Our measure of shipping efficiency in January 2020 was 0.880, which was about 1.5 times larger than the lowest value of z_{AW} at the end of 2021. Holding z_{AW} at its January 2020 level in the counterfactual requires raising the exogenous component x_{AW} enough to offset the higher congestion that arises as shipping firms reallocate more ships onto the route. Due to the higher shipping efficiency in the counterfactual economy, shipping firms find it optimal to reallocate ships from other Asian routes to the Asia-West Coast route. In contrast, the capacity allocated to Europe, the Middle East, and South America is practically unchanged and more ships remain idle.

The increase in capacity allocated to the Asia-West Coast route drives firms to increase the number of voyages along that route. Instead of 3 trips per month at the end of 2021, shipping firms would make about 4 trips. That increase comes at the expense of fewer trips per

month along the other Asian routes. The U.S.-bound potential shipping supply increases from 48 million metric tons at the end of 2021 to 55 million metric tons. Due to increased shipping efficiency, the U.S.-bound effective shipping supply increases by more than the potential shipping supply, from 34 to 47 million metric tons. The increase in shipping supply is accompanied by a 31% fall in the price of shipping services from the Asia-West Coast route.

With the increase in U.S.-bound shipping supply, imports rise. The import share of GDP increases from less than 12.7% to 14.0% at the end of 2021. That increase is driven by more imports of Asian goods despite a fall in imports from other regions. Sourcing goods from the Asia-West Coast route becomes more profitable, leading more importers to specialize in these goods. The boost in imports is driven by a 14% decline in the retail price of Asian goods at the end of 2021. The aggregate price index falls by much less as most goods consumed are produced domestically. The price index falls by 1.4% in December 2021 relative to the baseline economy.

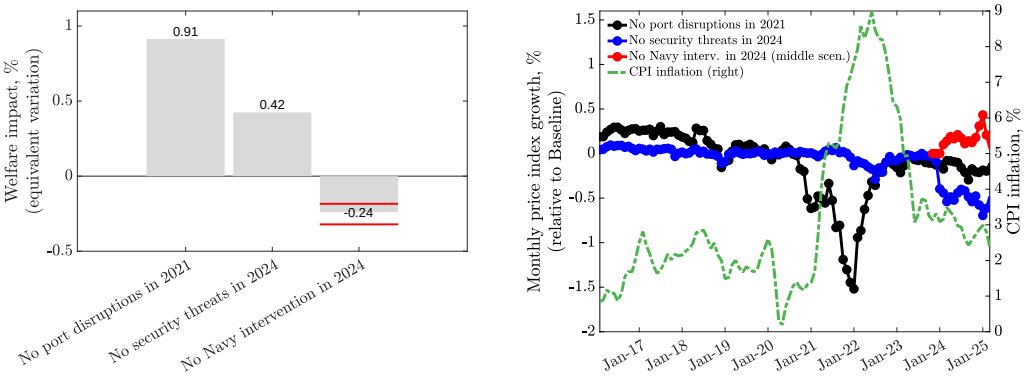
Figure 6.3a plots the welfare impact of the shipping disruptions related to the 2021 West Coast port congestion. The welfare impact corresponds to the value of ε_{ev} that solves Equation (6.1)

$$(1+\varepsilon_{\text{ev}})\sum_{\tau=t}^{T}\beta^{\tau-t}u(c_{A_t}^{\text{Base}},c_{E_t}^{\text{Base}},c_{M_t}^{\text{Base}},c_{S_t}^{\text{Base}},d_t^{\text{Base}})=\sum_{\tau=t}^{T}\beta^{\tau-t}u(c_{A_t}^{\text{Exp}},c_{E_t}^{\text{Exp}},c_{M_t}^{\text{Exp}},c_{S_t}^{\text{Exp}},d_t^{\text{Exp}}), \quad (6.1)$$

where the left-hand side corresponds to the utility in the baseline economy and the right-hand side to the utility in the counterfactual economy, β is the consumer's monthly discount factor assumed to be 0.9966, and t corresponds to January 2021 and T to December 2021.

The value of ε_{ev} represents the change in consumer income, at the prices obtained in the baseline economy, that is equivalent to the utility that the consumer would get in the counterfactual economy without shipping disruptions. As the utility is higher in a world with lower shipping disruptions, consumers would pay a positive amount to live in the counterfactual economy. Consumers would be willing to pay 0.91% of GDP to avoid the shipping disruptions from the 2021 West Coast port congestion.

FIGURE 6.3.—Welfare and price impact of shipping disruptions



(a) Welfare impact of disruptions

(b) Price impact of disruptions

Note: Panel (a) shows the welfare impact of shipping disruptions, measured as in Equation (6.1), that affected the Asia-West Coast route in the summer and fall of 2021 and the Asia-East Coast route via the Suez Canal and the Middle East-East Coast route due to security threats along the Red Sea in early 2024. Figure 6.3 also shows the welfare impact of the Navy intervention following the Houthi attacks in 2024 for low, medium, and high scenarios. Panel (b) shows the monthly growth rate of the price index in the counterfactual economy relative to the same-month index in the baseline economy.

Figure 6.3b shows the evolution of the growth rate of the total price index, P_t^{total}, in the counterfactual economy relative to the baseline economy in the same month. The average price in the economy without the 2021 port disruptions would be 1.4% lower at the end of 2021. To put this number into perspective, annualized CPI inflation in December 2021 was 7.2%. Although the model is not designed to capture the inflation dynamics observed over the period, a back-of-the-envelope inflation rate without the impact of the West Coast port disruptions would have been, all else equal, 5.6%.[26]

6.3. *Security threats in the Red Sea in early 2024*

Houthi forces began launching attacks on commercial vessels transiting the Red Sea and the Gulf of Aden in late 2023. The attacks forced shipping companies to reroute vessels away from the Suez Canal to the Cape of Good Hope. We showed in Section 3 that this added 700–1,200 nautical miles to the journeys passing through the Suez Canal, corresponding to about 4 to 5 additional days of travel in our sample. Our micro-level estimates of shipping efficiency along the routes from Asia to the East Coast via the Suez Canal and from the Middle East to the East Coast, z_{AS} and z_{ME}, fell by 21 and 31 p.p. between March 2023 and March 2024.

To study the aggregate impact of the Houthi attacks in the Red Sea in early 2024, we build a counterfactual economy in which shipping disruptions along the Asia-to-East Coast route via the Suez Canal and the Middle East-to-East Coast route are absent. That is achieved by solving

[26] This is calculated as $\pi_t^{\text{Exp}} \approx (1-0.014)P_t/P_{t-12} - 1 = 0.072 \times (1-0.014) - 0.014$.

for the values of x_{AS} and x_{ME} in each month that keep the shipping productivities, z_{AS} and z_{ME}, at their values as of August 2023. Figures C.6 and C.7 in Appendix C.4 contrast the counterfactual economies for each route with the baseline.

Our measure of shipping efficiency in August 2023 was 0.857 and 0.809 for the routes from Asia via the Suez Canal and from the Middle East to the East Coast. These values are more than 26 p.p. higher than their May 2024 values. Without shipping disruptions from the security threats, congestion increases mostly on the route from Asia via the Suez Canal. The increase in congestion is driven by a reallocation of ships from other Asian routes to the one via the Suez Canal as idle capacity stays about the same as in the baseline economy. Shipping firms increase the number of trips from 1.6 to about 3 a month along the Suez Canal and from 0.6 to 0.8 from the Middle East. Despite the change in the composition of shipping supply away from goods transported along the routes from Asia to the West Coast and to the East Coast via the Panama Canal, the total U.S.-bound potential shipping supply increases modestly from 42 million metric tons to 45 million metric tons in May 2024.

The import share of GDP in May 2024 rises in the counterfactual economy from 11.2 to 11.7%, driven by more imported goods from Asia and the Middle East. The increase in imports is driven by a fall in the retail price of goods from Asia and the Middle East of 5.8% and 21.3% in May 2024 relative to the baseline economy. The retail prices of goods from Europe and South America stay practically unchanged. The aggregate price index falls by 0.5% in May 2024 relative to the baseline economy.

Figure 6.3a above plots the welfare impact of the shipping disruptions related to the Houthi attacks in the Red Sea in 2024. The equivalent variation is annualized and refers to the period from December 2023 to March 2025, which is when our measure of shipping efficiency was significantly below trend for both affected routes. Consumers would be better off without the shipping disruptions in the Red Sea. The welfare cost of the security threats from the Houthi attacks between November 2023 and March 2025 amounted to 0.4% of GDP. The 2024 attacks in the Red Sea were considerably less detrimental than the 2021 port disruptions, partly because U.S. naval forces helped contain the disruptions before they deteriorated further. The value of that intervention is quantified in the next section.

6.4. *Robustness*

We assess the sensitivity of the welfare estimates to the elasticities governing the markups of shipping firms and importers (σ and θ), shipping costs (ζ), importers' sourcing decision (λ), consumer demand (ρ), and to the choice of the pre-disruption anchor date. For each perturbation, we hold the model's fit to the data fixed, which requires recalibrating the internally determined parameters and simulating the model so that the baseline economy continues to re-

produce the targeted moments and the observed time paths of the variables described in Section 5.3.[27]

Table C.3 in Appendix C.6 shows the equivalent variation for the 2021 West Coast port disruptions and the 2024 security threats in the Red Sea under $\pm 10\%$ perturbations to σ, θ, ζ, λ, and ρ as well as an alternative pre-disruption anchor date (one month earlier, i.e., December 2019 and July 2023). The estimated welfare costs remain within 0.76–1.15% of GDP for the 2021 West Coast port disruptions and 0.31–0.68% of GDP for the 2024 security threats in the Red Sea, leaving the qualitative conclusions unchanged.

7. The value of Navy intervention

Was the U.S. Navy's intervention in the Red Sea worth its cost? We infer the fiscal costs of the military operations from military records and use our model to estimate the economic losses averted. We find that the benefits to U.S. consumers exceeded the budgetary costs by roughly an order of magnitude—though, as we emphasize below, this comparison depends on assumptions about the counterfactual evolution of disruptions in the absence of the intervention.

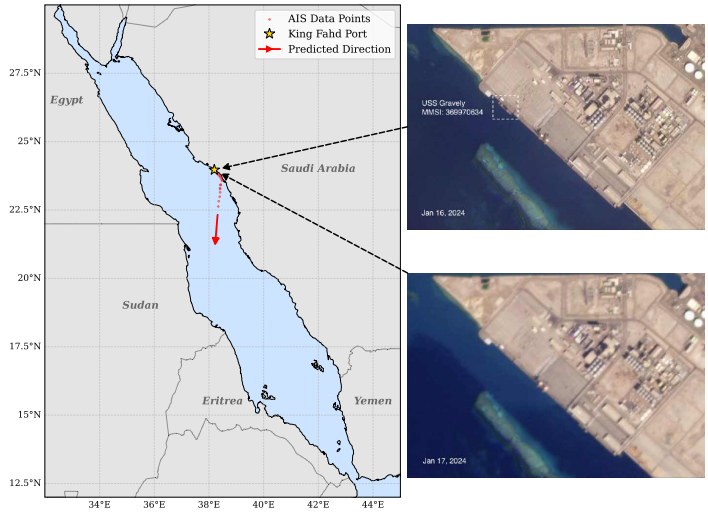
In response to the Houthi attacks in the Red Sea, the U.S. Navy and other allies formed a coalition in December 2023 and launched *Operation Prosperity Guardian* to patrol the Red Sea and actively shoot down incoming missiles and drones. Following the attack on the *Maersk Hangzhou*, the U.S. Navy sent destroyers USS Laboon and USS Gravely as well as the aircraft carrier USS Dwight D. Eisenhower on December 30, 2023. The first airstrikes were launched against Houthi targets in Yemen on January 12, 2024. To illustrate the tangible and highly mobilized nature of these operations, Figure 7.1 maps the movements of the USS Gravely in the Red Sea on January 17, 2024.[28] This visual evidence captures the destroyer's departures for and returns from patrol, underscoring the instrumental military presence required to safeguard this critical shipping corridor. The campaign coincided with a subsequent decline in attacks on U.S. vessels, culminating in a ceasefire in May 2025.

We begin by estimating the fiscal cost of the U.S. Navy's intervention in the Red Sea. Table 7.1 reports our estimate, derived from naval operations and munitions used in the conflict, as documented in military records. The naval operations totaled \$1.3 to 3.0 billion, or 0.004 to 0.01% of GDP, for the seven naval ships used for about eight months to patrol the Red Sea between late 2023 and the summer of 2024. The range depends on whether overhead and other

[27]The welfare estimates are, by construction, invariant to the congestion externality parameters ε_k and ϕ as the counterfactuals hold the observed shipping efficiency path z_r fixed at its pre-disruption level. The congestion externality will, however, shape the policy experiments of Section 8, where z_r responds endogenously.

[28]The USS Gravely played a prominent role in *Operation Prosperity Guardian*, frequently engaging Houthi anti-ship ballistic missiles and unmanned aerial vehicles to protect critical commercial shipping lanes. Additional figures detailing the USS Gravely's earlier deployment at NSA Bahrain on December 13, 2023, and its subsequent presence at the Port of Duqm in Oman on March 8, 2024, are provided in Appendix A.

FIGURE 7.1.—USS Gravely operations in the Red Sea (January 17, 2024)



Note: The figure illustrates the movement of the Arleigh Burke-class guided-missile destroyer USS Gravely (DDG 107) using AIS data. Because AIS transmissions for U.S. Navy ships are typically disabled during active military operations for security reasons, the available data are limited and primarily concentrated around periods when the ship was departing for operations or docking afterward. Satellite images are included alongside the map as an external validation to confirm that the USS Gravely was at the dock of the respective port prior to its departure.

indirect costs are included in the estimates. The different types of missiles used to counter the Houthi attacks amounted to an additional $1.2 to 2.4 billion, or 0.004 to 0.008% of GDP. The House passed the Israel Security Supplemental Appropriations Act in April 2024 providing emergency funding for military aid to Israel, which included $2.44 billion allocated to help address the additional expenses related to the increased U.S. naval operations against Houthi threats. These additional funds likely covered part of the expenses associated with naval operations and munitions. The total cost of the U.S. Navy's intervention in the Red Sea was between $2.4 and 5.5 billion, or 0.008 to 0.02% of U.S. GDP, without the supplemental budget increase. When these additional funds are included, the U.S. Navy's intervention cost between $4.9 and 7.9 billion, or 0.02 to 0.03% of GDP.

The model is now used to provide an estimate of the value of the Navy intervention, complementing direct estimates of the welfare cost of maritime insecurity such as Besley et al. (2015) for Somali piracy. Specifically, we construct three counterfactual economies in which shipping disruptions along routes from Asia to the East Coast via the Suez Canal and from the Middle East to the East Coast would continue to grow throughout 2024 and early 2025. Attacks on commercial vessels were escalating in the months before the coalition deployed in the region and would likely have worsened absent the Navy intervention, so the deterioration in shipping efficiency would plausibly have continued. Figures C.8 and C.9 in Appendix C.5 display the time paths for the affected shipping efficiencies, z_{AS} and z_{ME}, as well as other relevant ag-

TABLE 7.1

ESTIMATED COST OF U.S. NAVY RED SEA OPERATIONS

	Quantity	Unit Cost (US$M)	Total Cost (US$M)	% of GDP	Source
		Panel A: Naval Operations			
Arleigh Burke class destroyer	4, 250 days	87–211	237–578	0.0008–0.0020	[1],[2],[3]
Carrier air wing	1, 250 days	575–1,395	394–956	0.0013–0.0033	[1],[2],[3]
Nimitz class aircraft carrier	1, 250 days	752–1,830	515–1,253	0.0018–0.0043	[1],[2],[3]
Ticonderoga class cruiser	1, 250 days	187–380	128–260	0.0004–0.0009	[1],[2],[3]
Total			**1,273–3,048**	**0.0043–0.0104**	
		Panel B: Munitions			
SM-2	120	3.6–4.3	438–519	0.0015–0.0018	[4],[5]
SM-3/ESSM	20	1.9–25.3	39–507	0.0001–0.0017	[4],[5],[6]
SM-6	80	4.0–9.6	321–766	0.0011–0.0026	[5],[6]
Tomahawk cruise missile	135	2.1–3.9	287–531	0.0010–0.0018	[1],[7]
AMRAAM/AIM-9X	60	0.9–1.1	55–67	0.0002	[6],[8]
JDAM/AGM-114 Hellfire	420	0.05–0.12	20–49	0.0001–0.0002	[6],[8]
Hypervelocity Projectile	160	0.1	17	0.0001	[5],[9]
Total			**1,176–2,439**	**0.0040–0.0083**	
		Panel C: Other			
Israel Security Supplemental (ISS) Appropriations Act, 2024			2,440	0.0083	[10]
		Panel D: Total Cost			
Naval Operations			**1,273–3,048**		
Munitions			**1,176–2,439**		
Total (without ISS)			**2,449–5,487**	**0.0084–0.0187**	
Total (with ISS)			**4,889–7,927**	**0.0167–0.0271**	

Notes: The table provides estimates of the cost of U.S. Navy operations in the Red Sea between late 2023 and July 2024 (shares are calculated using 2024 nominal GDP of $29.3 trillion).
Panel A: Naval operations include one Nimitz-class aircraft carrier (USS Dwight D. Eisenhower), four Arleigh Burke-class destroyers (USS Gravely, USS Mason, USS Laboon, and USS Carney), one carrier air wing (Carrier Air Wing 3), and one Ticonderoga-class cruiser (USS Philippine Sea) deployed for approximately 250 days between October 2023 and July 2024. The lower bound for unit cost refers to direct costs (which include the costs of the combat unit and the personnel assigned to the unit itself), and the upper bound adds overhead and other indirect costs (which include costs such as medical care, training personnel, and other administrative costs).
Panel B: SM and ESSM stand for Standard Missiles and Evolved SeaSparrow Missiles; SM, ESSM, and Tomahawk cruise missiles are ship-launched surface-to-air missiles. AMRAAM and AIM-9X stand for Advanced Medium-Range Air-to-Air Missiles and Air Intercept Missile-9X; these are air-to-air missiles. JDAM stands for Joint Direct Attack Munition; JDAM and AGM-114 Hellfire are air-to-surface missiles. Hypervelocity Projectiles are versatile surface-to-air/surface missiles and correspond to rounds from a five-inch gun.
Panel C: The Israel Security Supplemental provided funding for the Central Command operations and helped address the additional expenses related to the increased U.S. naval operations against Houthi threats. The amount shown likely covered part of the expenses in Panels A and B.
Sources: [1] U.S. Navy (2024); [2] Congressional Budget Office (2021); [3] Congressional Budget Office (2025); [4] Department of the Navy (2024); [5] Ziezulewicz (2025); [6] Department of Defense (2024); [7] Department of the Navy (2023); [8] Trevithick (2024); [9] Congressional Research Service (2021); [10] House Committee on Appropriations (2024).

gregates under low, medium, and high disruptions.[29] The three scenarios differ in how severe and persistent this deterioration is. For the Asia-East Coast route via the Suez Canal, in the low scenario shipping efficiency stabilizes at around 57% in August 2024, in the medium scenario it continues its downward trend and reaches that level in November 2024, and in the high scenario the decline accelerates and persists until March 2025.[30]

Figure 6.3a shows the welfare impact of shipping disruptions if the attacks on container ships had worsened and lasted longer. As consumer welfare is lower without the Navy's protection, consumers are worse off relative to the baseline economy. The annualized value of the Navy's support between February 2024 and March 2025 amounted to 0.24% of GDP in the medium scenario. In the less disruptive scenario, the Navy intervention would have saved 0.18% of GDP, while the scenario with long-lasting attacks is valued at 0.32% of GDP. These values are measured as the consumer-welfare equivalent variation and so exclude non-consumer surplus,

[29] As before, they are computed by solving for the values of the exogenous component of shipping productivity, x_{AS} and x_{ME}, that deliver the paths of z_{AS} and z_{ME}.
[30] For the Middle East-East Coast route, the shipping efficiency stabilizes at 45%, close to its February 2024 value.

such as the risk borne by crews and vessels. The magnitudes are nonetheless consistent with the modest but non-negligible share of U.S. imports transiting these routes.

To sum up, relative to the 0.4% of GDP cost that materialized with the Navy in place (Section 6.3), the intervention averted an additional 0.18 to 0.32% of GDP in losses across the three scenarios, which exceeds the fiscal outlay (ranging from 0.008 to 0.03% of GDP) by roughly an order of magnitude. Table C.3 in Appendix C.6 also reports the sensitivity of the welfare gains from the Navy intervention under alternative parameter values. For the medium scenario, the value of the Navy intervention ranges between 0.20–0.26% of GDP.

8. TAX POLICY: TARIFFS AND PORT FEES

Motivated by the escalation of the trade war in 2025, we now append a government to this economy to study the role of tariffs and port fees. The 2025 tariffs have led to a substantial increase in the U.S. average effective tariff rate, applied widely across many trading partners. Although some of these duties have been eliminated for agricultural products, the average effective tariff rate was nearly 18% as of October 2025—the highest level since 1934. In October 2025, the U.S. government also started imposing fees on Chinese-built and Chinese-owned vessels. The fee for non-Chinese operators of Chinese-built ships was set to $18 per net ton (or $120 per container) per voyage, while the fee on Chinese-operated ships was $50 per net ton per voyage, both up to a cap of five voyages per vessel per year. The fees were later suspended in November 2025 for one year following China's retaliatory fees.

8.1. *The shipping market with tax policy*

To study the impact of tax policies when the shipping market is a key sector shaping the allocation of goods, we now introduce port fees and tariffs in our framework. Let $\mathfrak{f}_o$ denote region-specific port fees and τ_o the region-specific tariff rate on goods originating from region o. The port fees are levied on shipping firms, raising their marginal cost of shipping along route r (Equation (4.8)) according to

$$mc_r = \frac{g(K_r)}{x_r}\left[\frac{\overline{p}_n}{1/\zeta}\right]^{1/\zeta}\left[\frac{(\overline{p}_o + \mathfrak{f}_o)}{1/\nu}\right]^{1/\nu}. \tag{8.1}$$

Hence, increases in port fees are passed on to importers through higher prices of shipping services. Tariffs, on the other hand, are imposed on importers. They affect their profit from sourcing goods from route r (Equation (4.15)), which is now given by

$$\Pi_r = \max_{\{y_r(j)\}}\left\{p_o\chi_r^{\theta}\left(\int_0^N y_r(j)^{\sigma}dj\right)^{\theta/\sigma} - (1+\tau_o)\int_0^N p_r(j)y_r(j)dj - f\right\}, \tag{8.2}$$

and their demand for imported goods from a shipping firm (Equation (4.18)) is

$$\mathrm{y}_r(j) = o_r \left[\frac{\theta \chi_r^{\sigma} \, p_o y_r^{(1-\sigma/\theta)}}{(1+\tau_o) p_r(j)} \right]^{1/(1-\sigma)} \mathcal{I}. \tag{8.3}$$

Raising tariffs reduces importers' demand for foreign goods as well as their profits, ultimately affecting their sourcing decisions.

The government collects the revenue from port fees and tariffs, and rebates it lump sum to consumers, where total revenue T is defined as

$$T = \sum_{o=\{A,E,M,S\}} \sum_{r=\mathcal{R}_o} \left[\int_0^N \mathfrak{f}_o (\ell_r(j) \kappa_r(j))^{\nu} dj + \tau_o \, o_r \mathcal{I} \int_0^N p_r(j) y_r(j) dj \right], \tag{8.4}$$

Adding these tax policy instruments also alters the labor market clearing condition.[31]

In partial equilibrium, tariffs reduce output and raise retail prices. They are, however, not necessarily detrimental in general equilibrium. Propositions B.3, B.4, and B.5 in Appendix B.4 show why. Tariffs can operate like a Pigouvian tax when the reduction in shipping costs resulting from lower congestion outweighs the direct tariff-induced increase in retail prices. An increase in tariffs on a particular region decreases congestion along routes originating in that same region, as $\frac{\partial g(K_h)}{\partial \tau_o} \frac{\tau_o}{g(K_h)} \leq 0$ (for route h originating in region o), and potentially leads to an increase in congestion on routes originating in other regions. A reduction in congestion boosts productivity for shipping firms, allowing them to supply more goods in less time and at lower prices. A fall in the price of shipping services leads to an increase in retail demand, which in turn translates into an increase in importers' output, as $\frac{\partial y_h}{\partial p_h(j)} \frac{p_h(j)}{y_h} \leq 0$.

An increase in tariffs on a particular region also puts upward pressure on the retail price of goods from that region as it increases the marginal cost of importers. If the tariff increase drives up shipping service prices, it can lead to higher retail prices. If, instead, the reduction in shipping costs from lower congestion outweighs the direct tariff-induced increase in retail prices, retail prices may fall, or at least not rise. As a result, consumers might be better off when tariffs are introduced. Which effect dominates is a quantitative question.

As Proposition B.4 shows, the importers' markup also conditions how tariffs transmit through retail output. The elasticity of retail output to tariffs scales with $\theta/(1-\theta)$, which decreases as the markup $1/\theta$ rises. So a higher markup dampens the direct output response to a tariff. Whether the higher markup ultimately raises or lowers retail prices and welfare is a gen-

[31] The labor demanded by domestic firms is now given by $l_d = 1 - \frac{1}{w} \int_0^N \sum_{r \in \mathcal{R}} \left\{ \overline{p}_n n_r(j)^{\varsigma} + \frac{\overline{p}_o}{\nu(\overline{p}_o + \mathfrak{f}_o)} \left[\varsigma \overline{p}_n n_r(j)^{\varsigma} - \mu_r(j) \right] + \overline{p}_{\kappa} \frac{\kappa_r(j)^2}{2} \right\} dj$.

eral equilibrium question. In the calibrated experiment with a 50% markup (columns (6)–(7) of Table C.4), the price effect dominates and consumers are worse off.

8.2. *Dissecting the effect of tariffs*

We now compare the baseline economy in March 2025 with a counterfactual economy in which U.S. imports from Asia are subject to an 18% tariff. In the economy with tariffs on Asian goods, we proceed with two experiments. First, the congestion externality is raised by 50%, i.e., $\varepsilon_k = 1.5$, which is equivalent to increasing shipping disruptions in all routes by 50%. Second, the retail markup is increased from 25% to 50%, i.e., $\theta = 1/1.5$. Table C.4 in Appendix C.7 summarizes the results.

Baseline effect (columns (2)–(3)). Levying tariffs on goods from Asia reduces importers' demand for goods originating there. This fall in demand leads shipping firms to lower the price of shipping services along the Asian routes by 5 to 6%, while the price of shipping services from other regions rises. Lower prices erode profits on the Asian routes by at least 18%, prompting firms to reallocate ships toward more profitable routes. Shipping firms shift capacity to the U.S.-bound routes from Europe, the Middle East, and South America, and leave a larger share of their fleet idle (the idle capacity share rises by 0.4%).

With fewer U.S.-bound ships from Asia, congestion falls across all Asian routes, acting like a positive productivity shock. Yet because capacity also contracts along these routes, the effective shipping supply from Asia falls by 9.0 to 11.3%, and the number of trips from Asia declines by 9.4 to 10.2%. On net, total effective shipping supply falls by 5.5%, from 18.9 to 17.9 million metric tons, despite the gains on the non-Asian routes.

Turning to the retail market, the decline in shipping prices encourages retailers to expand their demand for imported goods, nudging the total import share from 11.3 to 11.6% of GDP. Imports from Europe, the Middle East, and South America rise by 7.5 to 14.0%. Even with the tariff in place, retail profits rise, drawing in new entrants (60.7% more retailers). Part of these gains is passed through to consumers, who face lower retail prices on imported goods. The price index of imported goods falls by 2.8% and that of all goods by 0.3%.

Tariff revenue amounts to 0.9% of GDP, lifting consumer income. With import prices lower and incomes higher, real GDP rises and consumers end up better off, with an equivalent variation of 1.3% of income. The gain stems entirely from the shipping market's adjustment. As firms reallocated supply and repriced services across routes, retail prices fell. Because the welfare gain hinges on the strength of this congestion channel, the next two experiments stress it—first by making congestion more costly, and then by raising importers' markup.

Shipping disruptions (columns (4)–(5)). We next let congestion bite harder on shipping firms. Although capacity falls across most routes, the congestion externality rises sharply, by 36 to

53% across routes. Total effective shipping supply almost halves to about 11 million metric tons. Supply contracts on every route as firms cut capacity and the number of trips falls because more congested routes take longer to traverse. Firms raise the price of shipping services to operate these routes, but the increase is not enough to offset the decline in profits, which fall across all routes. Higher shipping prices, compounded by the tariff, push retailers to raise their own prices, lifting the ideal price index of imported goods by 11.7%. As a result, the import share of GDP falls by 9.4%. Tariff revenue reaches 0.8% of GDP, slightly below the previous experiment. In this case the tariff makes consumers worse off, with a welfare loss of 0.6% of income in equivalent variation.

Higher importer markup (columns (6)–(7)). Finally, we raise importers' markups. Even though shipping prices fall, retail prices climb. The ideal price index of imported goods rises by 20.7%. As imports become more expensive, consumers buy fewer of them, and the import share of GDP falls from 11.3 to 9.5%. Weaker retail demand feeds back to the shipping sector. Effective shipping supply falls to about 13.4 million metric tons. Firms make fewer trips each month and leave more capacity idle, which in turn relieves congestion along the Asian routes. Tariffs still raise 0.6% of GDP in revenue, but consumers are now worse off, with a welfare loss of 0.4% of income.

8.3. *Dissecting the effect of port fees*

Port fees operate similarly to tariffs. However, since they are levied on shipping firms, they have a weaker transmission mechanism than tariffs levied on importers. Propositions B.6, B.7, and B.8 in Appendix B.5 provide the theoretical details. To obtain an estimate of port fees, $\mathfrak{f}_o$, an implied price per ton per voyage is needed. We use Census data and divide the value of containerized shipping imports by our measure of effective shipping capacity by region. On average, the implied price per ton per trip for ships originating from Asia corresponds to about \$5,000.[32] Hence, a fee of \$50 per ton per voyage would represent 1% of the implied price per ton per voyage. The model counterpart for the price per ton per voyage is $\overline{p}_o$. We thus set $\mathfrak{f}_o = 0.01 \times \overline{p}_o$. Table C.5 in Appendix C.8 presents the impact of imposing port fees on ships departing from Asia. As with tariffs, we report the baseline effect and then stress the two margins that govern transmission: a more costly congestion externality ($\varepsilon_k = 1.5$) and a higher importer markup ($\theta = 1/1.5$).

Baseline effect (columns (2)–(3)). Port fees raise the marginal cost of operating the taxed routes, which shipping firms pass on as higher shipping prices of about 2 to 2.5% across routes. Because the fee is levied on shipping firms and enters their cost rescaled by the exponent $1/\nu$,

[32] Our measure of shipping capacity in early 2025 was severely affected by tariff announcements and the ratio of imports to capacity would be lower, which would translate into a higher price per ton per trip.

its direct footprint is small: it raises only 0.02% of GDP in revenue, an order of magnitude less than the Asian tariff. Shipping firms make more trips (up about 3% across routes) and leave less of the fleet idle (its share falls by 0.4%), so total effective shipping supply goes up by 2.3%.

Stronger retail profitability draws in new entrants, with the mass of importers expanding by 49.7%. The ideal price index of imported goods falls by 4.9% (and that of all goods by 0.6%), so the import share of output rises from 11.3 to 11.8% of GDP, with imports increasing from every region by 4.3 to 5.2%. On net, consumers are modestly better off, with an equivalent variation of 0.7% of income. Unlike the tariff, this gain does not come from congestion relief, but from the entry of retailers and the resulting fall in retail prices.

Shipping disruptions (columns (4)–(5)). When congestion bites harder, port fees become sharply contractionary. The congestion externality rises by about 43% across routes, total effective shipping supply falls by 40%, and the number of trips drops by roughly 11%. Shipping firms raise prices by about 44%, but the increase falls short of their higher costs and profits decline by about 20% on every route. The higher shipping prices pass through to retail. The ideal price index of imported goods rises by 17.8% and the import share of output falls by 13.6%, with imports contracting across all regions. Even though retail entry remains strong (50.3% more importers), consumers are substantially worse off, with a welfare loss of 2.0% of income.

Higher importer markup (columns (6)–(7)). With higher markups, retail prices climb even though the fee itself is small. The ideal price index of imported goods rises by 33.1% and the import share of output falls from 11.3 to 8.7% of GDP, the steepest contraction in either table. Weaker import demand feeds back to shipping firms, whose effective supply falls by 24.9% and whose profits drop by as much as 55%. More idle capacity and fewer trips relieve congestion along the Asian routes (down 5 to 21%). Fiscal revenues from port fees are negligible (0.01% of GDP) and consumers are worse off by 2.2% of income.

Port fees versus tariffs. Although both instruments affect shipping costs, port fees are a blunter policy tool. Because they are levied on shipping firms and are scaled down by $1/\nu$ in their pricing decisions, they generate substantially less fiscal revenue than tariffs while producing larger welfare losses. As a result, port fees are more distortionary, dollar for dollar, than tariffs.

9. Improving port infrastructure

Improvements in port infrastructure have emerged as a first-order priority to overcome shipping disruptions. Recent investments have targeted reductions in turnaround times, the expansion of physical capacity, and better inland connectivity. These port upgrades are likely to be quantitatively significant as they alleviate congestion, facilitate vessel scheduling, and effectively increase the utilization of existing shipping infrastructure. To analyze the general equilibrium effect of port infrastructure improvements that alleviate congestion, we lower the congestion

shifter to $\varepsilon_k = 0.9$. Because ε_k scales the congestion-time relationship we estimate in Section 5, the experiment has a direct empirical interpretation: holding the number of port calls fixed, it reduces the hours container ships wait in a port's anchorage area before docking at a berth by 10%. A 10% improvement is modest relative to the congestion that accumulated during the 2021–2022 supply chain crisis, when aggregate shipping efficiency fell from roughly 89% to below 70%. Table C.6 in Appendix C.9 contrasts the outcomes from this counterfactual economy with the baseline economy matched to March 2025 aggregates.

Improvements in port infrastructure reduce congestion and lead to an increase in the productivity of shipping firms, allowing them to deliver more goods faster. The effective shipping supply increases by about 10% across all routes. Although ε_k falls by 10% relative to the baseline, the congestion factor falls by less than 3%. The reduction in congestion leads firms to reallocate ships that were idle to U.S.-bound routes, with the total share of idle supply decreasing by 2.0%. The fall in congestion also encourages more shipping firms to enter the U.S.-bound routes, with the number of shipping firms increasing by 5.4%. As the productivity of shipping firms increases, the price of shipping services falls by about 2.7%. As a result, the number of importers expands by 33.4%, the import share of output increases by 6.9%, and retail prices of imported goods from all regions fall by 7.3%. Consumers are better off with port upgrades that decongest shipping routes. They would need an additional 1% of their monthly income in the baseline to be as well off as they are in the economy with better port infrastructure.

10. Conclusion

This paper develops a new framework for measuring and quantifying the macroeconomic role of maritime shipping. Combining high-frequency AIS satellite data for the universe of U.S.-bound container vessels with vessel registry data, we construct route-specific measures of potential shipping capacity, effective shipping capacity, and shipping efficiency. We show that recent disruptions substantially reduced effective shipping capacity despite large reallocations of vessel capacity toward U.S.-bound routes. To interpret these empirical patterns, we develop a multi-route general equilibrium model in which shipping firms endogenously allocate capacity, choose routes and sailing speeds, and respond to disruptions, congestion, and trade policy.

The theoretical analysis shows that a route-specific disruption propagates through the entire shipping network because shipping firms reallocate vessels and capacity across routes, while importers adjust both import volumes and sourcing patterns. These responses interact with congestion externalities, shipping and retail markups, and changes in the number of active importers and shipping firms. As a result, the aggregate effect of a shipping disruption depends jointly on how shipping firms reallocate capacity, how importers adjust sourcing, and how these

adjustments reshape congestion and prices across routes. It therefore cannot be inferred from a route's Domar weight, the domestic expenditure share, or the trade elasticity alone.

Our quantitative analysis shows that maritime shipping is a key transmission mechanism through which supply chain disruptions affect the macroeconomy. The model attributes sizable welfare losses to the 2021 West Coast port crisis during the COVID-19 pandemic and to the 2024 Red Sea disruptions, and suggests that the U.S. Navy's intervention in the Red Sea generated consumer welfare gains substantially larger than its fiscal cost. More broadly, the policy experiments show that policies traditionally evaluated in environments with exogenous trade costs can have markedly different effects once shipping is treated as an endogenous sector. Tariffs may alleviate congestion on saturated shipping routes, though their welfare effects depend on the underlying market structure. Port fees are less effective because they raise limited revenue while generating larger distortions. These findings highlight the importance of incorporating endogenous shipping decisions and operational frictions into macroeconomic models.

Our analysis also points to several important extensions. The framework treats the world fleet as predetermined; embedding shipbuilding decisions would allow it to speak to longer horizons. Foreign producer prices and bunker fuel costs are taken as exogenous; integrating them would close the global feedback loop. And while we model the shipping sector as monopolistically competitive, the largest carriers operate within alliances whose strategic interactions could matter for pricing during periods of disruption. We leave these extensions for future work.

REFERENCES

D. Acemoglu, V. M. Carvalho, A. Ozdaglar, and A. Tahbaz-Salehi. The Network Origins of Aggregate Fluctuations. *Econometrica*, 80(5):1977–2016, 2012.

G. Alessandria, S. Y. Khan, A. Khederlarian, C. Mix, and K. J. Ruhl. The Aggregate Effects of Global and Local Supply Chain Disruptions: 2020–2022. *Journal of International Economics*, 146:103788, 2023.

T. Allen and C. Arkolakis. The Welfare Effects of Transportation Infrastructure Improvements. *The Review of Economic Studies*, 89(6):2911–2957, 2022.

M. Amiti, S. J. Redding, and D. E. Weinstein. The Impact of the 2018 Tariffs on Prices and Welfare. *Journal of Economic Perspectives*, 33(4):187–210, 2019.

J. E. Anderson and D. Marcouiller. Insecurity and the Pattern of Trade: An Empirical Investigation. *The Review of Economics and Statistics*, 84(2):342–352, 2002.

C. Arkolakis, A. Costinot, and A. Rodríguez-Clare. New Trade Models, Same Old Gains? *American Economic Review*, 102(1):94–130, 2012.

J. Asturias. Endogenous Transportation Costs. *European Economic Review*, 123:103366, 2020.

X. Bai, Z. Ma, Y. Hou, Y. Li, and D. Yang. A Data-Driven Iterative Multi-Attribute Clustering Algorithm and Its Application in Port Congestion Estimation. *IEEE Transactions on Intelligent Transportation Systems*, 24(11): 12026–12037, 2023.

X. Bai, J. Fernández-Villaverde, Y. Li, and F. Zanetti. The Causal Effects of Global Supply Chain Disruptions on Macroeconomic Outcomes: Evidence and Theory. Working Paper 32098, National Bureau of Economic Research, 2024.

X. Bai, J. Fernández-Villaverde, Y. Li, and F. Zanetti. State Dependence of Monetary Policy During Global Supply Chain Disruptions. Working Paper 35209, National Bureau of Economic Research, 2026.

D. R. Baqaee and E. Farhi. The Macroeconomic Impact of Microeconomic Shocks: Beyond Hulten's Theorem. *Econometrica*, 87(4):1155–1203, 2019.

D. R. Baqaee and E. Farhi. Productivity and Misallocation in General Equilibrium. *The Quarterly Journal of Economics*, 135(1):105–163, 2020.

T. Besley, T. Fetzer, and H. Gould. The Welfare Cost of Lawlessness: Evidence From Somali Piracy. *Journal of the European Economic Association*, 13(2):203–239, 2015.

J. Bhagwati and V. K. Ramaswami. Domestic Distortions, Tariffs and the Theory of Optimum Subsidy. *Journal of Political Economy*, 71(1):44–50, 1963.

J. Blaum, F. Esposito, and S. Heise. Input Sourcing Under Climate Risk: Evidence From U.S. Manufacturing Firms. *Review of Economic Studies*, 2026.

C. E. Boehm, A. Flaaen, and N. Pandalai-Nayar. Input Linkages and the Transmission of Shocks: Firm-Level Evidence From the 2011 Tohoku Earthquake. *The Review of Economics and Statistics*, 101(1):60–75, 2019.

G. Brancaccio, M. Kalouptsidi, and T. Papageorgiou. Geography, Transportation, and Endogenous Trade Costs. *Econometrica*, 88(2):657–691, 2020.

G. Brancaccio, M. Kalouptsidi, and T. Papageorgiou. Investment in Infrastructure and Trade: The Case of Ports. Working Paper 32503, National Bureau of Economic Research, 2024.

G. Brancaccio, M. Kalouptsidi, and T. Papageorgiou. Rigidities in Transportation and Supply Chain Disruptions. *AEA Papers and Proceedings*, 115:543–550, 5 2025.

J. K. Brueckner. Airport Congestion When Carriers Have Market Power. *American Economic Review*, 92(5): 1357–1375, 2002.

Bureau of Transportation Statistics. On National Maritime Day and Every Day, U.S. Economy Relies on Waterborne Shipping. Bureau of Transportation Statistics Data Spotlight, 2021. URL https://www.bts.gov/data-spotlight/national-maritime-day-and-every-day-us-economy-relies-waterborne-shipping

L. Caliendo and F. Parro. Estimates of the Trade and Welfare Effects of NAFTA. *The Review of Economic Studies*, 82(1):1–44, 2015.

L. Caliendo, M. Dvorkin, and F. Parro. Trade and Labor Market Dynamics: General Equilibrium Analysis of the China Trade Shock. *Econometrica*, 87(3):741–835, 2019.

Y. Carrière-Swallow, P. Deb, D. Furceri, D. Jiménez, and J. D. Ostry. Shipping Costs and Inflation. *Journal of International Money and Finance*, 130:102771, 2023.

V. M. Carvalho, M. Nirei, Y. U. Saito, and A. Tahbaz-Salehi. Supply Chain Disruptions: Evidence From the Great East Japan Earthquake. *The Quarterly Journal of Economics*, 136(2):1255–1321, 2021.

A. Cavallo, G. Gopinath, B. Neiman, and J. Tang. Tariff Pass-Through at the Border and at the Store: Evidence From U.S. Trade Policy. *American Economic Review: Insights*, 3(1):19–34, 2021.

A. K. Coşar, S. Osotimehin, and L. Popov. The Long-Run Effects of Transportation Productivity on the US Economy. Working Paper 33248, National Bureau of Economic Research, 2024.

D. A. Comin, R. C. Johnson, and C. J. Jones. Supply Chain Constraints and Inflation. Working Paper 31179, National Bureau of Economic Research, 2023.

Congressional Budget Office. The U.S. Military's Force Structure: A Primer, 2021 Update. Publication 57088, Congressional Budget Office, 2021. URL https://www.cbo.gov/publication/57088

Congressional Budget Office. The U.S. Military's Force Structure: Fiscal Year 2025 Update to Personnel Numbers and Costs. Publication 61278, Congressional Budget Office, 2025. URL https://www.cbo.gov/publication/61278

Congressional Research Service. Navy Lasers, Railgun, and Gun-Launched Guided Projectile: Background and Issues for Congress. CRS Report R44175, Congressional Research Service, 2021. URL https://crsreports.congress.gov/product/pdf/R/R44175

B. De Borger, S. Proost, and K. Van Dender. Port Activities, Hinterland Congestion, and Optimal Government Policies: The Role of Vertical Integration in Logistic Operations. *Journal of Transport Economics and Policy*, 45 (2):247–275, 2011.

Department of Defense. FY 2025 Program Acquisition Costs by Weapon System. Budget materials, Office of the Under Secretary of Defense (Comptroller), 2024. URL https://comptroller.defense.gov/Portals/45/Documents/defbudget/FY2025/FY2025_Weapons.pdf

Department of the Navy. FY 2024 Weapons Procurement. Budget estimates, Department of the Navy, 2023. URL https://www.secnav.navy.mil/fmc/fmb/Documents/24pres/WPN_Book.pdf

Department of the Navy. FY 2025 Weapons Procurement. Budget estimates, Department of the Navy, 2024. URL https://www.secnav.navy.mil/fmc/fmb/Documents/25pres/WPN_Book.pdf

J. di Giovanni, Ş. Kalemli-Özcan, A. Silva, and M. A. Yıldırım. Quantifying the Inflationary Impact of Fiscal Stimulus Under Supply Constraints. Working Paper 30892, National Bureau of Economic Research, 2023.

J. Dunn and F. Leibovici. Navigating the Waves of Global Shipping: Drivers and Aggregate Implications. Working Paper 2023-002, Federal Reserve Bank of St. Louis, 2023.

P. D. Fajgelbaum and E. Schaal. Optimal Transport Networks in Spatial Equilibrium. *Econometrica*, 88(4): 1411–1452, 2020.

P. D. Fajgelbaum, P. K. Goldberg, P. J. Kennedy, and A. K. Khandelwal. The Return to Protectionism. *The Quarterly Journal of Economics*, 135(1):1–55, 2020.

R. C. Feenstra, P. Luck, M. Obstfeld, and K. N. Russ. In Search of the Armington Elasticity. *The Review of Economics and Statistics*, 100(1):135–150, 2018.

J. Fernández-Villaverde, Y. Li, L. Xu, and F. Zanetti. Charting the Uncharted: The (Un)Intended Consequences of Oil Sanctions and Dark Shipping. Working Paper 33486, National Bureau of Economic Research, 2025.

S. Ganapati, W. F. Wong, and O. Ziv. Entrepôt: Hubs, Scale, and Trade Costs. *American Economic Journal: Macroeconomics*, 16(4):239–278, 10 2024.

R. Glick and A. M. Taylor. Collateral Damage: Trade Disruption and the Economic Impact of War. *The Review of Economics and Statistics*, 92(1):102–127, 2010.

R. Greenwood and S. G. Hanson. Waves in Ship Prices and Investment. *The Quarterly Journal of Economics*, 130 (1):55–109, 2015.

I. Heiland, A. Moxnes, K. H. Ulltveit-Moe, and Y. Zi. Trade From Space: Shipping Networks and the Global Implications of Local Shocks. *The Review of Economics and Statistics*, pages 1–45, 7 2025. ISSN 0034-6535.

House Committee on Appropriations. House Passes Series of Security Supplemental Bills. Press Release, 2024. URL https://appropriations.house.gov/news/press-releases/house-passes-series-security-supplemental-bills

C. R. Hulten. Growth Accounting With Intermediate Inputs. *The Review of Economic Studies*, 45(3):511–518, 1978.

D. Hummels. Transportation Costs and International Trade in the Second Era of Globalization. *Journal of Economic Perspectives*, 21(3):131–154, 2007.

D. Hummels and A. Skiba. Shipping the Good Apples Out? An Empirical Confirmation of the Alchian-Allen Conjecture. *Journal of Political Economy*, 112(6):1384–1402, 2004.

D. Hummels, V. Lugovskyy, and A. Skiba. The Trade Reducing Effects of Market Power in International Shipping. *Journal of Development Economics*, 89(1):84–97, 2009.

M. Isaacson and H. Rubinton. Shipping Prices and Import Price Inflation. *Federal Reserve Bank of St. Louis Review*, 105(2):89–107, 2023.

M. Kalouptsidi. Time to Build and Fluctuations in Bulk Shipping. *American Economic Review*, 104(2):564–608, 2014.

J. LaBelle and A. M. Santacreu. Global Supply Chain Disruptions and Inflation During the COVID-19 Pandemic. *Federal Reserve Bank of St. Louis Review*, 104(2):78–91, 2022.

N. Limão and A. J. Venables. Infrastructure, Geographical Disadvantage, Transport Costs, and Trade. *The World Bank Economic Review*, 15(3):451–479, 2001.

V. Lugovskyy, A. Skiba, and D. Terner. Unintended Consequences of Environmental Regulation of Maritime Shipping: Carbon Leakage to Air Shipping. *Journal of International Economics*, 155:104081, 2025. ISSN 0022-1996.

M. J. Melitz and S. J. Redding. New Trade Models, New Welfare Implications. *American Economic Review*, 105(3): 1105–1146, 2015.

T. Notteboom, A. Pallis, and J.-P. Rodrigue. *Port Economics, Management and Policy*. Routledge, London, 1 edition, 2021.

T. Notteboom, H. Haralambides, and K. Cullinane. The Red Sea Crisis: Ramifications for Vessel Operations, Shipping Networks, and Maritime Supply Chains. *Maritime Economics & Logistics*, 26(1):1–20, 2024.

Z. Qiu, Y. Wang, L. Xu, and F. Zanetti. Monetary Policy in Open Economies With Production Networks. *Journal of Monetary Economics*, 159:103918, 2026.

M. Stopford. *Maritime Economics*. Routledge, London, 3 edition, 2008.

S. P. Strandenes and P. B. Marlow. Port Pricing and Competitiveness in Short Sea Shipping. *International Journal of Transport Economics*, 27(3):315–334, 2000.

J. Trevithick. 770 Weapons Expended by Eisenhower Carrier Strike Group on Historic Red Sea Deployment. The War Zone, 2024. URL https://www.twz.com/news-features/770-weapons-expended-by-eisenhower-carrier-strike-group-on-historic-red-sea-deployment

UNCTAD. Review of Maritime Transport 2022. Report, United Nations Conference on Trade and Development, 2022.

UNCTAD. Review of Maritime Transport 2024. Report, United Nations Conference on Trade and Development, 2024.

U.S. Navy. Unprecedented: Dwight D. Eisenhower Carrier Strike Group Returns From Combat Deployment. Press Release, 2024. URL https://www.navy.mil/Press-Office/News-Stories/Article/3838261/unprecedented-dwight-d-eisenhower-carrier-strike-group-returns-from-combat-depl/

W. F. Wong. The Round Trip Effect: Endogenous Transport Costs and International Trade. *American Economic Journal: Applied Economics*, 14(4):127–166, 2022.

L. Xu, Y. Yu, and F. Zanetti. The Adoption and Termination of Suppliers Over the Business Cycle. *Journal of Monetary Economics*, 151:103730, 2025.

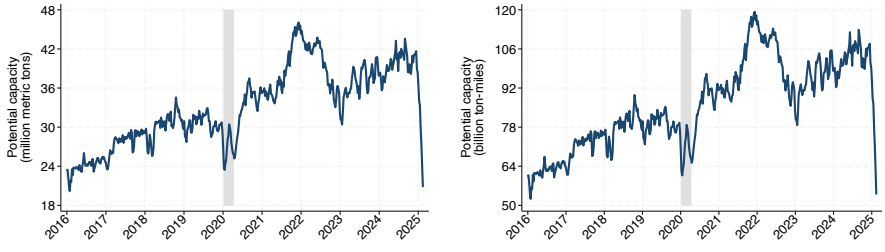
W. Y. Yap and D. Yang. Geopolitical Tension and Shipping Network Disruption: Analysis of the Red Sea Crisis on Container Port Calls. *Journal of Transport Geography*, 121:104004, 2024.

G. Ziezulewicz. Navy Just Revealed Tally of Surface-to-Air Missiles Fired in Ongoing Red Sea Fight. The War Zone, 2025. URL https://www.twz.com/news-features/navy-just-disclosed-how-many-of-each-of-its-surface-to-air-missiles-it-fired-during-red-sea-fight

ONLINE APPENDIX

A: EMPIRICS

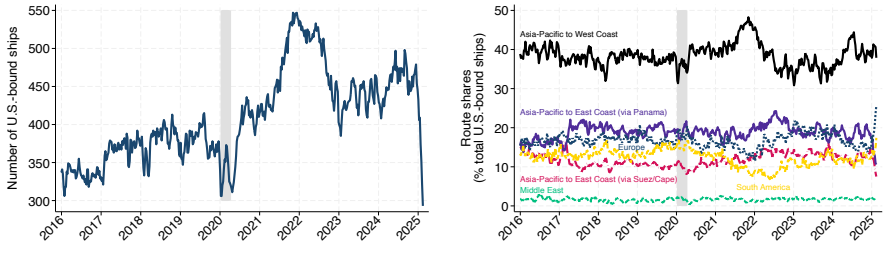
FIGURE A.1.—Potential capacity from unique container ships on U.S.-bound routes, 2016–2025



(a) Potential capacity (tons) (b) Potential capacity (ton-miles)

Note: This figure plots aggregate potential shipping supply in million metric tons (Panel A.1a) and billion ton-miles (Panel A.1b). Estimates are derived from the set of unique container ships operating on U.S.-bound routes. Shaded areas indicate recessions.

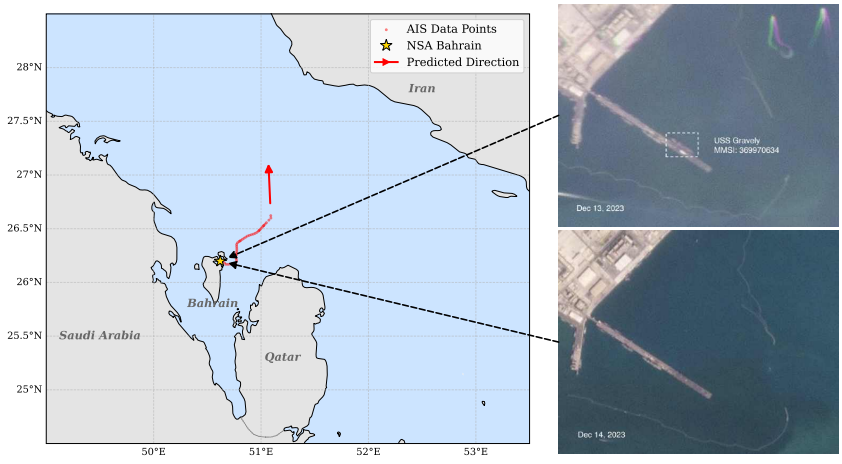
FIGURE A.2.—U.S.-bound container ships, 2016–2025



(a) Total Quantity (b) Route Shares

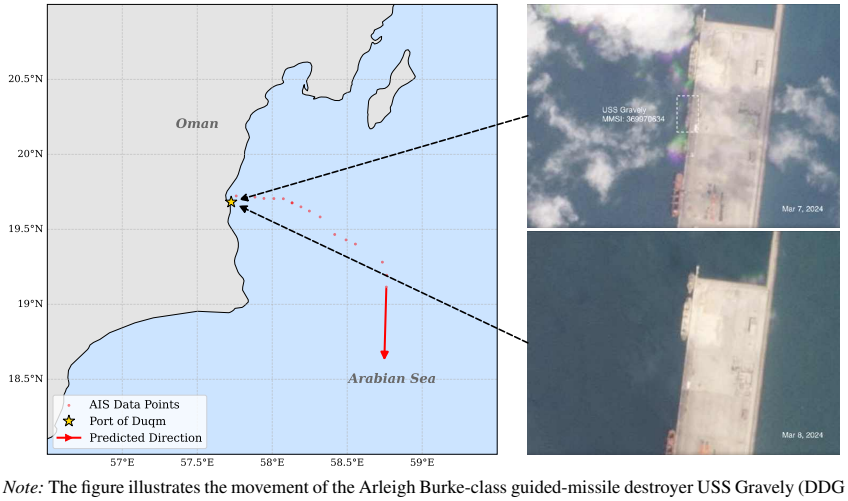
Note: Panel A.2a plots the total number of container ships operating on U.S.-bound routes. Panel A.2b shows the share of ships by specific route. Shaded areas indicate recessions.

FIGURE A.3.—USS Gravely near NSA Bahrain (December 13, 2023)



Note: The figure illustrates the movement of the Arleigh Burke-class guided-missile destroyer USS Gravely (DDG 107) near Naval Support Activity (NSA) Bahrain using AIS data.

FIGURE A.4.—USS Gravely near the Port of Duqm, Oman (March 8, 2024)



Note: The figure illustrates the movement of the Arleigh Burke-class guided-missile destroyer USS Gravely (DDG 107) near the Port of Duqm in Oman using AIS data.

B: THEORY

B.1. *Proof of Proposition 4.1 (Impact of shipping disruptions on real aggregate output)*

In this economy, real aggregate output is equivalent to consumer welfare and thus $Y \equiv \left[\gamma_d d^{\varrho} + (1-\gamma_d)c^{\varrho}\right]^{1/\varrho}$. Applying the chain rule, the elasticity of aggregate output to route-r aggregate shipping productivity, $\left(\partial Y/\partial X_r\right)/\left(X_r/Y\right)$, where the route-$r$ aggregate productivity is defined as $X_r \equiv \left[\int_0^N x_r(j)^{\sigma/(1-\sigma)}dj\right]^{(1-\sigma)/\sigma}$, is given by

$$\frac{\partial Y}{\partial X_r}\frac{X_r}{Y} = \left(\frac{\partial Y}{\partial d}\frac{d}{Y}\right)\left(\frac{\partial d}{\partial X_r}\frac{X_r}{d}\right) + \left(\frac{\partial Y}{\partial c}\frac{c}{Y}\right)\left\{\sum_{o\in\{A,E,M,S\}}\left(\frac{\partial c}{\partial c_o}\frac{c_o}{c}\right)\right. \tag{B.1}$$

$$\left.\times\sum_{h|o}\omega_h\left[\left(\frac{\partial y_h}{\partial X_r}\frac{X_r}{y_h}\right) + \left(\frac{\partial o_h}{\partial X_r}\frac{X_r}{o_h}\right) + \left(\frac{\partial \mathcal{I}}{\partial X_r}\frac{X_r}{\mathcal{I}}\right)\right]\right\},$$

where $\omega_h \equiv o_h y_h \mathcal{I}/c_o$ is the share of route h goods in the consumption of goods from region o. As there is only one route for goods from Europe, the Middle East, and South America to arrive in the U.S., $\omega_h = 1$ for $o \in \{E, M, S\}$.

From the consumer's first-order conditions, it is straightforward to deduce that

$$\frac{\partial Y}{\partial d}\frac{d}{Y} = \frac{p_d d}{w+\Lambda} \equiv \text{Domestic share in aggregate output},$$

$$\frac{\partial Y}{\partial c}\frac{c}{Y} = \frac{P^{\text{imp}}c}{w+\Lambda} \equiv \text{Total import share in aggregate output},$$

and

$$\frac{\partial c}{\partial c_o}\frac{c_o}{c} = \frac{p_o c_o}{P^{\text{imp}}c} \equiv \text{Region } o\text{'s import share of total imports},$$

where $P^{\text{imp}} \equiv \left(\sum_{o\in\mathcal{O}}\gamma_o^{1/(1-\rho)}p_o^{\rho/(\rho-1)}\right)^{(\rho-1)/\rho}$ is the imported goods price index. The route's Domar weight is then simply given by

$$\text{Route } h\text{'s share in aggregate output} \equiv \frac{\partial Y}{\partial c}\frac{c}{Y} \times \frac{\partial c}{\partial c_o}\frac{c_o}{c} \times \frac{o_h y_h \mathcal{I}}{c_o}$$

The impact of shipping disruptions along route r on the consumption of and spending on domestic goods depends on how the shipping disruptions affect the labor demanded by producers of domestic goods through general equilibrium effects. This in turn depends on how shipping

profits and entry are affected by the disruptions. Similarly, the impact of shipping disruptions on the number of retailers depends on the free-entry condition in the retail sector.

B.2. *Impact of shipping disruptions on importers' output and sourcing*

B.2.1. *Proposition B.1 (Impact of shipping disruptions on importers' output and sales)*

PROPOSITION B.1: (IMPACT OF SHIPPING DISRUPTIONS ON IMPORTERS' OUTPUT AND SALES) A one percent increase in shipping productivity along route r raises importers' output and sales from that same route by

$$\frac{\partial p_o y_r}{\partial X_r}\frac{X_r}{p_o y_r} = \frac{\partial y_r}{\partial X_r}\frac{X_r}{y_r} \approx \frac{\theta}{1-\theta} > 0.$$

In contrast, a one percent increase in shipping productivity along route r has no effect on importers' output and sales from other routes, i.e.,

$$\frac{\partial p_{\hat{o}} y_h}{\partial X_r}\frac{X_r}{p_{\hat{o}} y_h} = \frac{\partial y_h}{\partial X_r}\frac{X_r}{y_h} \approx 0.$$

PROOF: Start with importers' demand for the shipping service provided by firm j along route r conditional on their optimal choice of specialization

$$y_r(j) = \left[\frac{\sigma\theta\chi_r^{\sigma}\, p_o y_r^{(1-\sigma/\theta)} x_r(j)}{g(K_r)\left(\frac{\overline{p}_n}{1/\zeta}\right)^{1/\zeta}\left(\frac{\overline{p}_o}{1/\nu}\right)^{1/\nu}}\right]^{1/(1-\sigma)},$$

where the price of the shipping services was replaced by the firm's markup and marginal cost and, for simplicity, an interior solution for the shipping firm's optimal loading was assumed. Exponentiate both sides, aggregate over all shipping firms, and rearrange to obtain importers' supply conditional on their optimal choice of specialization, or

$$y_r = \left[\frac{\sigma\theta\chi_r\, p_o X_r}{g(K_r)\left(\frac{\overline{p}_n}{1/\zeta}\right)^{1/\zeta}\left(\frac{\overline{p}_o}{1/\nu}\right)^{1/\nu}}\right]^{\theta/(1-\theta)}$$

as well as their sales

$$p_o y_r = \left[\frac{\sigma\theta\chi_r p_o^{1/\theta} X_r}{g(K_r)\left(\frac{\overline{p}_n}{1/\zeta}\right)^{1/\zeta}\left(\frac{\overline{p}_o}{1/\nu}\right)^{1/\nu}} \right]^{\theta/(1-\theta)}.$$

The elasticity of retail output to shipping disruptions is

$$\frac{\partial y_h}{\partial X_r}\frac{X_r}{y_h} = \begin{cases} \frac{\theta}{1-\theta}\left[\underbrace{1}_{\text{PE effect}} + \underbrace{\frac{\partial p_o}{\partial X_r}\frac{X_r}{p_o} - \frac{\partial g(K_h)}{\partial X_r}\frac{X_r}{g(K_h)}}_{\text{GE effect}} \right] & \text{if route } h = r \\ \frac{\theta}{1-\theta}\left[\underbrace{0}_{\text{PE effect}} + \underbrace{\frac{\partial p_{\hat{o}}}{\partial X_r}\frac{X_r}{p_{\hat{o}}} - \frac{\partial g(K_h)}{\partial X_r}\frac{X_r}{g(K_h)}}_{\text{GE effect}} \right] & \text{if route } h \neq r, \end{cases}$$

where $p_{\hat{o}}$ is the retail price of the goods associated with route h when the region of origin is not o. The elasticity of retail sales to shipping disruptions is

$$\frac{\partial p_{\tilde{o}} y_h}{\partial X_r}\frac{X_r}{p_{\tilde{o}} y_h} = \begin{cases} \frac{\theta}{1-\theta}\left[\underbrace{1}_{\text{PE effect}} + \underbrace{\frac{1}{\theta}\frac{\partial p_o}{\partial X_r}\frac{X_r}{p_o} - \frac{\partial g(K_h)}{\partial X_r}\frac{X_r}{g(K_h)}}_{\text{GE effect}} \right] & \text{if route } h = r \text{ and } p_{\tilde{o}} = p_o \\ \frac{\theta}{1-\theta}\left[\underbrace{0}_{\text{PE effect}} + \underbrace{\frac{1}{\theta}\frac{\partial p_{\hat{o}}}{\partial X_r}\frac{X_r}{p_{\hat{o}}} - \frac{\partial g(K_h)}{\partial X_r}\frac{X_r}{g(K_h)}}_{\text{GE effect}} \right] & \text{if route } h \neq r \text{ and } p_{\tilde{o}} = p_{\hat{o}}. \end{cases}$$

Q.E.D.

B.2.2. *Proposition B.2 (Impact of shipping disruptions on retail sourcing)*

PROPOSITION B.2: (IMPACT OF SHIPPING DISRUPTIONS ON RETAIL SOURCING) A one percent increase in shipping productivity along route r raises the share of importers sourcing goods from that same route by

$$\frac{\partial o_r}{\partial X_r}\frac{X_r}{o_r} \approx (1-o_r)\lambda\frac{\theta}{1-\theta}(\Pi_r + f) > 0,$$

where importers' profit from selling goods transported along route r (net of the fixed cost) is $\Pi_r + f = (1-\theta)\left[\frac{\sigma\theta\chi_r p_o^{1/\theta} X_r}{g(K_r)\left(\frac{w}{1/\zeta}\right)^{1/\zeta}\left(\frac{\overline{p}_o}{1/\nu}\right)^{1/\nu}}\right]^{\theta/(1-\theta)}$. A one percent increase in shipping productivity along route r decreases the share of importers sourcing goods from other routes according

to

$$\frac{\partial o_h}{\partial X_r}\frac{X_r}{o_h} \approx -o_r\lambda\frac{\theta}{1-\theta}(\Pi_r + f) < 0,$$

where the optimal sourcing choice, o_r, is given by Equation (4.17).

PROOF: Using importers' first-order conditions, the profit from producing goods from route r conditional on their sourcing decision is

$$\Pi_r = (1-\theta)\left[\frac{\sigma\theta\chi_r p_o^{1/\theta} X_r}{g(K_r)\left(\frac{\overline{p}_n}{1/\zeta}\right)^{1/\zeta}\left(\frac{\overline{p}_o}{1/\nu}\right)^{1/\nu}}\right]^{\theta/(1-\theta)} - f.$$

The impact of route-r shipping disruptions on importers' sourcing choice of goods transported along route h is given by

$$\begin{aligned}\frac{\partial o_h}{\partial X_r}\frac{X_r}{o_h} &= \lambda X_r\left(\frac{\partial \Pi_h}{\partial X_r} - \sum_\kappa o_\kappa \frac{\partial \Pi_\kappa}{\partial X_r}\right)\\ &= \lambda(1-\theta)X_r\left(\frac{\partial p_{\tilde{o}} y_h}{\partial X_r} - \sum_\kappa o_\kappa \frac{\partial p_{\tilde{o}} y_\kappa}{\partial X_r}\right)\end{aligned}$$

Ceteris paribus, the first-order effect of shipping disruptions on the share of importers sourcing goods from route r is

$$\frac{\partial o_r}{\partial X_r}\frac{X_r}{o_r} \approx (1-o_r)\lambda\theta p_o y_r = (1-o_r)\lambda\frac{\theta}{1-\theta}(\Pi_r + f),$$

and the first-order effect of shipping disruptions on the share of importers sourcing goods from routes $h \neq r$ is given by

$$\frac{\partial o_h}{\partial X_r}\frac{X_r}{o_h} = -o_r\lambda\theta p_o y_r = -o_r\lambda\frac{\theta}{1-\theta}(\Pi_r + f),$$

where o_r is given by Equation (4.17). Note that the weighted sum of these elasticities is such that $\sum_\kappa o_\kappa\left(\frac{\partial o_\kappa}{\partial X_r}\frac{X_r}{o_\kappa}\right) = 0$.

Q.E.D.

B.3. *The constrained social planner's problem*

The planner's problem can be solved in four stages: (1) an inner cost-minimization problem over speed and loading per route given capacity; (2) the social price of shipping per route that takes into account that importers have a downward-sloping demand curve and that they can reallocate their sourcing decisions across routes; (3) a capacity allocation per route that internalizes the congestion effect that additional capacity generates; and (4) the characterization of the social marginal values as Lagrange multipliers emerging from the optimization such that all markets clear.

B.3.1. *Stage 1: Per-route shipping cost minimization*

For each route r and given capacity K_r, the choice of average speed s_r and loading ℓ_r is a self-contained cost-minimization problem. It involves only the route's own shipping technology and own input prices, and thus does not interact with any other route's choices. In Stage 1, the planner solves a cost-minimization problem over these margins for each route, subject to the aggregate shipping technology $Q_r \equiv x_r\, A_r\, s_r^{\alpha}\, \ell_r\, K_r \,/\, g(K_r)$ and taking K_r as given. The solution to the shipping cost-minimization problem yields the same marginal cost of shipping as in Equation (4.8) as a function of K_r.[33]

B.3.2. *Stage 2: The social price of shipping*

The planner sets the route-level social price of shipping v_r^{social} for each $r \in \mathcal{R}$, taking as given importers' demand for shipping services and their sourcing decisions. Given that there are redeployment costs, the planner sets the social price of shipping as a markup over the marginal cost as in Equation (4.10) to cover these resources, and the markup is also given by Equation (4.11). However, the price elasticity of demand differs from the decentralized equilibrium as the planner takes into account the price impact on importers' sourcing decisions, and the relevant elasticity is not the firm's inner elasticity.

Denote importers' total demand for shipping services from route r conditional on sourcing goods from that route by $Y_r^{\text{input}} \equiv N y_r(j)$, so that the aggregate shipping output is equal to the aggregate importer demand in line with $Q_r = Y_r^{\text{input}} o_r \mathcal{I}$. The output from that route (Equation (4.14)) can now be expressed as $y_r = \left[\chi_r N^{(1-\sigma)/\sigma} Y_r^{\text{input}}\right]^{\theta}$ and the optimal input demand that maximizes social profits (the analog to Equation (4.15)) is $Y_r^{\text{input}} = \left[\frac{\theta \chi_r^{\sigma}\, v_o^{c,\text{social}} N^{(1-\sigma)\theta/\sigma}}{v_r^{\text{social}}}\right]^{1/(1-\theta)}$, where $v_o^{c,\text{social}}$ is the social marginal value of consumption from region o.

[33] The corner case for loading $\ell_r = 1$ is handled by a multiplier $\mu_r > 0$ on the loading bound, with the marginal cost modified accordingly (cf. footnote 21).

The price elasticity of demand now depends on how total demand for shipping services from route r, Y_r^{input}, responds to changes in the social price of shipping and how importers reallocate across routes when that price changes. In the decentralized equilibrium, the price elasticity of demand depends solely on the inner elasticity of substitution between shipping firms (and is equivalent to $1/(1-\sigma)$). In the planner's problem, the price elasticity of demand is $\xi_r = \frac{1}{1-\theta}\left\{1 - \lambda(1-o_r)\left[(1-\theta)v_r^{\text{social}}Y_r^{\text{input}} - \theta f\right]\right\}$. The relevant elasticity is now the elasticity of retail output to the total demand for imports, θ, not the firm-specific σ. It also takes into account that importers can reallocate their sourcing to other goods. The resulting social markup is

$$m_r^{\text{social}} = \frac{1}{\theta}\left\{\frac{1 - \lambda(1-o_r)\left[(1-\theta)v_r^{\text{social}}Y_r^{\text{input}} - \theta f\right]}{1 - \lambda(1-o_r)/\theta\left[(1-\theta)v_r^{\text{social}}Y_r^{\text{input}} - \theta f\right]}\right\}, \tag{B.2}$$

which could be greater or smaller than $1/\theta$ and the decentralized markup $1/\sigma$. The social markup is now a fixed point as it enters both the left- and right-hand sides.

B.3.3. *Stage 3: Capacity allocation*

As the planner sets the social price of shipping services as a markup over the marginal cost, the planner has resources to cover the aggregate capacity adjustment costs. When choosing where to allocate capacity, the planner takes congestion, $g(K_r)$, and the aggregate capacity constraint, $\sum_{r\in\mathcal{R}} K_r \leq K$, into account. The more capacity is allocated to a route, the higher is the marginal cost of shipping.

The first-order condition of the planner's problem for route-r total capacity, K_r, when the optimal loading of ships is interior (i.e., $\ell_r < 1$), yields a similar expression to Equation (4.13)

$$N\left\{\underbrace{\frac{\left(v_r^{\text{social}} - (1+\phi)mc_r\right)x_r n_r(s_r^\star)\ell_r^\star}{g(K_r)}}_{\text{profit per ton traveled along route } r} - \underbrace{\frac{1}{|\mathcal{R}|}\sum_h \frac{\left(v_h^{\text{social}} - (1+\phi)mc_h\right)x_h n_h(s_h^\star)\ell_h^\star}{g(K_h)}}_{\text{average profit per ton traveled}}\right\} = \overline{p}_\kappa\left[K_r - \underbrace{\frac{1}{|\mathcal{R}|}(K-\overline{K})}_{\text{average capacity per route}}\right], \tag{B.3}$$

which equates the marginal benefit of reallocating capacity to route r to its marginal cost. The right-hand side of Equation (B.3) is the same as each firm's (Equation (4.13)) summed over all N firms. The left-hand side differs in two important ways. First, the congestion effect is taken into account, which raises the marginal cost of shipping by a factor of ϕ. Second, the social price of shipping includes a markup that takes into account how importers reallocate across

routes and how total demand for imported goods changes when the social price of shipping changes.

B.3.4. *Stage 4: The social price of consumption and labor*

The social marginal values of consumption, $v_o^{c,\text{social}}$, are now obtained from the Lagrange multipliers on the imported goods market clearing condition for each region o, so that $v_o^{c,\text{social}} = \partial u/\partial c_o$. Similarly, the social price of domestically-produced goods is $v_d^{\text{social}} = \partial u/\partial d$. The multiplier on the labor resource constraint is fixed at 1 by the numeraire normalization (equivalent to normalizing $w = 1$), which implies that $v_d^{\text{social}} = 1/z_d$.

Finally, the social planner ensures that the labor resource constraint holds, so that $l_d + \sum_{r\in\mathcal{R}} \{mc_r Q_r - N\mu_r^{\text{loading}}/\nu + \overline{p}_\kappa K_r^2/(2N)\} = 1$. This guarantees that all resources at the disposal of the social planner, $1 + f\mathcal{I}$, are allocated efficiently.

B.4. *The impact of tariffs on real aggregate output*

PROPOSITION B.3: (IMPACT OF TARIFFS ON REAL AGGREGATE OUTPUT) The elasticity of real aggregate output Y to tariffs τ_o on goods from region $o \in \mathcal{O}$ is given by

$$\frac{\partial Y}{\partial \tau_o}\frac{\tau_o}{Y} = \sum_{h\in\mathcal{R}} \left(\begin{smallmatrix}\text{Route } h\text{'s share in}\\ \text{aggregate output}\end{smallmatrix}\right) \times \left(\frac{\partial y_h}{\partial \tau_o}\frac{\tau_o}{y_h} + \frac{\partial o_h}{\partial \tau_o}\frac{\tau_o}{o_h}\right)$$
$$+ \left(\begin{smallmatrix}\text{Import share in}\\ \text{aggregate output}\end{smallmatrix}\right) \times \left(\frac{\partial \mathcal{I}}{\partial \tau_o}\frac{\tau_o}{\mathcal{I}}\right) + \left(\begin{smallmatrix}\text{Domestic share in}\\ \text{aggregate output}\end{smallmatrix}\right) \times \left(\frac{\partial d}{\partial \tau_o}\frac{\tau_o}{d}\right),$$

where $\left(\begin{smallmatrix}\text{Route } h\text{'s share in}\\ \text{aggregate output}\end{smallmatrix}\right) = o_h y_h \mathcal{I}/(w + \Lambda + T)$, $\left(\begin{smallmatrix}\text{Domestic share in}\\ \text{aggregate output}\end{smallmatrix}\right) = p_d d/(w + \Lambda + T)$, and $\left(\begin{smallmatrix}\text{Import share in}\\ \text{aggregate output}\end{smallmatrix}\right) = 1 - \left(\begin{smallmatrix}\text{Domestic share in}\\ \text{aggregate output}\end{smallmatrix}\right)$.

PROOF: The result follows from the same steps as the proof of Proposition 4.1. *Q.E.D.*

Propositions B.4 and B.5 below decompose the route-specific elasticities $\frac{\partial y_h}{\partial \tau_o}\frac{\tau_o}{y_h}$ and $\frac{\partial o_h}{\partial \tau_o}\frac{\tau_o}{o_h}$.

PROPOSITION B.4: (IMPACT OF TARIFFS ON IMPORTERS' OUTPUT AND SALES) The elasticity of retail output to tariffs is

$$\frac{\partial y_h}{\partial \tau_o}\frac{\tau_o}{y_h} = \begin{cases} -\frac{\theta}{1-\theta}\left[\underbrace{\frac{\tau_o}{1+\tau_o}}_{\text{PE effect}} + \underbrace{\frac{\partial g(K_h)}{\partial \tau_o}\frac{\tau_o}{g(K_h)} - \frac{\partial p_o}{\partial \tau_o}\frac{\tau_o}{p_o}}_{\text{GE effect}}\right] & \text{if route } h\text{'s origin} = o \\ -\frac{\theta}{1-\theta}\left[\underbrace{0}_{\text{PE effect}} + \underbrace{\frac{\partial g(K_h)}{\partial \tau_o}\frac{\tau_o}{g(K_h)} - \frac{\partial p_{\hat{o}}}{\partial \tau_o}\frac{\tau_o}{p_{\hat{o}}}}_{\text{GE effect}}\right] & \text{if route } h\text{'s origin} \neq o, \end{cases}$$

where $p_{\tilde{o}}$ is the retail price of the goods associated with route h when the region of origin is not o. The elasticity of retail sales to tariffs is

$$\frac{\partial p_{\tilde{o}} y_h}{\partial \tau_o} \frac{\tau_o}{p_{\tilde{o}} y_h} = \begin{cases} -\frac{\theta}{1-\theta} \left[\underbrace{\frac{\tau_o}{1+\tau_o}}_{\text{PE effect}} + \underbrace{\frac{\partial g(K_h)}{\partial \tau_o} \frac{\tau_o}{g(K_h)} - \frac{1}{\theta} \frac{\partial p_o}{\partial \tau_o} \frac{\tau_o}{p_o}}_{\text{GE effect}} \right] & \text{if route } h = r \text{ and } p_{\tilde{o}} = p_o \\ -\frac{\theta}{1-\theta} \left[\underbrace{0}_{\text{PE effect}} + \underbrace{\frac{\partial g(K_h)}{\partial \tau_o} \frac{\tau_o}{g(K_h)} - \frac{1}{\theta} \frac{\partial p_{\hat{o}}}{\partial \tau_o} \frac{\tau_o}{p_{\hat{o}}}}_{\text{GE effect}} \right] & \text{if route } h \neq r \text{ and } p_{\tilde{o}} = p_{\hat{o}}. \end{cases}$$

PROOF: Retail output of goods sourced from route h with port fees, $\mathfrak{f}_o$, and tariffs, τ_o, is now given by

$$y_h = \left[\frac{\sigma \theta \chi_h \, p_o X_h}{(1+\tau_o) g(K_h) \left(\frac{\overline{p}_n}{1/\zeta} \right)^{1/\zeta} \left(\frac{\overline{p}_o + \mathfrak{f}_o}{1/\nu} \right)^{1/\nu}} \right]^{\theta/(1-\theta)} \tag{B.4}$$

and importers' sales are

$$p_o y_h = \left[\frac{\sigma \theta \chi_h \, p_o^{1/\theta} X_h}{(1+\tau_o) g(K_h) \left(\frac{\overline{p}_n}{1/\zeta} \right)^{1/\zeta} \left(\frac{\overline{p}_o + \mathfrak{f}_o}{1/\nu} \right)^{1/\nu}} \right]^{\theta/(1-\theta)}. \tag{B.5}$$

Differentiating both with respect to τ_o yields the elasticity of retail output and sales to tariffs. *Q.E.D.*

Proposition B.4 shows that an increase in tariffs does not necessarily reduce retail output. The impact depends on how it affects retail prices and congestion. On one hand, an increase in tariffs on region o puts upward pressure on the retail price of goods from that same region, i.e., $\frac{\partial p_o}{\partial \tau_o} \frac{\tau_o}{p_o} \geq 0$. An increase in retail prices encourages importers to supply more foreign goods, but reduces consumer demand. On the other hand, an increase in tariffs decreases congestion along routes originating in the region where tariffs are levied, since $\frac{\partial g(K_h)}{\partial \tau_o} \frac{\tau_o}{g(K_h)} \leq 0$, and potentially leads to an increase in congestion on routes originating in other regions. A fall in congestion works like a productivity boost for shipping firms, allowing them to supply more goods in a shorter amount of time and at cheaper prices. The cheaper shipping services in turn encourage importers to purchase more foreign goods since retail demand slopes down in the price of shipping services, $\frac{\partial y_h}{\partial p_h(j)} \frac{p_h(j)}{y_h} \leq 0$, which then leads to an increase in retail output.

PROPOSITION B.5: (IMPACT OF TARIFFS ON RETAIL SOURCING) The elasticity of importers' sourcing decision to tariffs is given by

$$\frac{\partial o_h}{\partial \tau_o}\frac{\tau_o}{o_h} = \lambda(1-\theta)\tau_o\left(\frac{\partial p_{\tilde{o}} y_h}{\partial \tau_o} - \sum_{\kappa} o_\kappa \frac{\partial p_{\tilde{o}} y_\kappa}{\partial \tau_o}\right),$$

where $p_{\tilde{o}}$ is the retail price of goods sourced from route κ.

PROOF: Importers source goods according to the discrete choice rule (4.17). Differentiating with respect to τ_o yields

$$\frac{\partial o_h}{\partial \tau_o}\frac{\tau_o}{o_h} = \lambda\tau_o\left(\frac{\partial \Pi_h}{\partial \tau_o} - \sum_{\kappa\in\mathcal{R}} o_\kappa \frac{\partial \Pi_\kappa}{\partial \tau_o}\right).$$

Retail profit from sourcing goods from route h is

$$\Pi_h = (1-\theta)\left[\frac{\sigma\theta\chi_h p_o^{1/\theta} X_h}{(1+\tau_o)g(K_h)\left(\frac{\overline{p}_n}{1/\zeta}\right)^{1/\zeta}\left(\frac{\overline{p}_o+\mathfrak{f}_o}{1/\nu}\right)^{1/\nu}}\right]^{\theta/(1-\theta)} - f. \tag{B.6}$$

As $\frac{\partial \Pi_h}{\partial \tau_o} = (1-\theta)\frac{\partial (p_o y_h)}{\partial \tau_o}$, substituting it into the expression above yields the result. *Q.E.D.*

The larger λ is, the more sensitive importers' sourcing decision is to tariff-induced differences in route profitability and the more imports reallocate away from the taxed routes toward routes whose profitability rises.

B.5. *The impact of port fees on real aggregate output*

PROPOSITION B.6: (IMPACT OF PORT FEES ON REAL AGGREGATE OUTPUT) The elasticity of real aggregate output Y to port fees $\mathfrak{f}_o$ on goods from region $o \in \mathcal{O}$ is given by

$$\begin{aligned}\frac{\partial Y}{\partial \mathfrak{f}_o}\frac{\mathfrak{f}_o}{Y} = &\sum_{h\in\mathcal{R}} \left(\tfrac{\text{Route } h\text{'s share in}}{\text{aggregate output}}\right) \times \left(\frac{\partial y_h}{\partial \mathfrak{f}_o}\frac{\mathfrak{f}_o}{y_h} + \frac{\partial o_h}{\partial \mathfrak{f}_o}\frac{\mathfrak{f}_o}{o_h}\right) \\ &+ \left(\tfrac{\text{Import share in}}{\text{aggregate output}}\right) \times \left(\frac{\partial \mathcal{I}}{\partial \mathfrak{f}_o}\frac{\mathfrak{f}_o}{\mathcal{I}}\right) + \left(\tfrac{\text{Domestic share in}}{\text{aggregate output}}\right) \times \left(\frac{\partial d}{\partial \mathfrak{f}_o}\frac{\mathfrak{f}_o}{d}\right),\end{aligned}$$

where $\frac{\text{Route } h\text{'s share in}}{\text{aggregate output}} = o_h y_h \mathcal{I}/(w+\Lambda+T)$, $\frac{\text{Domestic share in}}{\text{aggregate output}} = p_d d/(w+\Lambda+T)$, and $\frac{\text{Import share in}}{\text{aggregate output}} = 1 - \frac{\text{Domestic share in}}{\text{aggregate output}}$.

PROOF: The result follows from the same steps as the proof of Proposition 4.1. *Q.E.D.*

Propositions B.7 and B.8 below decompose the route-specific elasticities $\frac{\partial y_h}{\partial \mathfrak{f}_o}\frac{\mathfrak{f}_o}{y_h}$ and $\frac{\partial o_h}{\partial \mathfrak{f}_o}\frac{\mathfrak{f}_o}{o_h}$.

PROPOSITION B.7: (IMPACT OF PORT FEES ON IMPORTERS' OUTPUT AND SALES) The elasticity of retail output to port fees is

$$\frac{\partial y_h}{\partial \mathfrak{f}_o}\frac{\mathfrak{f}_o}{y_h} = \begin{cases} -\frac{\theta}{1-\theta}\left[\underbrace{\frac{1}{\nu}\frac{\mathfrak{f}_o}{(\overline{p}_o+\mathfrak{f}_o)}}_{\text{PE effect}} + \underbrace{\frac{\partial g(K_h)}{\partial \mathfrak{f}_o}\frac{\mathfrak{f}_o}{g(K_h)} - \frac{\partial p_o}{\partial \mathfrak{f}_o}\frac{\mathfrak{f}_o}{p_o}}_{\text{GE effect}}\right] & \text{if route } h\text{'s origin} = o \\ -\frac{\theta}{1-\theta}\left[\underbrace{0}_{\text{PE effect}} + \underbrace{\frac{\partial g(K_h)}{\partial \mathfrak{f}_o}\frac{\mathfrak{f}_o}{g(K_h)} - \frac{\partial p_{\hat{o}}}{\partial \mathfrak{f}_o}\frac{\mathfrak{f}_o}{p_{\hat{o}}}}_{\text{GE effect}}\right] & \text{if route } h\text{'s origin} \neq o, \end{cases}$$

where $p_{\hat{o}}$ is the retail price of the goods associated with route h when the region of origin is not o. The elasticity of retail sales to port fees is

$$\frac{\partial p_{\tilde{o}} y_h}{\partial \mathfrak{f}_o}\frac{\mathfrak{f}_o}{p_{\tilde{o}} y_h} = \begin{cases} -\frac{\theta}{1-\theta}\left[\underbrace{\frac{1}{\nu}\frac{\mathfrak{f}_o}{(\overline{p}_o+\mathfrak{f}_o)}}_{\text{PE effect}} + \underbrace{\frac{\partial g(K_h)}{\partial \mathfrak{f}_o}\frac{\mathfrak{f}_o}{g(K_h)} - \frac{1}{\theta}\frac{\partial p_o}{\partial \mathfrak{f}_o}\frac{\mathfrak{f}_o}{p_o}}_{\text{GE effect}}\right] & \text{if route } h = r \text{ and } p_{\tilde{o}} = p_o \\ -\frac{\theta}{1-\theta}\left[\underbrace{0}_{\text{PE effect}} + \underbrace{\frac{\partial g(K_h)}{\partial \mathfrak{f}_o}\frac{\mathfrak{f}_o}{g(K_h)} - \frac{1}{\theta}\frac{\partial p_{\hat{o}}}{\partial \mathfrak{f}_o}\frac{\mathfrak{f}_o}{p_{\hat{o}}}}_{\text{GE effect}}\right] & \text{if route } h \neq r \text{ and } p_{\tilde{o}} = p_{\hat{o}}. \end{cases}$$

PROOF: Differentiating Equations (B.4) and (B.5) with respect to $\mathfrak{f}_o$ yields the elasticity of retail output and sales to port fees. *Q.E.D.*

As was the case with tariffs, Proposition B.7 shows that an increase in port fees does not necessarily reduce retail output. First, the direct effect now operates through the input price $\mathfrak{f}_{o_h}/(\overline{p}_{o_h}+\mathfrak{f}_{o_h})$ rather than the tariff wedge $\tau_o/(1+\tau_{o_h})$, and is rescaled by the cost exponent $1/\nu$ because port fees are levied on shipping firms rather than retailers. This makes their direct transmission weaker than that of tariffs. Second, an increase in port fees on a particular region decreases congestion along routes originating in that same region and potentially raises congestion on routes originating in other regions. It can also lead to an increase in retail prices as port fees increase the cost of shipping services.

PROPOSITION B.8: (IMPACT OF PORT FEES ON RETAIL SOURCING) The elasticity of importers' sourcing decision to port fees is given by

$$\frac{\partial o_h}{\partial \mathfrak{f}_o}\frac{\mathfrak{f}_o}{o_h} = \lambda(1-\theta)\mathfrak{f}_o\left(\frac{\partial\left(p_o y_h\right)}{\partial \mathfrak{f}_o} - \sum_{\kappa\in\mathcal{R}} o_\kappa \frac{\partial\left(p_{\tilde{o}} y_\kappa\right)}{\partial \mathfrak{f}_o}\right),$$

where $p_{\tilde{o}}$ is the retail price of goods sourced from route κ.

PROOF: Importers source goods according to the discrete choice rule (4.17). Differentiating with respect to $\mathfrak{f}_o$ yields

$$\frac{\partial o_h}{\partial \mathfrak{f}_o}\frac{\mathfrak{f}_o}{o_h} = \lambda \mathfrak{f}_o \left(\frac{\partial \Pi_h}{\partial \mathfrak{f}_o} - \sum_{\kappa \in \mathcal{R}} o_\kappa \frac{\partial \Pi_\kappa}{\partial \mathfrak{f}_o} \right).$$

Retail profit from sourcing goods from route h is given by Equation (B.6). As $\frac{\partial \Pi_h}{\partial \mathfrak{f}_o} = (1-\theta)\frac{\partial (p_o y_h)}{\partial \mathfrak{f}_o}$, substituting it into the expression above yields the result. *Q.E.D.*

The larger λ is, the more sensitive importers' sourcing decision is to fee-induced differences in route profitability and the more imports reallocate away from the fee-affected routes toward routes whose profitability rises.

C: QUANTITATIVE ANALYSIS

C.1. *Calibration and baseline simulation*

TABLE C.1

AVERAGE NUMBER OF TRIPS AND AVERAGE SPEED

	Log(Average Number of Trips per Vessel)			
	OLS		WLS	
	(1)	(2)	(3)	(4)
Log(Average Sailing Speed)	-0.197	0.035	0.674***	0.663**
	(0.140)	(0.148)	(0.233)	(0.327)
Route FE	Yes	Yes	Yes	Yes
Year & Month FEs	No	Yes	No	Yes
Weights	None	None	DWT	DWT
Observations	666	666	666	666
R^2	0.901	0.955	0.853	0.940

Note: Robust standard errors in parentheses. *** p<0.01, ** p<0.05, * p<0.1.

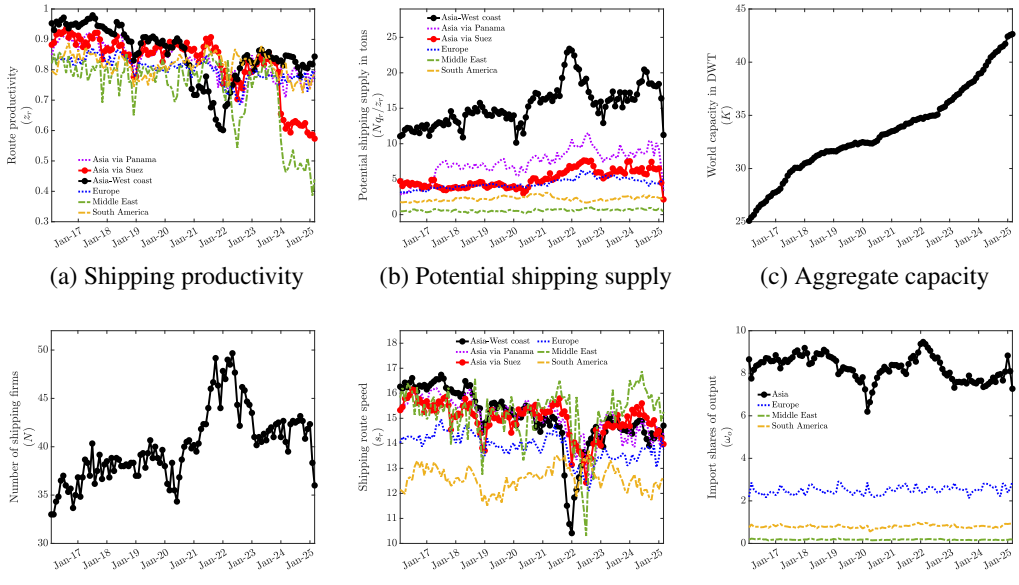
TABLE C.2

TOTAL PORT CONGESTION TIME AND TOTAL NUMBER OF PORT CALLS

	Log(Total Congestion Time)			
	OLS		WLS	
	(1)	(2)	(3)	(4)
Log(Total Port Calls)	1.409***	1.750***	0.868***	1.296***
	(0.074)	(0.076)	(0.080)	(0.085)
Port FE	Yes	Yes	Yes	Yes
Year & Month FEs	No	Yes	No	Yes
Weights	None	None	Port Calls	Port Calls
Observations	5,139	5,139	5,139	5,139
R^2	0.751	0.776	0.760	0.784

Note: Robust standard errors in parentheses. *** p<0.01, ** p<0.05, * p<0.1.

FIGURE C.1.—Targeted time series, February 2017–March 2025

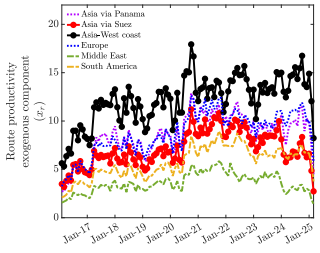


(a) Shipping productivity (b) Potential shipping supply (c) Aggregate capacity

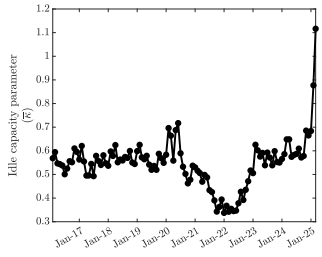
(d) Number of shipping firms (e) Average sailing speeds (f) Import shares

Note: Panel C.1a shows our measure of shipping productivity defined as the ratio of effective shipping supply to potential shipping supply for the six shipping routes. Panel C.1b shows the potential shipping supply in tons for the six shipping routes. Panel C.1c shows the world capacity in DWT. Panel C.1d shows the number of shipping firms. Panel C.1e shows the average sailing speeds along the six shipping routes. Panel C.1f shows the import shares of output from Asia, Europe, the Middle East, and South America. The targeted number of retail firms is equal to one over the same period. All these model-implied time series match the data.

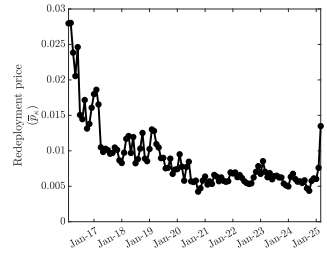
FIGURE C.2.—Evolution of the underlying exogenous variables, February 2017–March 2025



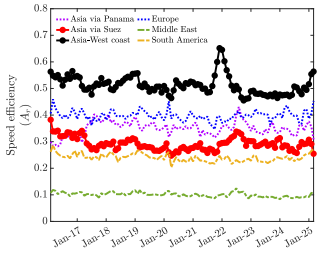
(a) Route productivity



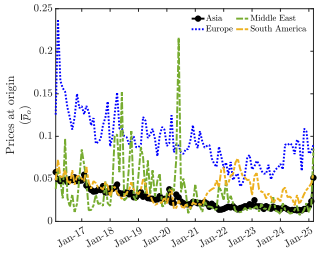
(b) Idle capacity parameter



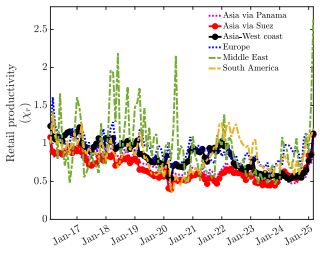
(c) Redeployment price



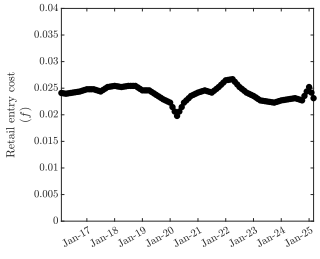
(d) Speed efficiency



(e) Origin prices



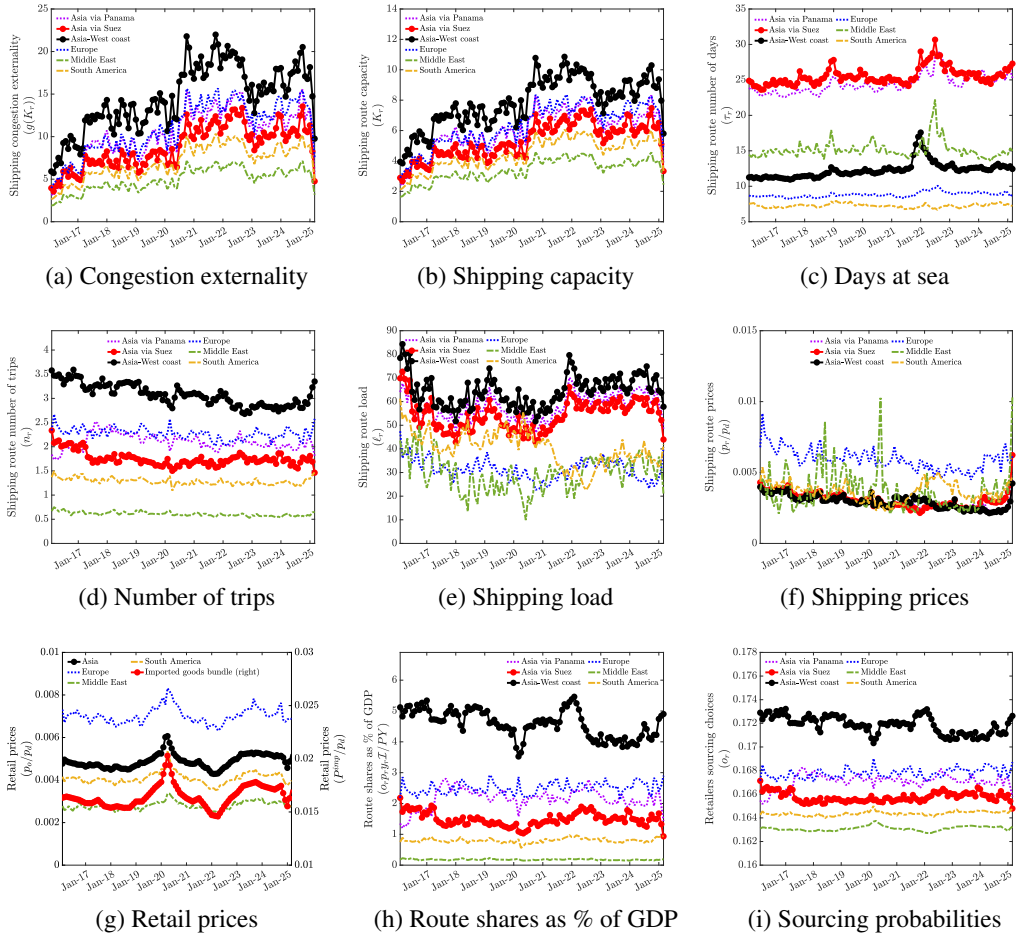
(f) Retail productivity



(g) Retail entry cost

Note: Panel C.2a shows the exogenous component of the shipping productivity. Panel C.2b shows the idle capacity parameter. Panel C.2c shows the price of redeployment. Panel C.2d shows the speed efficiency. Panel C.2e shows the origin prices of goods produced in Asia, Europe, the Middle East, and South America. Panel C.2f shows retailers' productivity. Panel C.2g shows the entry cost in the retail market. These exogenous variables match the time series displayed in Figure C.1 together with the constraint on the number of retail firms.

FIGURE C.3.—Evolution of other endogenous variables, February 2017–March 2025



(a) Congestion externality (b) Shipping capacity (c) Days at sea

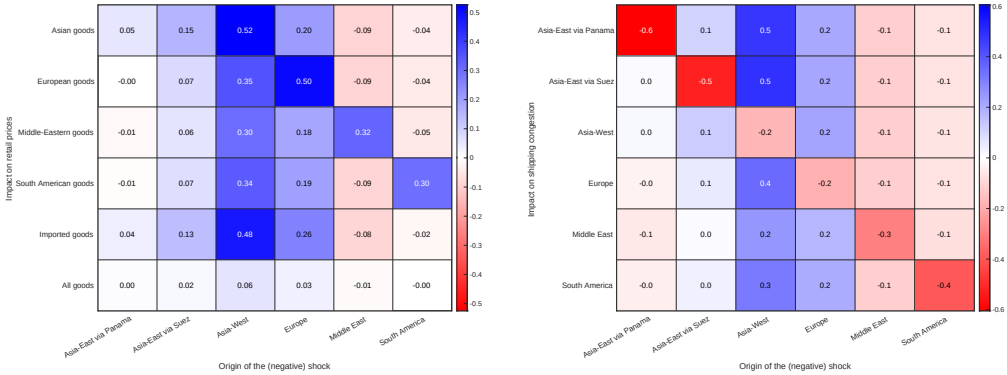
(d) Number of trips (e) Shipping load (f) Shipping prices

(g) Retail prices (h) Route shares as % of GDP (i) Sourcing probabilities

Note: Panel C.3a shows the congestion externality in shipping productivity. Panel C.3b shows the aggregate shipping capacity. Panel C.3c shows the average number of days spent on voyages to the U.S. Panel C.3d shows the average number of trips. Panel C.3e shows the shipping load. Panel C.3f shows the price of shipping services. Panel C.3g shows the retail price of imported goods. Panel C.3h shows the route shares as a fraction of GDP. Panel C.3i shows the retailers' sourcing probabilities.

C.2. *Proposition 4.1 on the impact of shipping disruptions on aggregate output and consumer welfare*

FIGURE C.4.—Impact of disruptions on retail prices and congestion

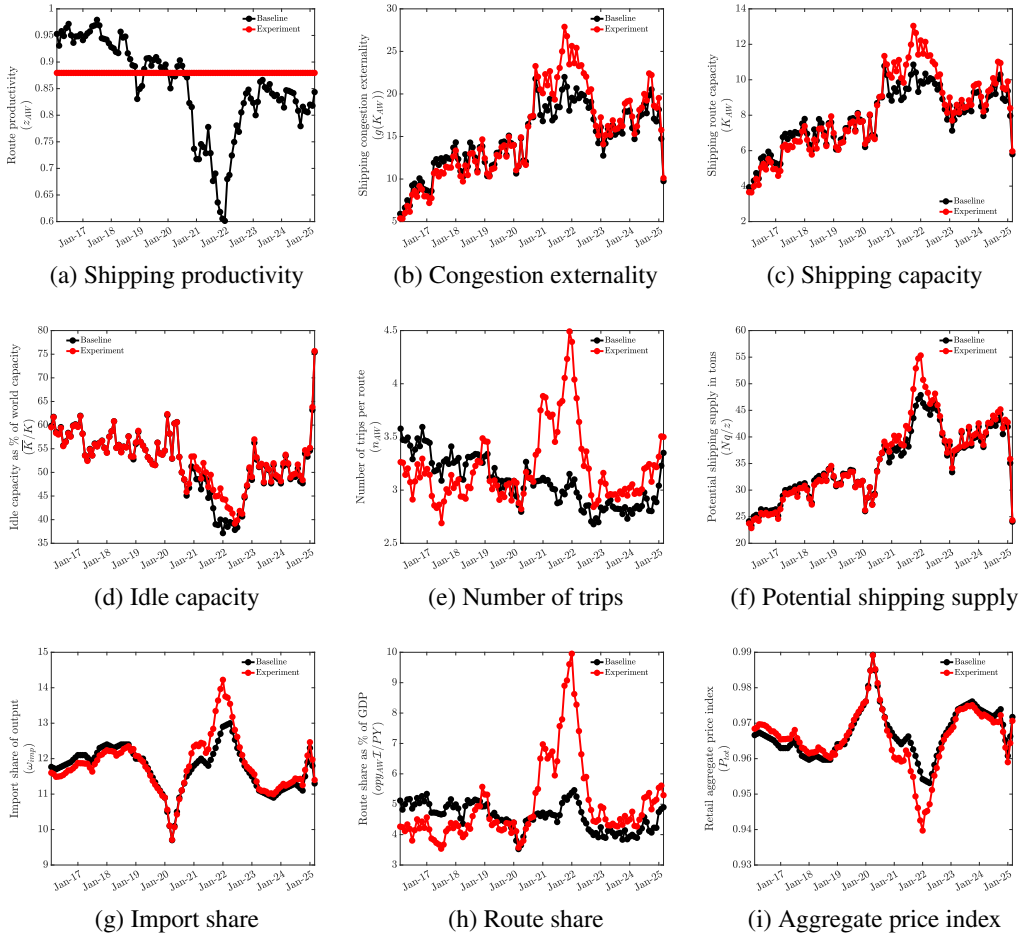


(a) Impact on retail prices (b) Impact on congestion

Note: Panel (a) displays the elasticity of retail prices of goods originating in region o to disruptions along route r, $-(\partial p_o/\partial X_r)(X_r/p_o)$. Panel (b) displays the elasticity of the congestion externality along route h to disruptions along route r, $-(\partial g(K_h)/\partial X_r)(X_r/g(K_h))$.

C.3. *Impact of port congestion in the summer and fall of 2021*

FIGURE C.5.—Evolution of selected aggregates: baseline vs. low shipping disruptions along the Asia to the West Coast route, 2017–2025



(a) Shipping productivity (b) Congestion externality (c) Shipping capacity

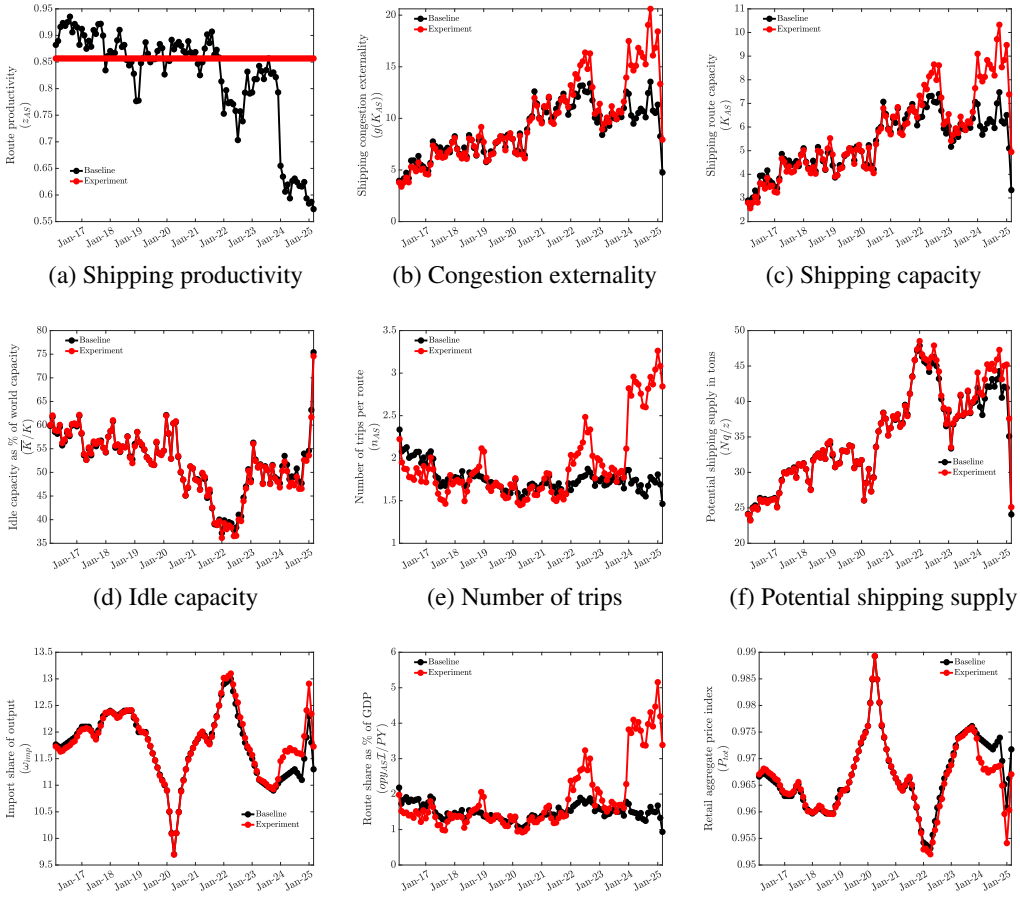
(d) Idle capacity (e) Number of trips (f) Potential shipping supply

(g) Import share (h) Route share (i) Aggregate price index

Note: Panel (a) shows the shipping productivity along the Asia to West Coast route. Panel (b) shows the congestion externality along the Asia to West Coast route. Panel (c) shows the shipping capacity allocated to the Asia to West Coast route. Panel (d) shows the idle capacity as a share of world capacity. Panel (e) shows the number of trips realized along the Asia to West Coast route. Panel (f) shows the U.S.-bound potential shipping supply. Panel (g) shows the import share of GDP. Panel (h) shows the Asia to West Coast route share of GDP. Panel (i) shows the aggregate price index.

C.4. *Impact of security threats in the Red Sea in early 2024*

FIGURE C.6.—Evolution of selected aggregates: baseline vs. low shipping disruptions along the Asia to the East Coast route via the Suez Canal, 2017–2025



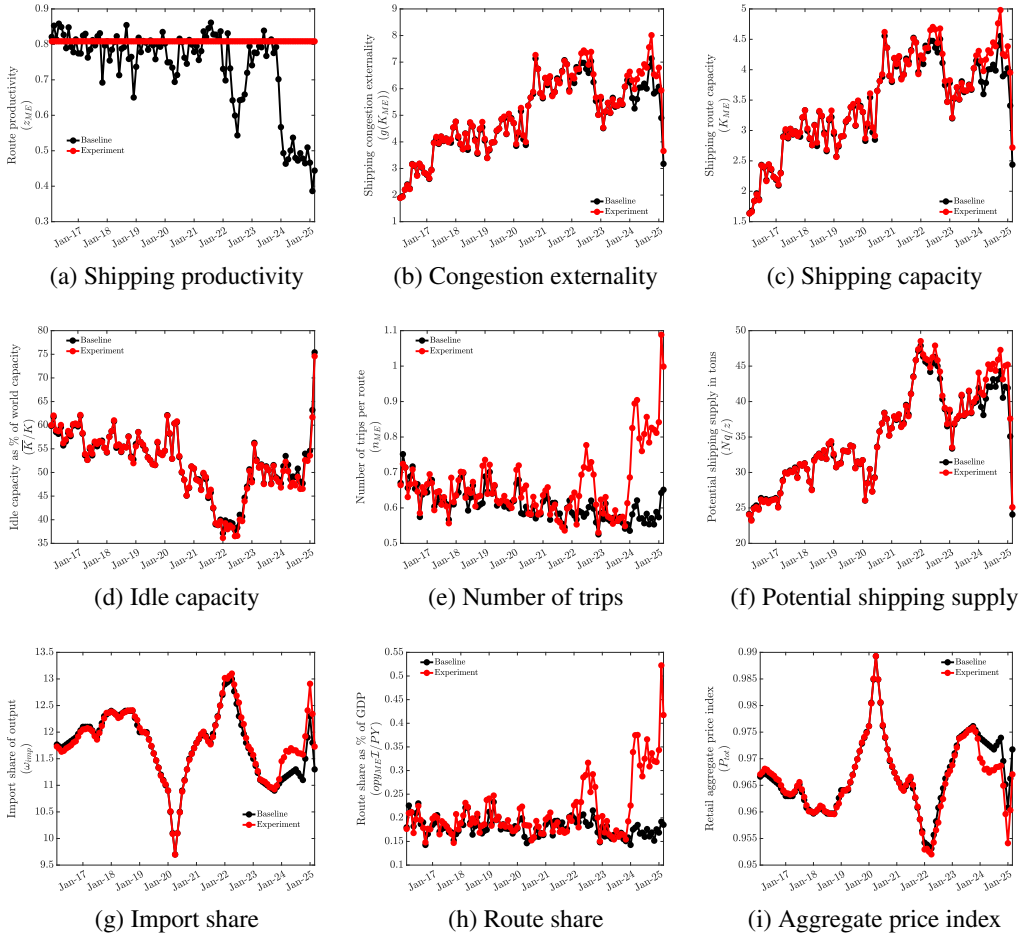
(a) Shipping productivity (b) Congestion externality (c) Shipping capacity

(d) Idle capacity (e) Number of trips (f) Potential shipping supply

(g) Import share (h) Route share (i) Aggregate price index

Note: Panel (a) shows the shipping productivity along the Asia to East Coast via the Suez Canal route. Panel (b) shows the congestion externality along the Asia to East Coast via the Suez Canal route. Panel (c) shows the shipping capacity allocated to the Asia to East Coast via the Suez Canal route. Panel (d) shows the idle capacity as a share of world capacity. Panel (e) shows the number of trips realized along the Asia to East Coast via the Suez Canal route. Panel (f) shows the U.S.-bound potential shipping supply. Panel (g) shows the import share of GDP. Panel (h) shows the Asia to East Coast via the Suez Canal route share of GDP. Panel (i) shows the aggregate price index.

FIGURE C.7.—Evolution of selected aggregates: baseline vs. low shipping disruptions along the Middle East to the East Coast route, 2017–2025



(a) Shipping productivity (b) Congestion externality (c) Shipping capacity

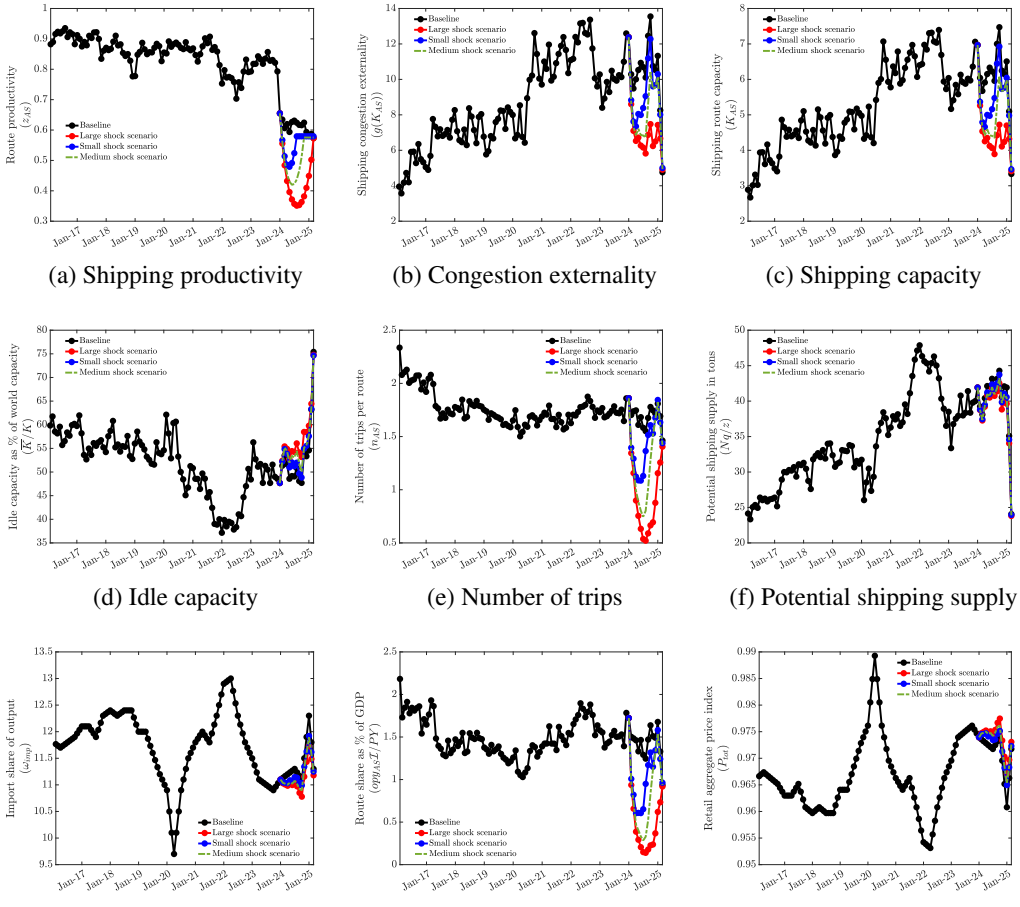
(d) Idle capacity (e) Number of trips (f) Potential shipping supply

(g) Import share (h) Route share (i) Aggregate price index

Note: Panel (a) shows the shipping productivity along the Middle East to the East Coast route. Panel (b) shows the congestion externality along the Middle East to the East Coast route. Panel (c) shows the shipping capacity allocated to the Middle East to the East Coast route. Panel (d) shows the idle capacity as a share of world capacity. Panel (e) shows the number of trips realized along the Middle East to the East Coast route. Panel (f) shows the U.S.-bound potential shipping supply. Panel (g) shows the import share of GDP. Panel (h) shows the Middle East to the East Coast route share of GDP. Panel (i) shows the aggregate price index.

C.5. *Impact of the Navy's intervention in the Red Sea in 2024*

FIGURE C.8.—Evolution of selected aggregates: baseline vs. no Navy support along the Asia to the East Coast route via the Suez Canal, February 2016–March 2025



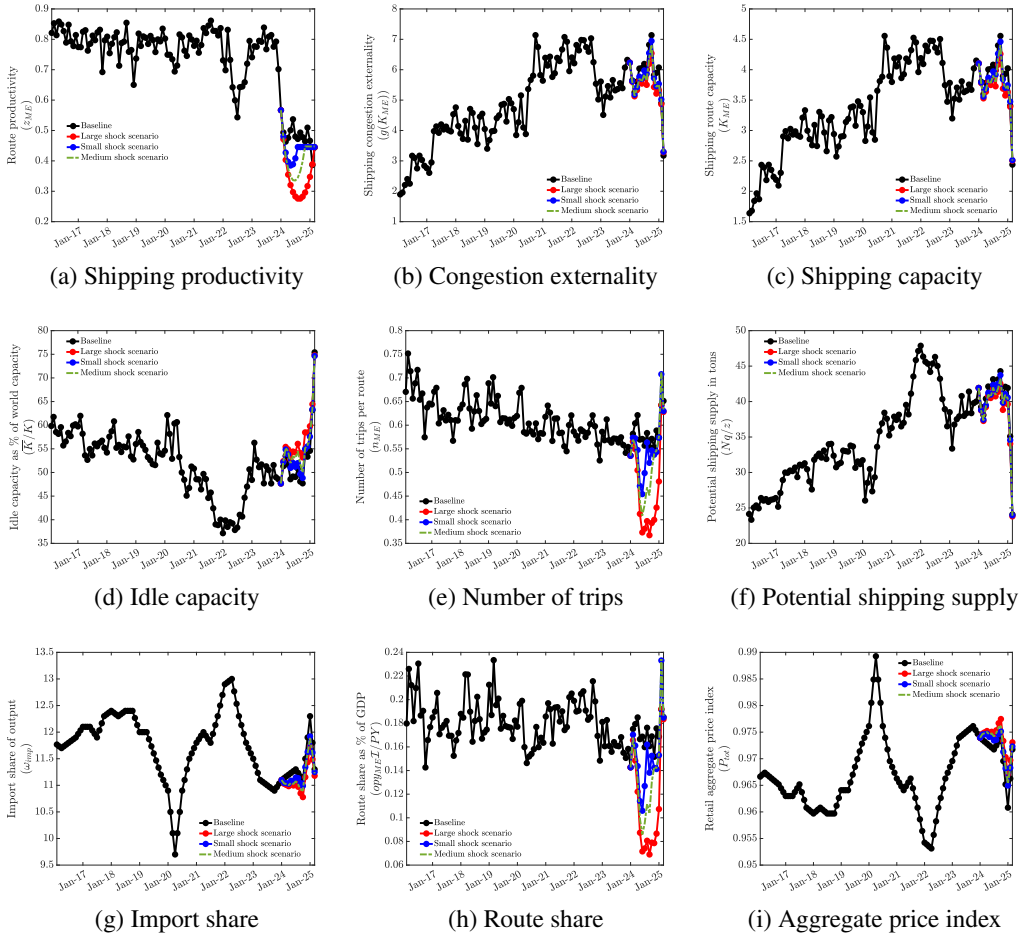
(a) Shipping productivity (b) Congestion externality (c) Shipping capacity

(d) Idle capacity (e) Number of trips (f) Potential shipping supply

(g) Import share (h) Route share (i) Aggregate price index

Note: Panel (a) shows the shipping productivity along the Asia to East Coast via the Suez Canal route. Panel (b) shows the congestion externality along the Asia to East Coast via the Suez Canal route. Panel (c) shows the shipping capacity allocated to the Asia to East Coast via the Suez Canal route. Panel (d) shows the idle capacity as a share of world capacity. Panel (e) shows the number of trips realized along the Asia to East Coast via the Suez Canal route. Panel (f) shows the U.S.-bound potential shipping supply. Panel (g) shows the import share of GDP. Panel (h) shows the Asia to East Coast via the Suez Canal route share of GDP. Panel (i) shows the aggregate price index.

FIGURE C.9.—Evolution of selected aggregates: baseline vs. no Navy support along the Middle East to the East Coast route, 2017–2025



(a) Shipping productivity (b) Congestion externality (c) Shipping capacity

(d) Idle capacity (e) Number of trips (f) Potential shipping supply

(g) Import share (h) Route share (i) Aggregate price index

Note: Panel (a) shows the shipping productivity along the Middle East to the East Coast route. Panel (b) shows the congestion externality along the Middle East to the East Coast route. Panel (c) shows the shipping capacity allocated to the Middle East to the East Coast route. Panel (d) shows the idle capacity as a share of world capacity. Panel (e) shows the number of trips realized along the Middle East to the East Coast route. Panel (f) shows the U.S.-bound potential shipping supply. Panel (g) shows the import share of GDP. Panel (h) shows the Middle East to the East Coast route share of GDP. Panel (i) shows the aggregate price index.

C.6. *Robustness of the welfare estimates*

TABLE C.3

ROBUSTNESS OF THE WELFARE ESTIMATES

Specification	Equivalent variation (% of GDP)		
	No 2021 port disruptions	No 2024 security threats	No 2024 Navy intervention
Baseline	0.914	0.424	-0.240
Panel A: Shipping markup and costs			
Lower shipping markup ($\sigma = 0.88$)	0.972	0.451	-0.229
Higher shipping markup ($\sigma = 0.72$)	0.851	0.396	-0.253
Lower trip cost curv. ($\zeta = 1.8$, $\nu = 2.2$)	0.914	0.424	-0.240
Higher trip cost curv. ($\zeta = 2.2$, $\nu = 1.8$)	0.914	0.424	-0.240
Panel B: Importers' markup and sourcing			
Lower retail markup ($\theta = 0.88$)	1.148	0.679	-0.196
Higher retail markup ($\theta = 0.72$)	0.758	0.310	-0.261
Lower sourcing variance ($\lambda = 0.9$)	0.911	0.424	-0.241
Higher sourcing variance ($\lambda = 1.1$)	0.917	0.425	-0.240
Panel C: Consumer demand			
Lower sub. imported goods ($\rho = 0.675$)	0.905	0.418	-0.242
Higher sub. imported goods ($\rho = 0.825$)	0.926	0.433	-0.238
Panel D: Pre-disruption anchor date			
Alternative anchor date (one month earlier)	0.997	0.373	-0.240

Notes: The table reports the consumer equivalent variation (as a percentage of GDP) for the counterfactual economies without the 2021 West Coast port disruptions, the 2024 security threats in the Red Sea, and the 2024 U.S. Navy intervention (central estimate), under alternative parameter values. Each row recalibrates the internally determined parameters and simulates the model so that the baseline economy continues to reproduce the same data targets and time paths. Panels A–C perturb each parameter by $\pm 10\%$ around its baseline value.

The welfare cost rises with σ, θ, and ρ, through two distinct channels. The first operates through market power. Raising either σ or θ lowers the corresponding markup and expands the retail sector toward its efficient size. A given proportional loss of shipping efficiency then falls on a larger base, raising the absolute welfare cost. The second channel operates through demand substitutability. A higher ρ makes imported varieties closer substitutes, so households respond to a shipping disruption by diverting demand toward less-affected origins and routes. This reallocation crowds onto a constrained network and raises marginal shipping costs across other routes, affecting demand for all other goods and therefore increasing the welfare cost of disruptions.

C.7. *Impact of tariffs on goods from Asia*

TABLE C.4

THE IMPACT OF TARIFFS ON ASIAN GOODS

		Baseline (1)	**Tariffs** (2)	Δ% (3)	↑ ϵ_k (4)	Δ% (5)	↓ θ (6)	Δ% (7)
Shipping market								
Q_r	Effective shipping supply (in DWT), *Total*	18.942	17.908	-5.5	10.853	-42.7	13.410	-29.2
	Asia-EC via Pan.	2.620	2.347	-10.4	1.425	-45.6	1.947	-25.7
	Asia-EC via Suez	1.229	1.090	-11.3	0.662	-46.1	0.995	-19.1
	Asia-West Coast	9.478	8.622	-9.0	5.219	-44.9	5.950	-37.2
	Europe to EC	3.852	3.970	3.1	2.406	-37.5	2.978	-22.7
	Middle East to EC	0.146	0.166	13.3	0.101	-31.1	0.168	15.2
	South Am. to EC	1.616	1.714	6.0	1.040	-35.7	1.372	-15.1
N	Number of shipping firms	36.000	37.462	4.1	40.507	12.5	47.836	32.9
$N\overline{\kappa}/K$	Idle capacity share	0.754	0.757	0.4	0.763	1.2	0.765	1.5
$g(K_r)$	Congestion factor, *Asia-EC via Pan.*	5.584	5.270	-5.6	7.666	37.3	5.156	-7.7
	Asia-EC via Suez	4.758	4.501	-5.4	6.548	37.6	4.587	-3.6
	Asia-West Coast	9.757	9.153	-6.2	13.286	36.2	7.748	-20.6
	Europe to EC	7.567	7.972	5.4	11.583	53.1	7.317	-3.3
	Middle East to EC	3.174	3.225	1.6	4.688	47.7	3.178	0.1
	South Am. to EC	4.771	4.974	4.3	7.233	51.6	4.735	-0.7
n_r	Number of trips/month, *Asia-EC via Pan.*	1.813	1.634	-9.9	1.477	-18.6	1.303	-28.1
	Asia-EC via Suez	1.463	1.314	-10.2	1.188	-18.8	1.121	-23.4
	Asia-West Coast	3.350	3.034	-9.4	2.735	-18.4	2.052	-38.8
	Europe to EC	2.577	2.633	2.1	2.376	-7.8	1.933	-25.0
	Middle East to EC	0.651	0.685	5.2	0.619	-4.9	0.607	-6.8
	South Am. to EC	1.468	1.514	3.1	1.367	-6.9	1.169	-20.4
p_r	Shipping prices, *Asia-EC via Pan.*	0.004	0.004	-5.6	0.006	37.3	0.004	-7.7
	Asia-EC via Suez	0.006	0.006	-5.4	0.009	37.6	0.006	-3.6
	Asia-West Coast	0.004	0.004	-6.2	0.006	36.2	0.003	-20.6
	Europe to EC	0.006	0.006	5.4	0.009	53.1	0.006	-3.3
	Middle East to EC	0.010	0.011	1.6	0.015	47.7	0.010	0.1
	South Am. to EC	0.005	0.005	4.3	0.007	51.6	0.005	-0.7
π_r ($\times 100$)	Shipping profits, *Asia-EC via Pan.*	0.007	0.005	-18.8	0.004	-33.7	0.003	-48.4
	Asia-EC via Suez	0.004	0.003	-19.4	0.003	-34.1	0.002	-41.3
	Asia-West Coast	0.022	0.018	-18.0	0.015	-33.4	0.008	-62.5
	Europe to EC	0.013	0.014	4.3	0.011	-15.0	0.007	-43.7
	Middle East to EC	0.001	0.001	10.6	0.001	-9.6	0.001	-13.2
	South Am. to EC	0.004	0.005	6.3	0.004	-13.3	0.003	-36.6
Retail market								
$\mathcal{I}$	Measure of retailers	1.000	1.607	60.7	2.931	193.1	3.173	217.3
o_r	Specialization, *Asia to EC via Pan.*	0.166	0.166	0.1	0.166	0.3	0.166	0.4
	Asia to EC via Suez	0.165	0.165	0.4	0.166	0.8	0.166	0.8
	Asia to West Coast	0.173	0.170	-1.3	0.168	-2.4	0.169	-2.3
	Europe to EC	0.169	0.168	-0.3	0.167	-0.8	0.168	-0.6
	Middle East to EC	0.163	0.164	0.7	0.166	1.4	0.165	1.2
	South Am. to EC	0.165	0.165	0.4	0.166	0.8	0.166	0.7
ω_o	Import share of output, *Total*	0.113	0.116	2.5	0.102	-9.4	0.095	-15.5
	Asia	0.073	0.072	-0.7	0.064	-12.2	0.058	-20.3
	Europe	0.029	0.031	7.5	0.028	-5.0	0.026	-11.7
	Middle East	0.002	0.002	14.0	0.002	1.1	0.003	36.2
	South America	0.009	0.010	9.5	0.009	-3.0	0.009	-0.5
P^{tot}/p_d	Retail price (rel. to domestic goods), *All goods*	0.972	0.969	-0.3	0.983	1.2	0.991	2.0
P^{imp}/p_d	*Imported*	0.017	0.017	-2.8	0.019	11.7	0.021	20.7
p_o/p_d	*Asia*	0.005	0.005	-1.7	0.006	12.9	0.006	23.1
	Europe	0.007	0.007	-4.3	0.008	9.9	0.008	18.9
	Middle East	0.003	0.003	-6.2	0.003	7.7	0.003	2.9
	South Am.	0.004	0.004	-4.9	0.004	9.2	0.005	14.3
Government								
T/Y	Tax revenues (% of GDP)		0.881		0.779		0.589	
Welfare								
	Equivalent variation (% of income, rel. to baseline)		1.295		-0.605		-0.395	

Note: The experiment is based on the model calibrated to March 2025 data.

C.8. *Impact of port fees on ships from Asia*

TABLE C.5

THE IMPACT OF PORT FEES ON ASIAN SHIPS

		Baseline (1)	**Port fees** (2)	Δ% (3)	↑ ϵ_k (4)	Δ% (5)	↓ θ (6)	Δ% (7)
Shipping market								
Q_r	Effective shipping supply (in DWT), *Total*	18.942	19.370	2.3	11.343	-40.1	14.221	-24.9
	Asia-EC via Pan.	2.620	2.677	2.2	1.569	-40.1	2.159	-17.6
	Asia-EC via Suez	1.229	1.256	2.2	0.736	-40.1	1.108	-9.8
	Asia-West Coast	9.478	9.662	1.9	5.656	-40.3	6.542	-31.0
	Europe to EC	3.852	3.959	2.8	2.319	-39.8	2.933	-23.9
	Middle East to EC	0.146	0.151	3.3	0.089	-39.5	0.156	6.8
	South Am. to EC	1.616	1.664	3.0	0.975	-39.7	1.323	-18.2
N	Number of shipping firms	36.000	35.450	-1.5	38.949	8.2	43.994	22.2
$N\overline{\kappa}/K$	Idle capacity share	0.754	0.751	-0.4	0.763	1.2	0.776	2.9
$g(K_r)$	Congestion factor, *Asia-EC via Pan.*	5.584	5.694	2.0	8.004	43.3	5.076	-9.1
	Asia-EC via Suez	4.758	4.852	2.0	6.821	43.4	4.507	-5.3
	Asia-West Coast	9.757	9.930	1.8	13.946	42.9	7.674	-21.3
	Europe to EC	7.567	7.724	2.1	10.853	43.4	6.516	-13.9
	Middle East to EC	3.174	3.239	2.0	4.552	43.4	2.909	-8.4
	South Am. to EC	4.771	4.871	2.1	6.846	43.5	4.253	-10.8
n_r	Number of trips/month, *Asia-EC via Pan.*	1.813	1.869	3.1	1.619	-10.7	1.423	-21.5
	Asia-EC via Suez	1.463	1.509	3.2	1.307	-10.7	1.226	-16.2
	Asia-West Coast	3.350	3.447	2.9	2.982	-11.0	2.238	-33.2
	Europe to EC	2.577	2.661	3.2	2.302	-10.7	1.888	-26.8
	Middle East to EC	0.651	0.674	3.4	0.583	-10.4	0.583	-10.5
	South Am. to EC	1.468	1.517	3.3	1.314	-10.5	1.135	-22.7
p_r	Shipping prices, *Asia-EC via Pan.*	0.004	0.005	2.5	0.006	44.0	0.004	-8.7
	Asia-EC via Suez	0.006	0.006	2.5	0.009	44.1	0.006	-4.8
	Asia-West Coast	0.004	0.004	2.3	0.006	43.6	0.003	-21.0
	Europe to EC	0.006	0.006	2.1	0.009	43.4	0.005	-13.9
	Middle East to EC	0.010	0.011	2.0	0.015	43.4	0.010	-8.4
	South Am. to EC	0.005	0.005	2.1	0.007	43.5	0.004	-10.8
π_r ($\times 100$)	Shipping profits, *Asia-EC via Pan.*	0.007	0.007	6.3	0.005	-20.3	0.004	-38.4
	Asia-EC via Suez	0.004	0.005	6.4	0.003	-20.2	0.003	-29.8
	Asia-West Coast	0.022	0.024	5.9	0.018	-20.8	0.010	-55.4
	Europe to EC	0.013	0.014	6.5	0.011	-20.2	0.007	-46.4
	Middle East to EC	0.001	0.001	7.0	0.001	-19.8	0.001	-19.9
	South Am. to EC	0.004	0.005	6.8	0.003	-20.0	0.003	-40.3
Retail market								
$\mathcal{I}$	Measure of retailers	1.000	1.497	49.7	1.503	50.3	1.652	65.2
o_r	Specialization, *Asia to EC via Pan.*	0.166	0.166	0.2	0.166	0.2	0.166	0.3
	Asia to EC via Suez	0.165	0.165	0.3	0.166	0.5	0.166	0.5
	Asia to West Coast	0.173	0.171	-1.0	0.170	-1.5	0.170	-1.4
	Europe to EC	0.169	0.168	-0.4	0.168	-0.5	0.168	-0.2
	Middle East to EC	0.163	0.164	0.6	0.165	0.9	0.164	0.5
	South Am. to EC	0.165	0.165	0.3	0.166	0.5	0.165	0.3
ω_o	Import share of output, *Total*	0.113	0.118	4.5	0.098	-13.6	0.087	-22.7
	Asia	0.073	0.076	4.3	0.063	-13.8	0.054	-25.3
	Europe	0.029	0.030	4.8	0.025	-13.4	0.023	-21.9
	Middle East	0.002	0.002	5.2	0.002	-12.9	0.002	16.6
	South America	0.009	0.010	5.0	0.008	-13.1	0.008	-13.0
P^{tot}/p_d	Retail price (rel. to domestic goods), *All goods*	0.972	0.966	-0.6	0.989	1.7	1.000	2.9
P^{imp}/p_d	*Imported*	0.017	0.016	-4.9	0.020	17.8	0.023	33.1
p_o/p_d	*Asia*	0.005	0.005	-4.8	0.006	17.9	0.007	34.6
	Europe	0.007	0.007	-5.0	0.008	17.7	0.009	32.6
	Middle East	0.003	0.003	-5.1	0.003	17.5	0.003	16.1
	South Am.	0.004	0.004	-5.0	0.005	17.6	0.005	28.0
Government								
T/Y	Tax revenues (% of GDP)		0.024		0.020		0.014	
Welfare								
	Equivalent variation (% of income, rel. to baseline)		0.682		-2.018		-2.159	

Note: The experiment is based on the model calibrated to March 2025 data.

C.9. *Impact of port infrastructure improvement*

TABLE C.6

THE IMPACT OF PORT INFRASTRUCTURE IMPROVEMENTS

		Baseline (1)	$\downarrow \varepsilon_k$ (2)	$\Delta\%$ (3)
Shipping market				
Q_r	Effective shipping supply (in DWT), *Total*	18.942	20.844	10.0
	Asia-East Coast via Panama	2.620	2.886	10.1
	Asia-East Coast via Suez	1.229	1.354	10.2
	Asia-West Coast	9.478	10.423	10.0
	Europe to East Coast	3.852	4.239	10.0
	Middle East to East Coast	0.146	0.161	10.2
	South America to East Coast	1.616	1.780	10.1
N	Number of shipping firms	36.000	37.928	5.4
$N\overline{\kappa}/K$	Idle capacity share	0.754	0.739	-2.0
$g(K_r)$	Congestion factor, *Asia-East Coast via Panama*	5.584	5.438	-2.6
	Asia-East Coast via Suez	4.758	4.633	-2.6
	Asia-West Coast	9.757	9.489	-2.7
	Europe to East Coast	7.567	7.364	-2.7
	Middle East to East Coast	3.174	3.090	-2.7
	South America to East Coast	4.771	4.644	-2.7
n_r	Number of trips/month, *Asia-East Coast via Panama*	1.813	1.829	0.9
	Asia-East Coast via Suez	1.463	1.476	0.9
	Asia-West Coast	3.350	3.375	0.8
	Europe to East Coast	2.577	2.599	0.8
	Middle East to East Coast	0.651	0.657	0.9
	South America to East Coast	1.468	1.481	0.9
p_r	Shipping prices, *Asia-East Coast via Panama*	0.004	0.004	-2.6
	Asia-East Coast via Suez	0.006	0.006	-2.6
	Asia-West Coast	0.004	0.004	-2.7
	Europe to East Coast	0.006	0.006	-2.7
	Middle East to East Coast	0.010	0.010	-2.7
	South America to East Coast	0.005	0.005	-2.7
π_r $(\times 100)$	Shipping profits, *Asia-East Coast via Panama*	0.007	0.007	1.8
	Asia-East Coast via Suez	0.004	0.004	1.9
	Asia-West Coast	0.022	0.023	1.5
	Europe to East Coast	0.013	0.013	1.6
	Middle East to East Coast	0.001	0.001	1.9
	South America to East Coast	0.004	0.004	1.8
Retail market				
$\mathcal{I}$	Measure of retailers	1.000	1.334	33.4
o_r	Specialization, *Asia to East Coast via Panama*	0.166	0.166	0.1
	Asia to East Coast via Suez	0.165	0.165	0.2
	Asia to West Coast	0.173	0.171	-0.7
	Europe to East Coast	0.169	0.168	-0.2
	Middle East to East Coast	0.163	0.164	0.4
	South America to East Coast	0.165	0.165	0.2
ω_o	Import share of output, *Total*	0.113	0.121	6.9
	Asia	0.073	0.078	6.9
	Europe	0.029	0.031	6.9
	Middle East	0.002	0.002	7.1
	South America	0.009	0.010	7.0
P^{tot}/p_d	Retail price (rel. to domestic goods), *All goods*	0.972	0.963	-0.9
P^{imp}/p_d	*Imported goods*	0.017	0.016	-7.3
p_o/p_d	*Asia*	0.005	0.005	-7.3
	Europe	0.007	0.006	-7.3
	Middle East	0.003	0.003	-7.4
	South America	0.004	0.004	-7.3
Welfare				
	Equivalent variation (% of income)		1.050	

Note: The experiment is based on the model calibrated to March 2025 data.